

**Cardiovascular Magnetic Resonance in patients with HIV  
Infection: Assessing the structural and functional  
abnormalities associated with remodelling of the  
myocardium**

**Magdalena Elizabeth (Leonie) Scholtz**

**Cardiovascular Magnetic Resonance in patients with HIV Infection:  
Assessing the structural and functional abnormalities associated with  
remodelling of the myocardium**

**Magdalena Elizabeth (Leonie) Scholtz**

Submitted in fulfilment of the requirements for the degree Philosophiae Doctor  
Diagnostic Radiology in the Faculty of Health Sciences

University of Pretoria

PRETORIA

March 2019

Supervisor: Prof. Anton Stoltz (University of Pretoria)

Co-supervisor: Prof. Ntobeko Ntusi (University of Cape Town)

Co-supervisor: Prof. James Ker Snr. (University of Pretoria)

*“The diagnostic radiologist is a clinician who has sacrificed one of the greatest glories of the practice of medicine and its greatest responsibility - the daily contact with the ill and their families - in order to concentrate more on the essence of our profession, the pathology of the living. This he sees through the medium of shadows, which has left him open to the charge of not quite being a real clinician.*

*But shadows, after all, are real. What are we to one another and what is the world to any of us, but an inverted image on the retina? Seeing is done with the mind. The camera does not see; it records. The radiologist perceived the shadow, sees a lesion, and imagines the man. The bedside physician sees the man, perceives the signs and imagines the lesion. They practice from the outside in and we from the inside out. Both are clinicians, for in truth there is no other kind of doctor worthy of the name. The decisive test for all is finally and always the bedside. This, then, is one concept of the radiologist - with a film on the view box, but the bedside in his or her mind.”*

Harry Z Mellins MD 1921-2009

## **Submission declaration**

I, Magdalena Elizabeth Scholtz, hereby declare that the thesis/dissertation that I herewith submit for the degree Philosophiae Doctor to the University of Pretoria contains my own work and has not been previously submitted by me for a degree to this or any other tertiary institution.

15/7/2019

Magdalena Elizabeth Scholtz

Date



## Plagiarism declaration

Full name: Magdalena Elizabeth Scholtz

Student number: 75016682

Title: Cardiovascular Magnetic Resonance in patients with HIV Infection: Assessing the structural and functional abnormalities associated with remodelling of the myocardium

### Declaration:

1. I understand what plagiarism entails and am aware of the University's policy in this regard.
2. I declare that this thesis is my own original work. Where somebody else's work was used (whether from a printed source, the internet or any other source) due acknowledgement was given and reference was made according to departmental requirements.
3. I did not make use of another student's previous work and submit it as my own.
4. I did not allow and will not allow anyone to copy my work with the intention of presenting it as his or her own work.

15/7/2019

Magdalena Elizabeth Scholtz

Date

## **Dedication**

To my children Xan, Inge, Johan, Daniella, Michail, Beate, Markus, Mia, Ian and my grandchildren  
Clarke and Kai.

LS

## **Acknowledgements**

I would like to express my sincere gratitude to my supervisor Prof Anton Stoltz for his support, encouragement and supervision. Also, to everyone from the Department of Internal Medicine at the University of Pretoria, who helped to source the patients, as well as my co-supervisor, lifelong mentor and friend, Prof James Ker snr. for his help, enthusiasm and wisdom.

I am forever grateful to Prof Ntobeko Ntusi, my co-supervisor from the University of Cape Town without whom the project would not have seen the light of day, for his valuable input, immense knowledge and expertise.

I would like to thank Mr Stephen Jermy from UCT, who meticulously performed the time-consuming image analysis and Drs Aneesah Mohamed Khan and Aqeela Moosa, who collected the patients and all their clinical data and had to deal with challenging logistics throughout the study.

I am also grateful to Prof Zarina Lockhat, colleague and friend from the Department of Radiology, for her precious support, encouragement and friendship.

Thanks to Dr André du Plessis from Scholtz and partners, who did a time-consuming backup of the image analysis, for his expertise and to Me Anelia Swart and her team of radiographers at Scholtz and Partners, (Veronica van der Walt, Busisiwe Macia and Linda-Marie Botha), who performed all the CMR scans meticulously and diligently and often worked extended hours in the process. Their commitment and dedication made the study possible.

To Philips Medical Systems, Best, The Netherlands and specifically Guillaume Thelissen as well as Lee Roering and Elizna Rodgers from Philips who helped with the scan protocols and applications, my sincere appreciation.

Lastly, I would like to thank all my children for their love, their honesty, their delightful senses of humour, and for becoming my best friends, my fiercest critics and my biggest supporters.

## **Executive summary**

*Background:* The pandemic of human immunodeficiency virus (HIV) infection in sub-Saharan Africa with its attendant dire impact on society and the economy continues. In 2016 it was estimated that the disease affected 36.7 million (30.8–42.9 million) people worldwide, with the majority living in Sub-Saharan Africa (7.1 million in South Africa). South Africa spent over 1 billion US dollars on the disease in 2014. In the pre-antiretroviral therapy (ART) era, once the myocardium was involved, life expectancy seriously declined and was estimated at less than 6 months. The widespread availability of ART profoundly altered the epidemiology, natural history and outcomes of HIV-associated cardiovascular disease (CVD). The functional, structural and tissue characteristics of the cardiovascular manifestations of HIV infection can be assessed with accuracy using cardiovascular magnetic resonance (CMR). This study was designed to ascertain the effects of HIV on the myocardium in untreated asymptomatic young patients, at a time when the national policy in South Africa (SA) was to prescribe ART only to HIV-infected patients with a CD4<sup>+</sup> count below 350 cells/mm<sup>3</sup>.

*Methods and results:* Systolic and diastolic functional parameters as well as structural and tissue characteristics were assessed using a single 1.5 Tesla magnet in 40 asymptomatic untreated young HIV-infected patients from Tshwane district, South Africa (median age 36±10 years, 78% female), who presented for the first time and the findings compared to 37 healthy controls (matched for age and sex with a median age 36±11 years, 70% female). Left ventricular volumes, mass and ejection fraction did not differ significantly between the two groups (59±21% in HIV infected versus 61±29% in controls, p=0.7). However, there was a significant difference in the strain rate assessment (peak systolic circumferential strain rate in the HIV- infected group was  $-1.2\pm 0.56\text{ s}^{-1}$  versus  $-0.1\pm 0.22\text{ s}^{-1}$  in controls, p=0.044; peak systolic longitudinal strain rate in the HIV-infected group was  $-1.0\pm 0.23\text{ s}^{-1}$  versus  $-0.8\pm 0.43\text{ s}^{-1}$  in controls, p=0.014 and peak systolic radial strain rate was  $2.2\pm 0.67\text{ s}^{-1}$  in the HIV-infected group versus  $1.8\pm 0.55\text{ s}^{-1}$  in the controls, p=0.004). Native T1 times were significantly higher in the HIV-infected patients (1085 ms versus 1052 ms in controls, p=0.037). There was no difference in the presence of myocardial oedema between the groups (1.95 versus 2.14 in the control group, p=0.082). There was

increased late gadolinium enhancement of the myocardium present in the HIV-infected patients (83.8% versus 48.6% in controls,  $p= 0.002$ ).

*Conclusions:*

HIV infection is associated with strain abnormalities, and focal myocardial fibrosis in asymptomatic, untreated, young patients, unlikely to have been affected by other risk factors for cardiovascular disease, early in the course of the disease.

## **Keywords**

Human immunodeficiency virus; acquired immunodeficiency virus; cardiovascular magnetic resonance; late gadolinium enhancement; T1 mapping

## Table of Contents

Submission declaration .....	iv
Plagiarism declaration .....	v
Dedication.....	vi
Acknowledgements.....	vii
Executive summary .....	viii
Keywords.....	x
List of figures .....	xiii
List of tables .....	xvi
Abbreviations.....	xvii
<b>Chapter 1: Introduction.....</b>	<b>1</b>
1.1 Problem statement .....	1
1.2 Aim and objectives.....	5
1.3 Hypothesis .....	6
<b>Chapter 2: Literature review .....</b>	<b>7</b>
2.1 Literature review methodology .....	7
2.2 Cardiac manifestations of HIV .....	8
2.2.1 Pericardial disease .....	8
2.2.2. Myocardial disease .....	10
2.2.3 Infective endocarditis .....	17
2.2.4 Coronary artery disease .....	18
2.2.5 Pulmonary hypertension .....	20
2.3 Cardiovascular MRI.....	21
2.3.1 History .....	21
2.3.2 Technique .....	23
2.4 Cardiac remodelling .....	38
2.4.1 Introduction .....	38
2.4.2 HIV and cardiac remodelling .....	40
<b>Chapter 3: Materials and Methods.....</b>	<b>42</b>
3.1 Study population .....	42
3.2 Design and procedure.....	44
3.2.1 General .....	44
3.2.2 Scout images.....	46
3.2.3 Functional analysis sequences .....	47
3.2.4 T2 Oedema imaging sequence .....	48
3.2.5 Perfusion sequence .....	49
3.2.6 Sequences performed for detection of hyperaemia, fibrosis, inflammation or infiltration .....	50
3.3 Post-processing analysis .....	54
3.3.1 General .....	54
3.3.2 Functional analysis .....	54
3.3.3 Oedema.....	57
3.3.4 Perfusion.....	58
3.3.5 Hyperaemia (early enhancement).....	58
3.3.6 Analysis of late gadolinium enhancement.....	58
3.3.7 Quantifying fibrosis using LGE and T1 mapping .....	60
3.3.8 Assessment of LV strain and diastolic function using tissue tracking .....	61
3.3.9 Data analysis summary .....	64
3.4 Statistics .....	65
3.4.1 Statistical considerations .....	65

3.4.2 Control of potential Bias .....	66
3.5 Safety .....	66
3.6 Ethical considerations .....	67
<b>Chapter 4: Results .....</b>	<b>68</b>
4.1 Demographics and weight .....	68
4.2 Serological markers .....	69
4.3 Structural and functional analyses.....	70
4.4 Tissue characterisation analyses.....	75
<b>Chapter 5: Discussion .....</b>	<b>80</b>
<b>Chapter 6: Impact of the Study and future considerations.....</b>	<b>84</b>
<b>Chapter 7: Published articles, articles under review and planned articles .....</b>	<b>87</b>
<b>Appendix 1 .....</b>	<b>88</b>
<b>Appendix 2 .....</b>	<b>94</b>
<b>Appendix 3 .....</b>	<b>96</b>
<b>References .....</b>	<b>99</b>



## List of figures

Figure 1a. People infected with HIV (2017).

Figure 1b. The number of people living with HIV in 2016 according to UNAIDS.<sup>6</sup>

Figure 2. Aetiology of HIV-associated myocarditis and heart failure.<sup>1</sup>

Figure 3. Due to its versatility, CMR can assess morphology, function, perfusion and tissue characteristics, making it an ideal imaging tool to evaluate the cardiac manifestations of HIV.

Figure 4. Three axial black-blood T1 weighted axial images through the chest with the blood and lungs appearing dark and the normal myocardium of the LV and RV and muscular structures of the chest wall homogenous and grey. The subcutaneous fat tissue appears white. The left ventricle (LV) is situated behind the right ventricle (RV) on axial images.

Figure 5. LV outflow tract view with the blood appearing white on the cine images and the left ventricle and the aorta (Ao) seen in a single plane.

Figure 6. Two chamber cine view with the left ventricle (LV) and left atrium (LA) in the same plane.

Figure 7. Four-chamber cine view with all four cardiac chambers visualised in the same plane. The left ventricle (LV) and the left atrium (LA) lies behind the right ventricle (RV) and the right atrium in the four-chamber plane.

Figure 8. The short axis white blood images are used for systolic functional analysis. The left ventricle (LV) is situated behind the right ventricle (RV).

Figure 9. Short axis perfusion sequence with the perfusion defect appearing as a dark area in the antero-septal left ventricular (LV) wall (arrows).

Figure 10. T2-oedema sequence showing an inferolateral area affected by acute myocarditis (arrow) appearing whiter than the rest of the myocardium.

Figure 11. Potential mechanisms of hyperenhancement in acute and chronic myocardial infarction. Kim RJ, Choi KM, Judd RM, Higgins CB, de Roos A, eds. Cardiovascular MRI and MRA. Philadelphia, PA: Lippincott Williams and Wilkins; 2003: 209-237.

Figure 12. The typical pattern of evolving myocardial infarction secondary to acute coronary occlusion can be explained by the pathophysiology of ischaemia progressing to transmural necrosis. Little or no cellular necrosis is found until about 15 minutes after occlusion. After 15 minutes, a 'wave-front' of necrosis begins in the subendocardium and gradually extends towards the epicardium over the next few hours. During this period the extent of the infarcted region within the ischaemic zone increases continuously towards transmural.<sup>1</sup>

Figure 13. Patterns of late gadolinium enhancement encountered in clinical practice.<sup>140</sup>

- A. Transmural: infarct, severe myocarditis or sarcoidosis
- B. Subepicardial: myocarditis, sarcoidosis
- C. Mid-myocardial: dilated cardiomyopathy, hypertrophic cardiomyopathy, pulmonary hypertension
- D. Subendocardial: infarct, amyloid, hyper-eosinophilic syndrome
- E. Diffuse: amyloid, hypertrophic cardiomyopathy

- Figure 14. T1-mapping image with a region of interest (ROI) drawn manually depicting the native T1 time.
- Figure 15. Three patterns of cardiac remodelling due to myocardial hypertrophy.<sup>152</sup>
- Figure 16. Axial scout image with the right ventricle (RV) and left ventricle (LV) on the same plane.
- Figure 17. Coronal scout image with the left ventricle (LV) and aorta (Ao) on the same plane.
- Figure 18. Sagittal scout image with the right ventricle (RV) in front of the left ventricle (LV).
- Figure 19. Short axis white blood cine images were used to perform the functional analysis.
- Figure 20. T2 weighted turbo spin echo short axis image. The blood pool appears black, surrounded by the myocardium.
- Figure 21. Short axis image during early perfusion with the contrast still in the LV and RV cavities and appearing white before perfusing the myocardial muscle.
- Figure 22. Four chamber PSIR LGE image with the myocardium appearing black due to effective “nulling”. Contrast enhancement would stand out as white patches.
- Figure 23. PSIR LGE short axis image also with the myocardium appearing black.
- Figure 24a. Short axis images with planimetry of the endo- and epicardial borders. The endocardial line is red and the epicardium traced in green.
- Figure 24b. Four chamber orientation to indicate the levels of the short axis images as seen in Figure 24a during diastole and systole. The yellow lines indicate the level of the prior images.
- Figure 25a. The short-axis views were utilised to perform the functional analysis with dedicated software. Papillary muscles were excluded in the calculations. The endocardium once again traced with a red line and the epicardium with a green line. The papillary muscles were traced with a pink line.
- Figure 25b. Three-dimensional image indicating the level of the short axis image obtained in Figure 24a.
- Figure 26. T2-weighted short axis images were evaluated for oedema using computer-aided analysis. The areas of oedema were colour coded according to its signal intensity.
- Figure 27. Intensity of LGE in the LV myocardium (colour coded in yellow).
- Figure 28. T1 mapping was performed on the short axis images. The T1 time was colour coded in shades of red and orange in this image, according to its value.
- Figure 29. Tissue tracking was performed using the software module included with the dedicated software package, CVI42. The fine yellow grid lines can be seen in the overlay over the LV myocardium and the distortion during contractility used to calculate the strain.
- Figure 30. The three types of strain patterns. The fibres shorten in the longitudinal and circumferential plane but lengthens in the radial plane.<sup>158</sup>

Figure 31. Coronary artery territories and left ventricular segments according to the AHA model. There are seventeen segments and they correspond to the three main coronary artery territories with the right coronary artery supplying mainly the inferior region, the left anterior descending coronary artery supplying the apex, anterior and septal regions and the circumflex artery supplying the lateral wall mainly.

Figure 32a. LGE PSIR-TFE image of a control HIV uninfected individual.

Figure 32b. LGE in the same individual with yellow colour overlay in the areas of enhancement colour coded according to the intensity of the enhancement.

Figure 33a. LGE PSIR-TFE image of an HIV infected patient showing brighter areas of enhancement in the anterolateral wall and septum.

Figure 33b. The same LGE image with colour overlay in the areas of enhancement. The yellow regions indicate enhancement.

Figure 34a. T1 map of an HIV uninfected individual in the control group.

Figure 34b. Abnormal T1 map of one of the HIV-infected patients. The T1 time in ms is colour coded in orange/red with darker intensity in areas of abnormality in the HIV infected patient in comparison to the normal patient in Figure 34a.

Figure 35. The association between the CD4<sup>+</sup> count and the peak longitudinal diastolic strain rate implying that the lower the CD4<sup>+</sup> count, the greater the degree of diastolic dysfunction.

Figure 36. The association between the CD4<sup>+</sup> count and the native T1 time, which demonstrates that the T1 time correlates with the decline in the CD4<sup>+</sup> count.

Figure 37. The association between the native T1 time and the peak longitudinal diastolic strain rate once again demonstrating that the degree of abnormality in the native T1 time correlates well with the degree of diastolic impairment.

## **List of tables**

Table 1. Methodology according to Pubmed

Table 2. Summary of the sequences performed

Table 3. Demographics, weight and BSA

Table 4. Baseline serological markers

Table 5a. Summary of the results of the systolic functional analysis

Table 5b. Results of the LV mass assessment

Table 6. Results for the circumferential strain patterns

Table 7. Results for the radial strain patterns

Table 8. Results for the longitudinal strain patterns

Table 9. Tissue characterisation results

## Abbreviations

ACE-I	Angiotensin-converting enzyme inhibitor
AIDS	Acquired immunodeficiency syndrome
AMI	Acute myocardial infarction
Ao	Aorta
ARB	Angiotensin receptor blocker
ART	Antiretroviral therapy
BB TSE	Black blood turbo spin echo
BSA	Body surface area
BTFE	Balanced turbo field echo
CAD	Coronary artery disease
CCT	Cardiac computerised tomography
CMI	Chronic myocardial infarction
CMR	Cardiovascular magnetic resonance
CTCA	Computerised tomography coronary angiography
CVD	Cardiovascular disease
DCM	Dilated cardiomyopathy
EDV	End-diastolic volume
EF	Ejection fraction
EGEr	Early gadolinium enhancement ratio
EMB	Endomyocardial biopsy
ESV	End-systolic volume
FFE	Fast field echo
FS	Fat suppression
GFR	Glomerular filtration rate
GRE	Gradient echo

HAART	Highly active antiretroviral therapy
HIV	Human immunodeficiency virus
IMT	Intima-media thickness
IR	Inversion recovery
LA	Long axis
LGE	Late gadolinium enhancement
LV	Left ventricle/ventricular
LVEDV	Left ventricular end diastolic volume
LVEDVI	Left ventricular end diastolic volume index
LVEF	Left ventricular ejection fraction
LVESVI	Left ventricular end systolic volume index
LVM	Left ventricular mass
LVMi	Left ventricular mass index
mL	Millilitre
MOLLI	Modified Look-Locker inversion
MRS	Magnetic Resonance Spectroscopy
NSF	Nephrogenic systemic fibrosis
NYHA	New York Heart Association
OIs	Opportunistic infections
PAH	Pulmonary arterial hypertension
PI	Protease inhibitor
PLHIV	People living with HIV
PSIR	Phase-sensitive inversion recovery
RAAS	Renin-angiotensin-aldosterone system
ROI	Region of interest
RV	Right ventricular

SA	Short axis
sBTFE	Saturation recovery with balanced turbo field echo pulse
SD	Standard deviation
SIR	Signal intensity ratio
SSA	Sub-Saharan Africa
SA	South Africa
SV	Stroke volume
TI	Inversion time
TIMI	Thrombolysis in myocardial infarction
2Ch	Two chamber
4Ch	Four chamber
cm <sup>3</sup>	Cubic centimetres
%	Percentage
kg	Kilograms
m <sup>2</sup>	Metre squared
pg	Picogram
μL	Microlitre

# Chapter 1: Introduction

## 1.1 Problem statement

Although the human immunodeficiency virus (HIV)/acquired immunodeficiency syndrome (AIDS) epidemic seems to be tapering off worldwide, the impact of the disease in sub-Saharan Africa (SSA), which accounts for 69% of all adults and 90% of all children affected, remains daunting.<sup>2</sup> Eighteen percent of all HIV infections globally are found in South Africa (SA), followed by Nigeria (9%) and India (6%). Approximately 7.1 million South Africans are infected with HIV (Figure 1a). In 2013, 340,000 new HIV infections were recorded in SA and 200,000 AIDS-related deaths occurred. The proportion of adults living with HIV in SA was then estimated at 19.1%. Young females comprise the largest proportion of infected individuals, and in the Kwazulu-Natal province of SA, a recent study demonstrated that 39.3% of pregnant women were HIV infected.<sup>3</sup> More recently it was estimated that the disease affected 36.7 million (30.8–42.9 million) people worldwide, according to the UNAIDS 2016 fact sheet,<sup>4</sup> with an estimated 19.4 million living in East and Southern Africa. UNAIDS reported that 20.9 million people globally had access to antiretroviral therapy (ART) by 2017.

AIDS-related deaths in 2016 were estimated at 1 million (830 000 - 1.2 million) globally, which is a decline of approximately 900,000 as compared to 2005. A decline in the number of AIDS-related deaths in South Africa from the 2006 peak of 345,185, down to an estimated 126,755 in 2017, has largely been attributed to the national rollout of ARTs.<sup>5</sup>



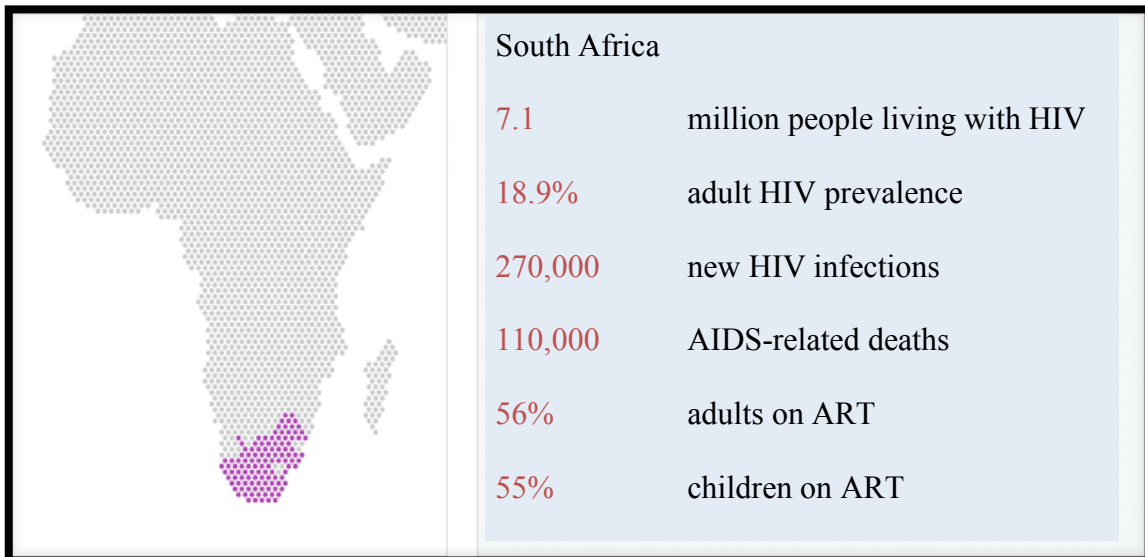


Figure 1a. People infected with HIV in South Africa according to the UNAIDS data of 2017.

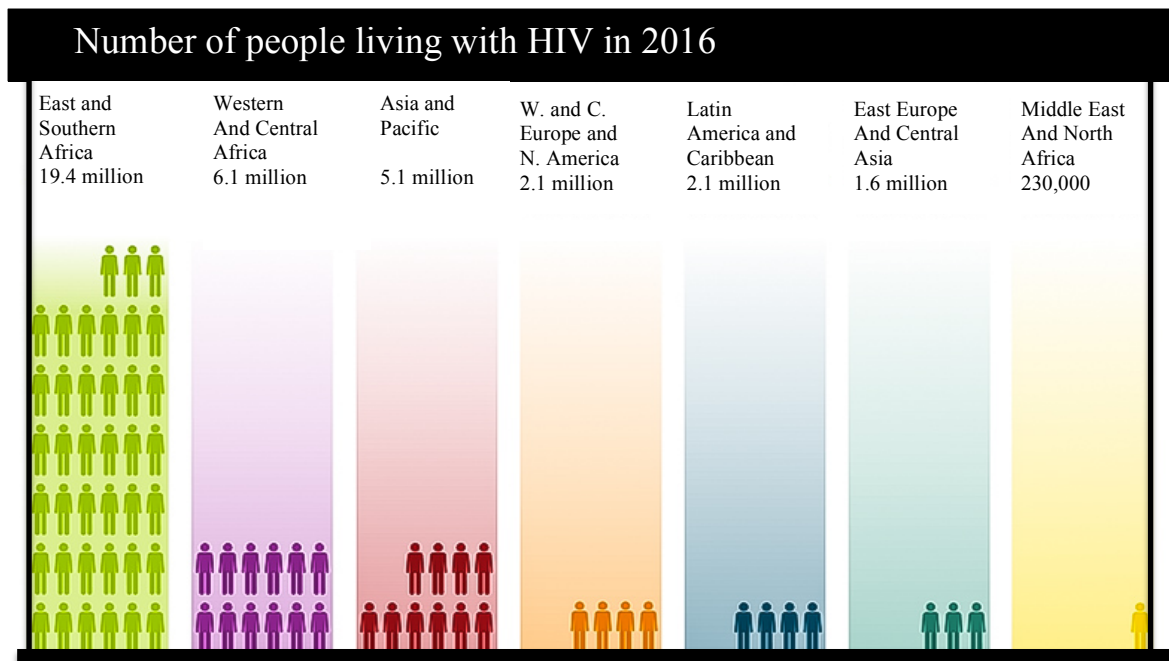


Figure 1b. The number of people living with HIV in 2016 according to UNAIDS.<sup>6</sup>

In dealing with this, in SA, 42% of all infected adults over 15 years and 90% of all pregnant HIV infected females, are currently receiving antiretroviral treatment (ART). SA now has the largest ART program globally and spends more than \$1 billion on HIV drugs annually. ART has increased life expectancy to nearly normal. Consequently, diseases of ageing, including cardiovascular diseases (CVD) are increasing in this population. Although ART decreases viral load with reduced immune

hyperactivity, complete functional immune restoration does not occur, nor is the viral load completely eradicated.<sup>7</sup>

The direct and indirect monetary cost and effect of HIV on the SA economy have not yet been accurately estimated. The financial burden of HIV on our society is complex and includes direct and indirect costs. A report by AVERT-Global Information and Education on HIV and AIDS- states that SA spent over 1.5 billion US dollars on its domestic HIV/AIDS program in 2014 alone.<sup>8</sup> In addition there is an indirect macroeconomic cost which includes countless lost working hours due to absenteeism related to the illness itself, the complications of HIV, and attendance at funerals as well as the additional burden of increased cost to medical schemes and pension benefits as well as the loss of skilled human resources leading to disruption of production.<sup>9</sup>

Trivialising the impact of HIV by putting a simple number to the casualties left behind in its wake completely undermines the deep-reaching socio-economic consequences of this pandemic. Countless lives are lost each year, and the impact on the individuals left behind cannot be quantified. The most vulnerable are the orphaned infants and children.

Cardiac involvement in HIV infection often goes undetected in this population. However, patients may present with advanced disease, and the pathophysiology and access to sophisticated imaging and prompt treatment in the developing world differ substantially from developed countries. The pericardium, myocardium, as well as the valvular structures may be affected by the virus *per se*, opportunistic infections (OIs), or treatment of the disease. The immune system plays a significant role in ventricular remodelling and the myocardial remodelling processes in immune compromised patients due to HIV is an important pathophysiological entity.

Cardiovascular magnetic resonance (CMR) is a robust and reproducible imaging modality, which is widely utilised internationally, but not yet widely available in SA. CMR does not make use of ionising radiation and is safe for assessing the cardiovascular system with no detrimental consequences to the patient. CMR is a versatile imaging technique that cannot only evaluate structure, perfusion, morphology and function but can also provide information on tissue characteristics, making it unique amongst available imaging modalities.<sup>10</sup>

HIV affects the myocardium in various ways, and CMR is the ideal imaging modality enabling this unique, comprehensive assessment. Compared to other non-invasive techniques, systolic and diastolic function can be more accurately quantified.<sup>11-14</sup> Also, the amount of scar tissue or fibrosis, an important aspect of remodelling and predictor of outcome, can be visualised. CMR has not yet been comprehensively used in research aimed at defining the cardiac manifestations of HIV/AIDS in Africa with only a few limited papers published in the literature so far. Once HIV affects the cardiovascular system, the prognosis is poor.<sup>15</sup> CMR can play an important role in the early diagnosis and management of these patients. Earlier detection of cardiac involvement and the response to treatment has the potential to improve outcomes in these patients substantially.

Only a few studies evaluating the effects of HIV on the myocardium with the help of CMR have been reported on in the literature.<sup>16-19</sup> Two of the studies were from the United Kingdom<sup>16, 17</sup>, one from Germany and the other one was from the United States.<sup>18</sup> The first two studies included 90 patients each with all the patients on ART treatment. The other study included 95 patients of which only 6 were treatment naïve.<sup>18</sup> No comprehensive studies specifically focused upon myocardium and tissue characteristics with CMR, have been performed in SSA and no studies have been conducted on patients not yet on ART.

The demographics differ between HIV infection in SSA and the rest of the world: in SSA, tuberculosis is endemic and access to ART is not universal, and therefore pericarditis and cardiomyopathy are the most frequent manifestations of HIV infection.<sup>20</sup> In the resource-rich countries where the majority of patients are on treatment, coronary artery disease and accelerated atherosclerosis are the main cardiac manifestations.<sup>20</sup> The effects of ART treatment on the cardiovascular system are well known and are discussed below.

The fact that many patients in SSA still present late during the infection and have not yet been on ART has opened the opportunity to study the direct effects of the disease on the myocardium and, again in this instance using CMR.

## **1.2 Aim and objectives**

The aim of this study was to identify and document the CMR findings of the myocardium, (structural and functional) in treatment naïve HIV-infected patients and the objective was to assess the degree of myocardial remodelling (changes in mass, volume and tissue characteristics) that occurs:

- a) To document functional abnormalities (ejection fraction [EF], diastolic function as well as volume and mass abnormalities) associated with left ventricular (LV) remodelling of the myocardium observed in patients with HIV-infection.
- b) To characterise the structural changes (tissue characteristics), affecting the myocardium in patients with HIV and verifying whether these changes are due to oedema, fibrosis or inflammation based on MRI findings.
- c) To compare the functional and structural CMR findings between HIV-infected and HIV-uninfected controls.

The CMR findings were correlated with other cardiac markers (NT-pro BNP) to ascertain whether cardiac involvement occurs early during the disease process.

### **1.3 Hypothesis**

Cardiovascular manifestations (structural and functional changes affecting the myocardium) of HIV occur early in the disease process and can be documented by CMR. The null hypothesis to be tested (rejected, nullified or disproved) was the assumption of no difference in the functional parameters and tissue characteristics in the HIV infected and control groups. The alternative hypothesis was that HIV infection *per se* causes structural or functional changes early in the course of the disease and that the findings documented in other studies could have been attributed to ART.

## Chapter 2: Literature review

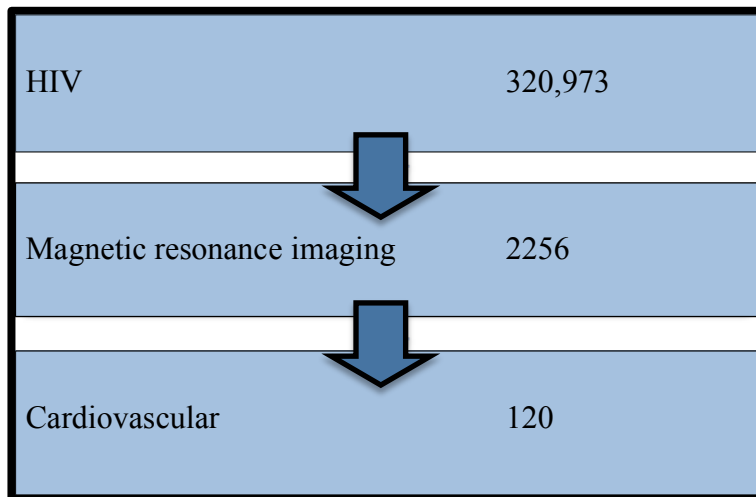
### 2.1 Literature review methodology

To expose the gaps in our understanding and knowledge of the diagnostic imaging of the cardiovascular manifestations of HIV, two research databases (Pubmed and MEDLINE) were used:

a. Pubmed

The keyword “HIV” delivered 320,973 articles and when “magnetic resonance imaging” was added to the search produced 2,256 articles. The added keyword “cardiovascular” reduced it to 120 articles, of which 13 were read and referred to in the literature review. The rest of the articles were rejected on the basis that they were either case reports or dealt with peripheral vascular or neurovascular manifestations of HIV.

Table 1. Methodology according to Pubmed



b. MEDLINE (Ovid)

The keyword “HIV” was combined with “magnetic resonance imaging,” and this produced 49 articles.

Most of these were case reports, dealt with peripheral or neurovascular manifestations or were not relevant. Fourteen were included in the literature review.

Although the cardiac manifestations of HIV were already documented as early as 1984, and MRI used extensively in other areas, CMR only became available for clinical use after 2000, and therefore all the relevant CMR articles between 2000 up to the date of the completion of the study were included in the search and the references.

## **2.2 Cardiac manifestations of HIV**

HIV, as well as its treatment, can affect any of the structural components of the heart, including the pericardium, the myocardium, the valve leaflets and their associated apparatus, the coronary vessels, aorta and pulmonary arteries. The effect of the disease on the myocardium was the focus of this study.<sup>21</sup>

### **2.2.1 Pericardial disease**

#### *Aetiology, pathophysiology and epidemiology of HIV-associated pericardial disease*

The pericardium is a frequent target in HIV infection: in high-income countries, acute and chronic pericarditis and pericardial constriction are usually due to viral infections (42-49%) and pericardial tuberculosis (3-6%) is uncommon.<sup>22</sup> In low- and middle-income countries (LMICs), where tuberculosis is endemic, as in SSA, pericardial tuberculosis is the most frequent cause of HIV-related pericardial disease.<sup>23</sup> Significant pericardial effusions are common in HIV/AIDS patients and are found in up to 46% of cases<sup>24</sup> although a decreased incidence of constriction has been reported in contrast to non-HIV infected aetiologies.<sup>25</sup>

Historically, in the pre-ART era, tuberculosis accounted for over 80% of pericardial effusions in HIV-infected persons in SSA.<sup>26</sup> Constrictive pericarditis was reported in 30-60% of these patients, despite prompt anti-tuberculous therapy and use of glucocorticosteroids.<sup>27</sup> A study of 185 African patients with tuberculous pericardial disease (40% of whom had clinical features or a confirmed diagnosis of HIV) found that patients with HIV infection were more likely to present with features of myopericarditis as opposed to pericardial involvement alone.<sup>28</sup>

### *Diagnostic imaging of HIV-associated pericardial disease*

Chest radiography is routinely performed during the workup of patients with HIV/AIDS (most often to exclude lung pathology) and is also the first imaging modality used in order to ascertain the possible presence of cardiac pathology, despite non-specific findings. Chest radiography is readily available in most parts of SSA, including rural areas. A study from the Western Cape in South Africa reported that almost half of the patients presenting with an enlarged cardiac contour due to pericardial effusion were HIV infected.<sup>29</sup> Conversely less than a third of HIV-infected persons with tuberculous pericarditis have evidence of pulmonary involvement on chest radiography, possibly due to a subdued immune response.<sup>30</sup> Smaller pericardial effusions may be present in up to 60% of HIV-infected patients, a common incidental finding in a recent CMR study from Europe (57% of patients on ART and 77% in untreated patients).<sup>17</sup> Echocardiography remains readily available to assess the pericardium, but few rural facilities are equipped or have expertise.

In situations where constriction needs to be differentiated from restrictive myocardial disease CMR and an invasive left and right heart catheterisation can be helpful, but restrictive cardiomyopathy has not been reported as a significant clinical problem in HIV infection.<sup>31</sup>

### *Prognosis of HIV-associated pericardial disease*

In a study from South Africa patients with tuberculous-associated pericardial disease had an overall mortality rate of 26%, with mortality higher in those who were HIV infected (40% vs. 17% in HIV uninfected individuals).<sup>32</sup> In the largest randomised clinical trial of patients with tuberculous pericarditis, conducted in Africa, 1400 patients (two thirds of whom were HIV infected) were included and randomised to receive prednisolone versus placebo or *Mycobacterium indicus pranii* vs. placebo. Neither agent demonstrated any increase in efficacy and prednisolone was associated with a significant increase in incidence of HIV-related cancers.<sup>33</sup>



## 2.2.2. Myocardial disease

### 2.2.2.1 Myocarditis

#### *Aetiology, evolving pathogenesis, epidemiology and prognosis of HIV-associated myocarditis*

Myocarditis due to HIV has been described, but the virus appears to infect the myocardial cells in a patchy distribution without a clear association between HIV viral load and cardiomyocyte dysfunction.<sup>34</sup> Myocarditis in HIV may also be related to opportunistic infections (OIs). In an autopsy study from the Congo, *Toxoplasma gondii*, *Cryptococcus neoformans* and *Mycobacterium avium intracellulare complex* were isolated from the myocardium of end-stage AIDS patients.<sup>35</sup> In a seminal study of HIV-associated cardiomyopathy from the US, endomyocardial biopsy (EMB) specimens revealed myocarditis with cardiotropic viral infections in most cases.<sup>36</sup> In contrast, a study from SA by Shaboodien and colleagues compared the prevalence of myocarditis and cardiotropic viral genomes in HIV-associated cardiomyopathy cases with HIV uninfected idiopathic dilated cardiomyopathy (DCM) patients and heart transplant recipients. They found myocarditis to be present in only 44% of HIV-associated cardiomyopathy cases.<sup>37</sup>

In a pre-ART autopsy series, myocarditis was documented in 52% of patients who died of AIDS, but since the widespread availability and utility of ART, the incidence of HIV-associated myocarditis has been markedly reduced.<sup>38</sup> There are no data on the epidemiology of HIV-associated myocarditis available from SSA.

#### *Diagnostic imaging of HIV-associated myocarditis*

An increased cardiothoracic ratio on chest X-ray is one of the features of underlying myocardial disease and chest roentgenograms are usually routinely performed on these patients. Depressed LV systolic function and wall motion abnormalities may be present on echocardiography in the acute setting of HIV related myocarditis. CMR is ideal because it can characterise myocardial tissue and diagnose myocardial and pericardial oedema/inflammation and necrosis with high accuracy while excluding the differential

diagnoses. Endomyocardial biopsy (EMB) is considered the gold standard for the diagnosis of myocarditis albeit one with flaws regarding its sensitivity and specificity. CMR is a non-invasive alternative and can also be of help in guiding the location of the biopsy site to enhance the diagnostic yield. Three CMR techniques were historically applied in myocarditis:

1. Late gadolinium enhancement (LGE) for detecting myocardial necrosis or fibrosis.
2. T2-weighted images for assessment of myocardial oedema.
3. T1-weighted sequences before and after contrast injection for detection of myocardial hyperaemia.

The initial 'Lake Louise criteria' for CMR diagnosis of myocarditis stated that CMR findings are consistent with myocarditis if 2 of the 3 above-mentioned criteria are found to be positive but revised criteria have been submitted stating that LGE, T1 and T2 mapping are the tools that should be relied upon.<sup>39</sup> Although the CMR findings in myocarditis are not specific, the criteria act as useful tools for the assessment of myocardial inflammation in patients with suspected acute myocarditis.<sup>40</sup> Antimyosin scintigraphy has been considered as a test to evaluate myocardial inflammation, albeit with exposure to radiation and with a poor diagnostic yield.<sup>41</sup>

#### **2.2.2.2 Cardiomyopathy with systolic dysfunction**

##### *Aetiology, evolving pathophysiology and epidemiology of HIV-associated cardiomyopathy*

The aetiology and mechanisms of development of HIV-associated cardiomyopathy are complex and multifactorial. Fluorescent *in situ* hybridisation of HIV in myocytes of patients with AIDS and primates with simian immunodeficiency virus demonstrated that the target of cardiac infection is the macrophage rather than the myocyte consistent with the observation that cardiac myocytes lack HIV receptor proteins (gp120 or p24).<sup>42, 43</sup> Additional evidence implicating direct myocyte infection by HIV, leading to LV systolic dysfunction, does exist.<sup>44</sup> Furthermore, gene products of HIV and HIV-related proteins contribute to the development of LV dysfunction.<sup>45</sup> HIV infection of cardiovascular dendritic cells may also play an important pathophysiological role as these cells may act as viral reservoirs and as antigen-presenting cells that result in chronic inflammation.<sup>46</sup> Opportunistic infections (OIs) may also cause

myocarditis that may lead to secondary cardiomyopathy in HIV-infected patients. Furthermore, some drugs used in the treatment of HIV, specifically zidovudine, may be associated with the development of a cardiomyopathy.<sup>47</sup>

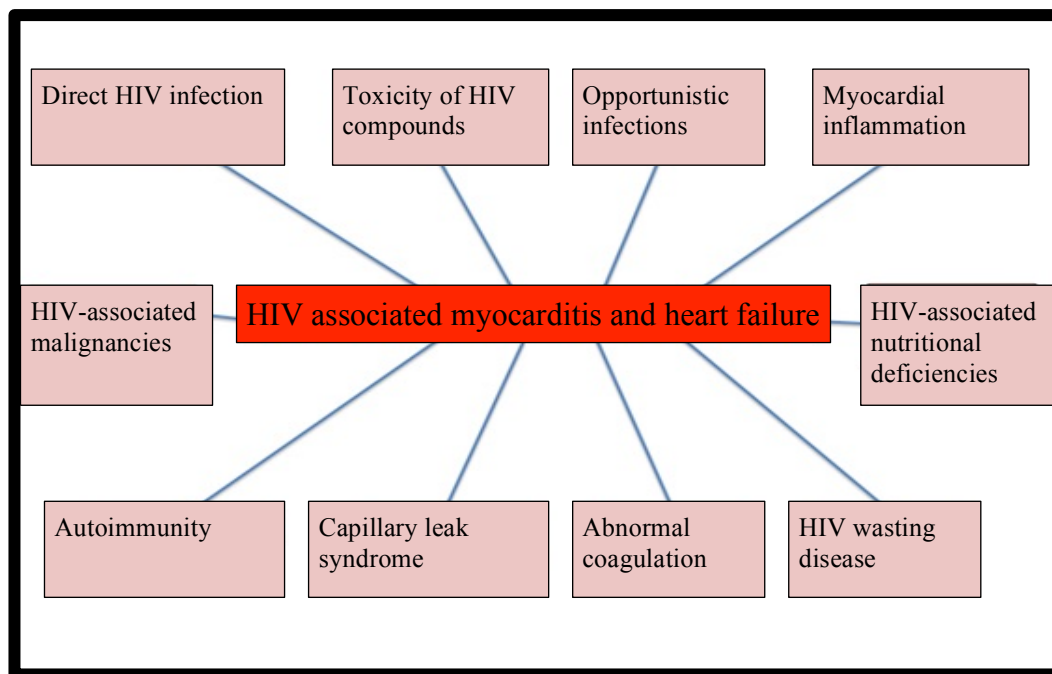


Figure 2. Aetiology of HIV-associated myocarditis and heart failure.<sup>21</sup>

Recent echocardiographic and CMR data suggest that the natural history of the disease in the era of ART is changing and these pathological features are likely to evolve as well.<sup>15</sup> The unfortunate delayed introduction of ART into SA has however provided an opportunity to study the natural history of HIV-associated cardiomyopathy.

The estimated annual incidence of HIV-associated cardiomyopathy in industrial countries in the pre-ART era was 15.9 per 1000, but was reported to occur much more commonly in SSA compared to resource-rich countries and in up to 38% in people living with HIV (PLWHIV) according to The Heart of Soweto study.<sup>48-51</sup>

The current prevalence of HIV-associated cardiomyopathy is substantially lower, mainly due to the ease of access to ART and reduction in OIs.<sup>15, 46</sup> In The Heart of Soweto Study, conducted in SA,

cardiomyopathy was reported in 38% of HIV infected patients<sup>52</sup> whereas the incidence in Rwanda<sup>51</sup> and Cameroon<sup>53</sup> was somewhat lower (18% and 15%, respectively). Since the introduction of ART, the typical phenotype of HIV-associated cardiomyopathy has changed from severe, dilated cardiomyopathy to subclinical LV dysfunction, with mildly reduced LV systolic function and frequent findings of impaired diastolic function. Few studies have measured the incidence at a population level.<sup>54</sup> The incidence of HIV-associated cardiomyopathy in the ART era seems to be declining in SSA, but there is unfortunately a paucity of population-based natural history data.

#### *Diagnostic imaging in HIV-associated cardiomyopathy*

Chest radiography is non-specific but does provide information regarding cardiac size and contour. In a study from Nigeria performed on adult patients presenting with HIV infection, 53% had normal chest x-rays. Most of the abnormal findings were due to concomitant lung infections (28%). Approximately 7% of untreated HIV-infected patients had cardiomegaly and 6% had changes compatible with congestive cardiac failure on chest x-ray.<sup>55</sup> Abnormalities of the cardiac silhouette seem to be more prevalent in HIV-infected children and in a study from SA, the second most common chest abnormality in children was found to be cardiomegaly (21%). Nonetheless, no correlation was found between the degree of cardiomegaly in these children and the level of their immunity, and differentiation between the causes of the cardiomegaly was not specified.<sup>56</sup>

Systolic cardiac failure causes reduced contractility and manifests as a decrease in the ejection fraction. Diastolic dysfunction or heart failure with preserved ejection fraction (HFpEF) occurs when the LV loses its ability to relax due to increased myocardial muscle stiffness.<sup>57</sup> Echocardiography remains the most practical and readily available diagnostic tool for assessment of cardiac morphology and function. In a large prospective multi-centre study, (the HIV-HEART study) conducted in Germany, 10% of HIV-infected patients (>80% on ART) demonstrated LV dilatation on echocardiography. Systolic dysfunction occurred in 34% and diastolic dysfunction in 48% of all patients.<sup>58</sup> In another large

prospective study of 656 HIV-infected persons (the SUN study), Mondy and co-workers monitored the effects of ART in asymptomatic patients. It was found that 26% had diastolic dysfunction. Systolic dysfunction occurred less frequently (18%).<sup>59</sup> A small study from Nigeria, performed on untreated, largely asymptomatic patients, found systolic dysfunction in 30% and diastolic dysfunction in 32% of patients.<sup>60</sup>

Inotropic contractile reserve during dobutamine stress echocardiography was shown to risk-stratify patients with HIV-associated cardiomyopathy and to predict subsequent improvement in LVEF.<sup>61</sup> Sixty patients with HIV-associated cardiomyopathy were included in the study. Improvement in the LVEF occurred in 56% of the patients and was more likely to occur in those demonstrating inotropic contractile reserve.

CMR, where available, should be considered and provides an accurate assessment of ventricular morphology and function, myocardial oedema, fibrosis, perfusion and viability, as well as a comprehensive evaluation of differential diagnoses. A high prevalence of CMR abnormalities has recently been reported in HIV-infected patients on ART.<sup>18, 62</sup> Systolic and diastolic dysfunction (lower peak myocardial systolic and diastolic longitudinal and circumferential strain and strain rates) occurred in asymptomatic HIV infected patients,<sup>16, 17, 63</sup> with diastolic dysfunction more severe than systolic dysfunction.<sup>16, 18</sup> Oedema, hyperaemia and increased myocardial mass also occurred more frequently in the HIV-infected patients.<sup>17, 63</sup> A recent novel finding was the presence of increased native T1 relaxation time, pointing to an underlying inflammatory process and diffuse myocardial fibrosis, found both in treated and in a small subgroup of patients not yet on ART.<sup>17, 18</sup>

#### *Prognosis of HIV-associated cardiomyopathy*

In the pre-ART era, HIV-associated cardiomyopathy was found almost exclusively in patients with advanced HIV infection and AIDS. The median survival was 101 days in patients with overt LV

dysfunction, and 472 days in patients with normal cardiac function on echocardiography, at a similar stage of immunosuppression.<sup>64</sup> With the routine use of ART, the outcome of HIV-associated cardiomyopathy is similar to that of heart muscle disease causing systolic LV dysfunction in HIV uninfected persons.<sup>65</sup> Despite optimal therapy LV systolic dysfunction and dilated cardiomyopathy are associated with significant mortality independent of age, gender and CD4<sup>+</sup> count.<sup>66</sup> Spontaneous recovery from HIV-associated cardiomyopathy has been described in patients treated with ART's.<sup>67</sup> More recently the presence of HIV infection has been demonstrated to be an independent predictor of mortality at 180 days for patients with acute decompensated heart failure and is associated with an increase in-hospital and 180-day mortality rate.<sup>68</sup>

### **2.2.2.3 Myocardial fibrosis and asymptomatic LV dysfunction**

In autopsy studies, up to 40% of HIV-infected patients were found to have histological evidence of interstitial myocardial fibrosis. Focal fibrosis (mostly present in the mid-ventricular and basal inferolateral wall) was seen on CMR in up to 76% of asymptomatic HIV-infected individuals, compared to 13% of control subjects,<sup>16</sup> findings, which have recently been confirmed by other groups.<sup>17, 63</sup> Similarly, diffuse fibrosis on CMR-determined extracellular volume estimation was found to be more frequent in HIV-infected persons, compared to matched controls.<sup>17, 18</sup>

### **2.2.2.4 Diastolic dysfunction**

Echocardiographic studies have reported a high prevalence of diastolic abnormalities in HIV-infected persons. Strain imaging has been increasingly used to document global and segmental systolic and diastolic dysfunction in asymptomatic HIV-infected patients with preserved LV systolic function.<sup>69-71</sup> In a cross-sectional study of 698 HIV-infected persons, 48% had diastolic dysfunction, which was associated with older age, higher body mass index, higher total cholesterol, arterial hypertension and diabetes mellitus.<sup>71</sup> HIV-associated diastolic dysfunction is more severe in patients with clinical AIDS.<sup>58, 72</sup> In one study the early and late longitudinal diastolic strain rates were impaired with a normal

mean strain rate<sup>70</sup> which implied an early abnormality in myocardial relaxation and in future could potentially be a useful marker of early cardiac involvement in asymptomatic young HIV-infected patients. A study from the Congo found the prevalence of diastolic dysfunction in HIV-infected patients to be much higher (86%) and also to be more severe in patients with clinical AIDS when compared to studies from Europe and North America.<sup>35</sup> Systolic function was preserved in the HIV infected (n=30) as well as in the AIDS group (n=19). Recently, CMR demonstrated high rates of diastolic dysfunction in cohorts of asymptomatic HIV-infected persons with preserved ejection fraction.<sup>16-18</sup>

#### **2.2.2.5 Myocardial lipidosis**

Two earlier studies (on asymptomatic HIV-infected patients on treatment), revealed the presence of myocardial steatosis.<sup>16, 18</sup> The 90 HIV-infected, asymptomatic individuals on combination ART had 47% higher median myocardial lipid levels on magnetic resonance spectroscopy (MRS), and 74% higher median plasma triglyceride levels.<sup>16</sup> Another report confirmed these findings.<sup>73</sup> Intra-myocardial lipid levels correlated with impaired strain, ART duration and visceral adiposity in a subsequent study.<sup>17</sup> In a more recent publication, pericardial fat accumulation was also demonstrated with CMR in HIV-infected patients on treatment.<sup>74</sup>

#### **2.2.2.6 Mitochondrial injury**

There is evidence of impaired mitochondrial injury in HIV-infected individuals.<sup>75</sup> Nonetheless, the clinical relevance of these findings remains uncertain and an area for further investigation. There is no evidence of increased mitochondrial genetic abnormalities in HIV-infected persons.<sup>76</sup>

#### **2.2.2.7 Cardiac masses**

There have been several reports of cardiac masses in HIV-infected persons and the aetiology for these has varied from tuberculomas, lymphomas and Kaposi's sarcoma to invasive angiosarcoma.<sup>77, 78</sup> Kaposi's sarcoma most commonly involves the epicardium and pericardium.<sup>79</sup> Tuberculomas have been

described in areas of high tuberculous prevalence. Lymphoma is the second commonest cardiac tumour in industrial nations, the majority of which are high-grade B cell tumours, like Burkitt's lymphoma or large cell immunoblastic lymphoma.<sup>80</sup> The right atrium is most commonly involved by malignant sarcomas and lymphomas. There is no evidence that cardiac tumours in HIV have a different outcome from those in HIV uninfected persons. Echocardiography, CCT and CMR are very important in the diagnosis and evaluation of HIV-associated cardiac masses.<sup>79</sup>

The goal of CMR for assessing cardiac and para cardiac masses includes confirming or excluding a mass suspected by X-ray or echocardiography, assessing its location, mobility and relationship to surrounding tissues, imaging the degree of vascularity, distinguishing solid lesions from fluid and determining tissue characteristics as well as the specific nature of a mass. Owing to its excellent resolution, tissue characterisation and multi-planar approach, the extent of intra- or pericardial mass lesions can be clearly visualised. The additional administration of gadolinium contrast agents can assess vascularity and help to differentiate a tumour from thrombus.

### **2.2.3 Infective endocarditis**

#### *Pathophysiology epidemiology and diagnosis of HIV-associated infective endocarditis*

Non-bacterial, thrombotic endocarditis and infective endocarditis have been described in patients with HIV infection. Unusual organisms such as *Candida*, *C. diphtheria* or *Aspergillus* may occur in this population.<sup>81</sup> The abuse of intravenous drugs increases the risk of developing right-sided infective endocarditis in HIV infection, which has a prevalence varying from 6.4% to 34% in HIV and is independent of the specific ART regimen.<sup>34</sup>

The overall incidence of infective endocarditis in HIV-infection is similar to that among HIV-uninfected individuals.<sup>34, 82</sup> A retrospective study of cases of infective endocarditis in HIV-infected individuals over a 12-year period from Italy revealed that the incidence of infective endocarditis had decreased following



the introduction of ART from 20.5 to 6.6 per 1,000 patient years.<sup>83</sup> Marantic endocarditis (previously found in 4-10% in HIV patients at autopsy) usually associated with HIV wasting disease, is less frequently reported in the ART era.<sup>84</sup> The complication and mortality rates are 30% higher in those patients with advanced HIV who develop infective endocarditis and this is related to the degree of immunosuppression.<sup>83</sup> Although CMR and novel methods and modalities are being developed echocardiography remains the primary imaging modality in infective endocarditis due to its availability.<sup>85</sup>

#### **2.2.4 Coronary artery disease**

##### *Pathophysiology of HIV-associated coronary artery disease*

There is an increasing occurrence of coronary artery disease (CAD) in intermediate to long-term survivors with HIV, with a histologically distinctive form of accelerated atherosclerosis.<sup>86</sup> Vessel involvement is frequently diffuse and circumferential,<sup>87</sup> with unusual proliferation of smooth muscle cells, mixed with abundant elastic fibres resulting in endoluminal protrusions.<sup>88</sup> The increased platelet activation in HIV,<sup>89</sup> altered adhesion of HIV-infected monocytes-macrophages and HIV-associated angiitis/vasculitis all contribute to coronary arteriopathy.<sup>90</sup> In South Africa, there are reports of *de novo* arteriothrombosis, with evidence of acute coronary syndromes marked by fresh thrombus, as opposed to atherosclerotic occlusion.<sup>89</sup> Atherosclerosis in HIV is a multifactorial pathogenic process with contributions from sequelae of ART and HIV-mediated endothelial dysfunction.<sup>91</sup> Protease inhibitors (PIs) may lead to increased atherosclerosis via increased dyslipidaemia, insulin resistance, increased levels of C peptide, lipodystrophy and endothelial dysfunction.<sup>92</sup> In a single centre-study, HIV-infected patients had lower TIMI, (thrombolysis in myocardial infarction) risk assessment scores and were more likely to have single-vessel CAD.<sup>93</sup> A study of 501 HIV-infected patients from Botswana, reported a striking clustering of atherosclerotic risk factors namely; hypertension, dyslipidaemia, obesity, dysglycaemia and smoking,<sup>94</sup> which could play an important role in the late presentation of CAD in this population. In this study, the age for the occurrence of CVD risk factors was about a decade after the

peak age for HIV infection in Botswana.

The on-going Randomised Trial to Prevent Vascular Events in HIV (REPRIEVE Trial) is the first large randomised clinical research trial evaluating the effects of a daily dose of a statin and whether it may reduce the risk of heart disease in HIV-infected individuals.<sup>95</sup>

#### *Epidemiology of HIV-associated coronary artery disease*

Coronary artery disease (CAD) in HIV-infected persons was reported early in the HIV epidemic.<sup>86</sup> Data from observational studies show that compared to the general population, HIV-infected individuals have a higher rate of CAD, particularly in those receiving PIs for longer than 18 months.<sup>96</sup> In the French Hospital Database, HIV-infected persons had a standardised CAD mortality ratio of 1.5 compared to the uninfected general population.<sup>97</sup> The mean age of myocardial infarction in HIV-infected patients was 48 years likely reflecting the earlier exposure of ART.<sup>98</sup> Increased risk for CAD has been reported in children who received ART from a young age and continued to receive these medications causing substantial risk of morbidity and mortality in this group.<sup>99</sup> The available data on HIV-associated CAD is based upon studies outside Africa. While CAD has not been reported as a significant issue among Africans; given the growing burden of cardiovascular risk factors and diabetes, HIV-associated CAD is likely to lead to an increasing prevalence on the continent and could in the future be a major contributor to the growing epidemic of CVD on the continent.<sup>100</sup>

#### *Diagnostic imaging of HIV-associated coronary artery disease*

Sonographic carotid intima-media thickness assessment (IMT) is a potent risk assessment imaging tool for underlying atherosclerotic disease and may be useful in long-term survivors of retroviral infection.<sup>101</sup> HIV-infected individuals have a greater IMT compared to uninfected individuals, and the progression is more rapid.<sup>101</sup>

The presence of coronary artery calcium deposits and non-calcified plaque on CT in HIV-infected men

was found to be higher and the degree of stenosis worse in the multicentre AIDS study in the US, especially in patients on prolonged ART and lower CD4+ T-cell count,<sup>102</sup> and CT assessment of risk will become increasingly important in the future. In a recent meta-analysis, the prevalence of non-calcified plaque on coronary computed tomographic angiography (CCTA) was also much higher (>threefold) in HIV patients.<sup>103</sup> CCTA has an increasing role to play in this setting.<sup>104</sup> In a gated myocardial SPECT study from France performed on 94 asymptomatic HIV-infected patients, the investigators concluded that in male patients older than 52, (with at least two other cardiovascular risk factors) the presence of underlying silent ischaemia is four times more common in HIV-infected patients when compared to matched, uninfected individuals.<sup>105</sup> In two recent PET studies, elevated 18 fluorine-2-deoxy-D-glucose uptake was observed in the aorta and carotid vessels respectively, indicating arterial wall inflammation.<sup>106, 107</sup> The patients in one study also had raised sCD163 counts, indicating the presence of increased macrophage activity.<sup>106</sup>

### **2.2.5 Pulmonary hypertension**

#### *Pathophysiology and epidemiology of HIV-associated pulmonary hypertension*

Right ventricular (RV) abnormalities secondary to pulmonary arterial hypertension are common as a result of prior infections, thromboembolic disease, chronic obstructive lung disease and lung malignancy, and are well documented.<sup>108</sup> The pathophysiology of primary pulmonary hypertension in HIV (in the absence of significant pulmonary disease), is complex and multifactorial and poorly understood.<sup>109</sup> A third of HIV-infected patients with pulmonary hypertension have AIDS or AIDS-related pulmonary infections. Pulmonary infection, low CD4<sup>+</sup> cell counts or hypoxemia are not needed for development of pulmonary hypertension however.<sup>110</sup>

HIV-associated pulmonary hypertension is estimated to occur in 0.5% of AIDS patients.<sup>111</sup> Ventricular dysfunction seems to be more severe in patients with PAH who are also infected with the HIV virus.<sup>112</sup> There is a lack of data from SSA on HIV-associated pulmonary hypertension. The Pan African

Pulmonary Hypertension Cohort (PAPUCO) registry provided valuable insights in this regard.<sup>113</sup> The patients were screened for the presence of pulmonary hypertension and their risk profiles documented. The study included 220 patients of which 35% were HIV-infected. Patients with pulmonary hypertension in SSA have a worse outcome in comparison to the rest of the world, probably due to delayed diagnosis and comorbidities, including the infectious diseases.<sup>113</sup>

#### *Imaging in patients with pulmonary hypertension*

Computerised tomography remains the imaging tool of choice in the assessment of patients with underlying pulmonary hypertension. CMR may add value in selected patients, especially when performed to assess the cardiac structures.<sup>114</sup> RV functional analysis can be performed in addition to assessment of RV dimensions as well as pulmonary artery size. Late gadolinium enhancement (LGE) classically occurs in the insertion points of the RV wall but the findings cannot be distinguished from findings occurring in primary pulmonary hypertension.<sup>114</sup>

#### *Prognosis of HIV-associated pulmonary hypertension*

Before the advent of ART, HIV-associated pulmonary hypertension was associated with a poor prognosis. In a study of 131 HIV-infected persons, half of the patients died during a median follow-up period of 8 months; and about half of these patients died within 6 months of diagnosis of pulmonary hypertension.<sup>115</sup>

## **2.3 Cardiovascular MRI**

### **2.3.1 History**

In 1946 Felix Bloch and Edward Mills Purcell independently discovered the magnetic resonance phenomenon. The first magnetic resonance scan of a human being was performed in 1980. Owing to initial obstacles, mainly related to cardiac motion and ECG triggering, CMR only established itself

within the cardiac imaging armamentarium long after its first diagnostic application in other disciplines. Faster and more effective sequences, coupled with ECG gating and breath holding, were subsequently developed to ‘freeze’ heart motion. Vector ECG gating, parallel imaging and other solutions have also minimised the initial problems during ECG triggering that resulted from the magneto-hydrodynamic effect of pulsatile blood in the aorta.<sup>116</sup>

Since the first MR images of the human heart were produced more than 20 years ago, the quality of CMR imaging has improved significantly and it is still advancing apace. CMR now represents one of the most versatile, non-invasive imaging modalities available, offering high spatial resolution and image contrast along with tissue characterisation and haemodynamic assessment, without the use of ionising radiation and with complete multi-planar coverage of the heart.<sup>10</sup> Because of its versatility, CMR is the ideal imaging modality to evaluate the cardiac effects of HIV. A multitude of sequences are available and different parameters can be assessed with CMR, but a lot of these are not applicable in this setting. The basic principles and the specific sequences used and parameters measured in this study will be alluded to and discussed in more detail.

CMR is the most versatile imaging modality in the diagnostic armamentarium for the evaluation of cardiovascular pathology (see Figure 3).

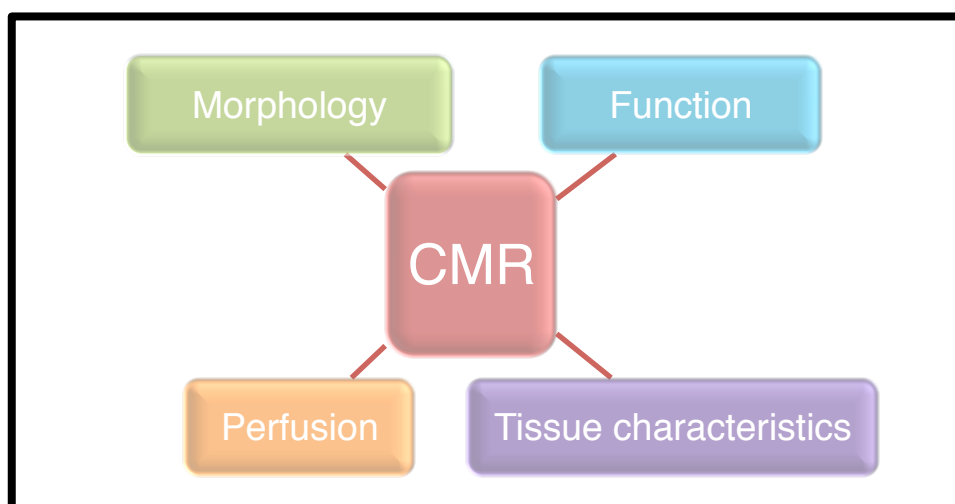


Figure 3. Due to its versatility, CMR can assess morphology, function, perfusion and tissue characteristics, making it an ideal imaging tool to evaluate the cardiac manifestations of HIV.

### **2.3.2 Technique:**

#### ***2.3.2.1 General principles:***

The effects of the virus on the myocardium were primarily assessed, and therefore functional and structural analysis and tissue characteristics were the main focus. To perform a CMR scan the patient needs to be placed in a high-strength magnetic field. A radio wave is then emitted and directed towards the patient, whose own hydrogen nuclei, which behave like minuscule spinning magnets, align parallel to the direction of the external magnetic field. These ‘magnets’ rotate or precess at a frequency proportional to the strength of the external field. If the frequency of the radio wave is identical to the precessing hydrogen nuclei, they are flipped horizontally. During their relaxation, they emit radio signals. The net longitudinal magnetisation increases with a speed defined by the T1 relaxation time, and the transverse magnetisation decreases with a speed defined by the T2 relaxation time. T1 and T2 relaxation times are tissue-specific and are related to the proton density. CMR images can be acquired (weighted) to show the distribution of tissue relaxation times (T1 and T2) or proton density. These sequences are applied to make the blood appear darker or brighter than the myocardium, generating static (dark blood or bright blood) or dynamic (cine bright-blood) images, which form the cornerstone of every study.<sup>117</sup> Although new sequences are continually being developed the basic principles of CMR remain unaltered.

#### ***2.3.2.2 Scout imaging***

Each examination starts with a series of scout views performed on each patient to establish the short- and long-axis views of the heart. These images act as localisers in planning the rest of the study. Approximately 27 scout images are required to define the thoracic contents, including 9 parallel images in each of the axial, coronal and sagittal planes.<sup>117</sup>

### ***2.3.2.3 Anatomical and morphological imaging***

To assess anatomy and morphology static images are required. Black-blood T1-weighted imaging is usually preferred because it allows a clear distinction between the inner portion of the vessel or myocardium from blood. Images can be oriented in any plane, but the main aim with black-blood T1 sequences is to obtain an overall anatomic image of the heart and its relation to the vascular structures (and therefore a larger field of view is sometimes preferred, which might include the rest of the intra-thoracic structures as well) (see figure 4). Because these are static images measurements are not derived from them and functional assessment cannot be performed with T1-weighted images.

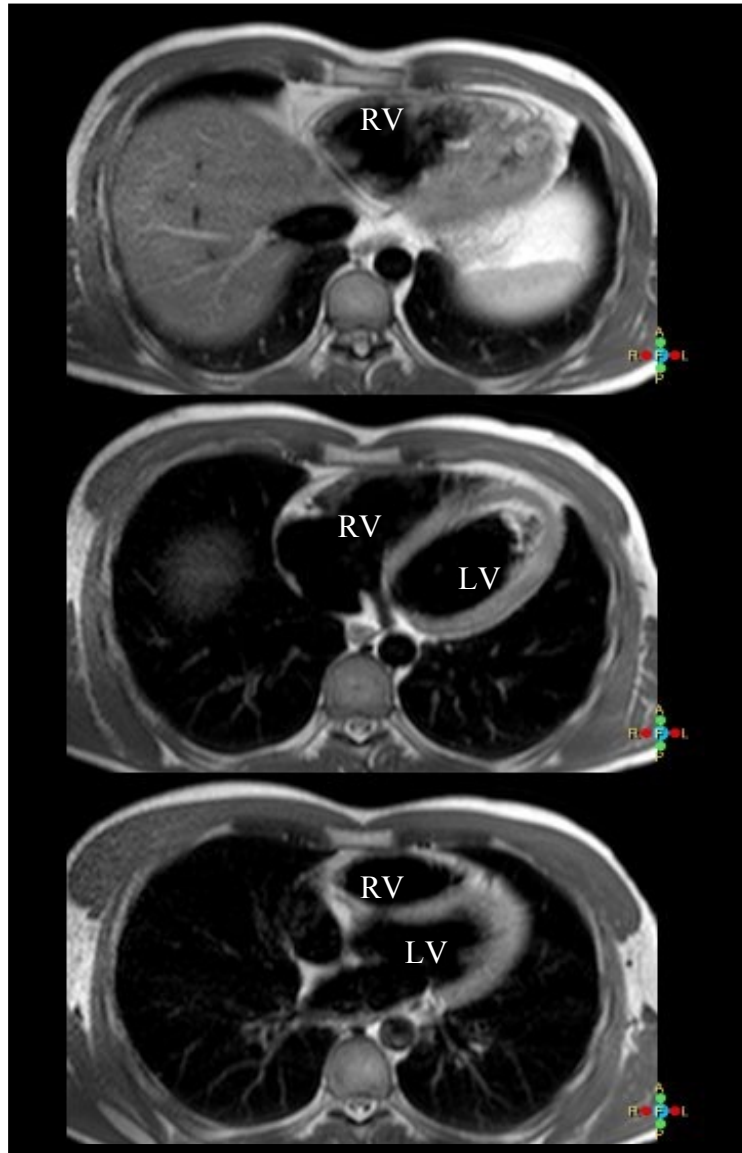


Figure 4. Three axial Black-blood T1 weighted axial images through the chest with the blood and lungs appearing dark and the normal myocardium of the LV and RV and muscular structures of the chest wall homogenous and grey. The subcutaneous fat tissue appears white. The left ventricle (LV) is situated behind the right ventricle (RV) on axial images.



#### 2.3.2.4 Functional imaging

Dynamic cine CMR (white-blood imaging) is used for global and regional LV and RV wall motion assessment, as well as ventricular volume, ejection fraction and mass measurements. For all these parameters, CMR is increasingly recognised as the gold standard when compared to echocardiography and nuclear studies<sup>11, 118-120</sup> and in providing acceptable endpoints in trials in which functional as opposed to clinical outcomes are the objectives.<sup>121</sup> Cine views are generally obtained in more than one orientation, but the functional analysis is mostly performed in the short axis plane (See Figures 5-8).

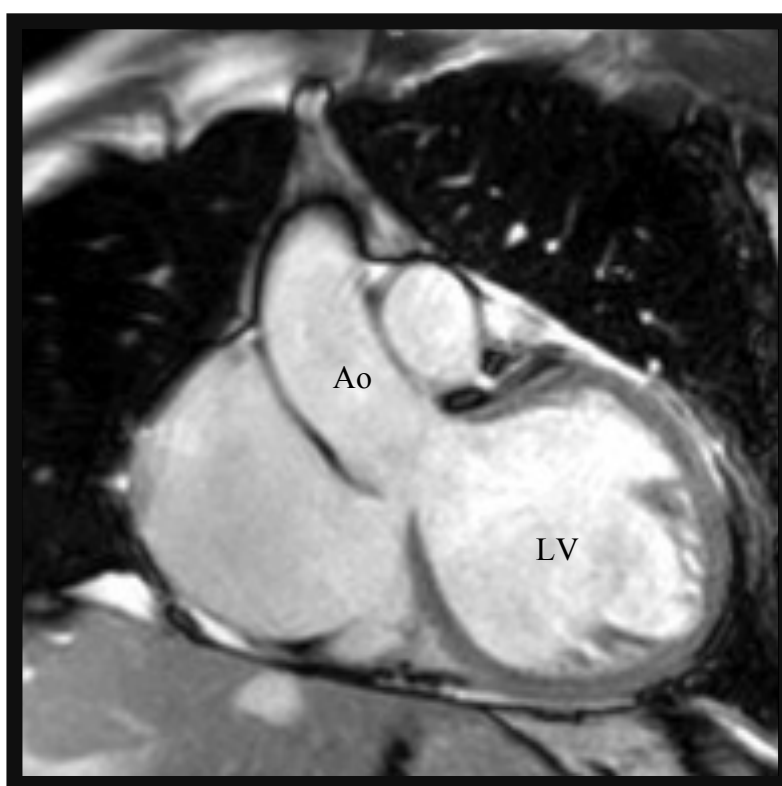


Figure 5. LV outflow tract view with the blood appearing white on the cine images and the left ventricle and the aorta (Ao) seen in a single plane.



Figure 6. Two chamber cine view with the LV and left atrium (LA) in the same plane.

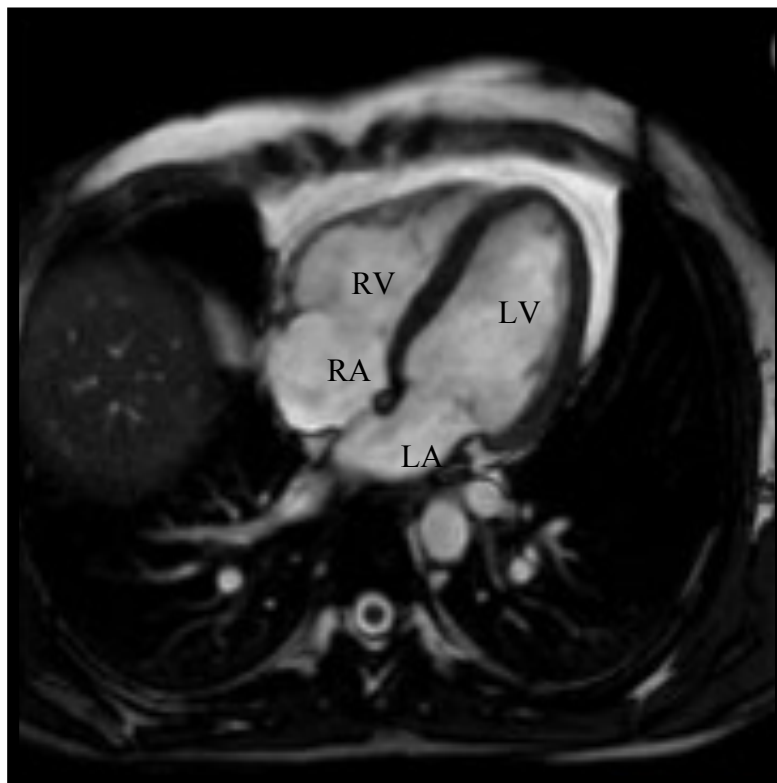


Figure 7. Four-chamber cine view with all four cardiac chambers visualised in the same plane.  
The LV and the LA lie behind the RV and the right atrium (RA) in the four-chamber plane.

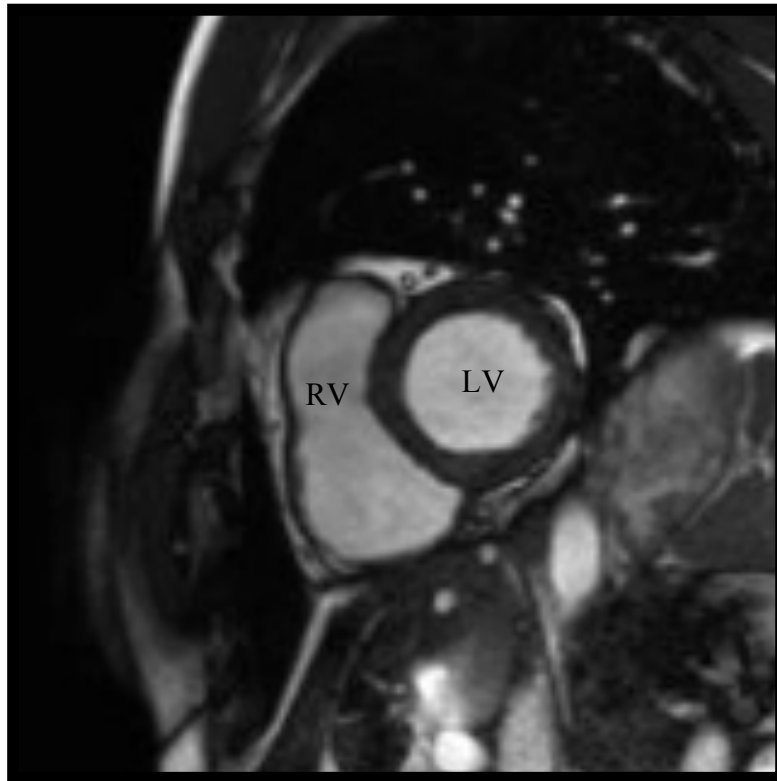


Figure 8. The short axis white blood images are used for systolic functional analysis. The LV is situated behind the RV.

#### ***2.3.2.5 Myocardial perfusion imaging***

During perfusion scanning a movie of the wash-in of gadolinium-based contrast through the myocardium is obtained (so-called “first-pass perfusion”). Perfusion defects appear as dark regions surrounded by bright contrast-enhanced, normally perfused myocardium (see Figure 9) and can be present at rest or induced during adenosine stress testing. CMR perfusion is playing an increasingly important diagnostic role in ischaemic heart disease but has a limited role in non-ischaemic cardiomyopathy.

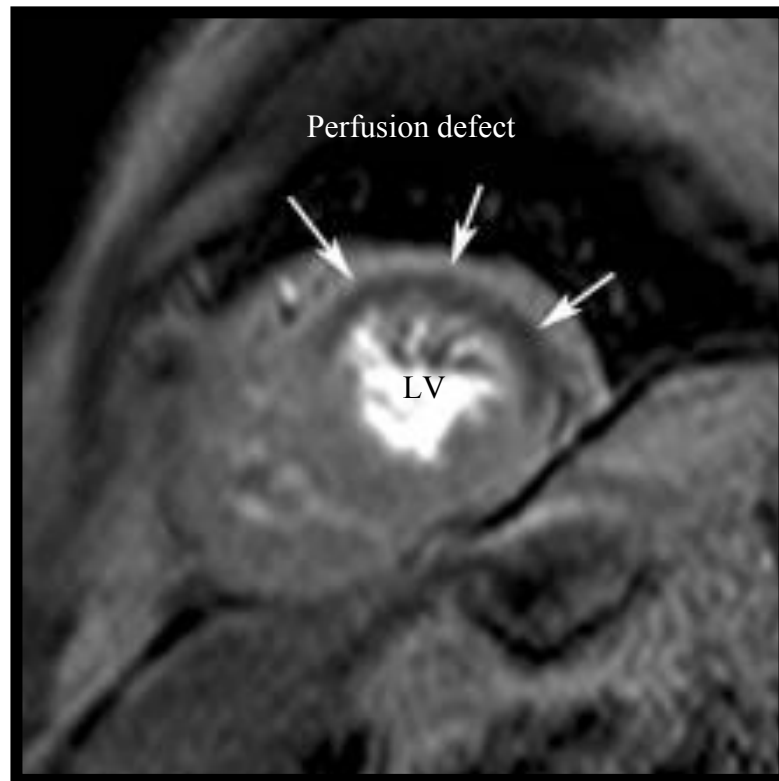


Figure 9. Short axis perfusion sequence with the perfusion defect appearing as a dark area in the antero-septal LV wall (arrows).

### ***2.3.2.6 Myocardial oedema imaging***

The water content within the tissue alters the T2 relaxation time within myocardial tissue. Myocardial oedema is, therefore, associated with prolonged T2 relaxation time. Static dark blood images of the myocardium can be obtained, confirming the presence or absence of oedema, which manifests as bright areas in contrast with the normal darker myocardium (see Figure 10). Myocardial oedema has been described in patients with acute myocardial infarction, myocarditis, stress-related cardiomyopathy, sarcoidosis and cardiac allograft rejection.

In the event of an acute myocardial infarct (AMI) myocardial oedema can be seen on T2 sequences as early as 30 minutes after the onset of ischaemia.<sup>122</sup> T2-weighted CMR imaging can help to differentiate between acute and chronic myocardial infarction.<sup>123</sup> Owing to an increase in water protons in the affected myocardium after an AMI, the T2-weighted signal increases. This lasts for many days after the

acute incident and disappears when the myocardial swelling subsides during the chronic phase. More importantly, high signal intensity on T2-weighted CMR, in the absence of LGE in the same area, reflects reversible ischaemic injury.<sup>122</sup>

There is excellent correlation between the area at risk (AAR), measured by T2-weighted imaging, and the angiographic APPROACH score, which is an anatomically and prognostically well-validated measure of the extent of myocardial jeopardy.<sup>124, 125</sup> This score indicates the size and location of the myocardial bed supplied by diseased vessels.



Figure 10. T2-oedema sequence showing an inferolateral area affected by acute myocarditis (arrow) appearing whiter than the rest of the myocardium.

Good image resolution depends on a stable and homogenous magnetic field. T2 decay (decay of transverse magnetisation) may be influenced by intrinsic defects in the magnet itself or by distortions (heterogeneity) caused by material or coils placed in the magnet.

Qualitative T2-weighted imaging performed with dark-blood turbo spin-echo sequences therefore has several limitations, including magnetic field heterogeneity from surface coil arrays, stagnant blood flow resulting in increased signal intensity (particularly along the sub-endocardium) and through-plane motion resulting in signal loss.<sup>126</sup> Optimal image quality also relies on regular heart rhythm with a ventricular rate within a relatively normal range, appropriate selection of repetition time tailored to the patient's heart rate, and the ability of the patient to breath-hold. T2W images may be rendered non-diagnostic, due to excessive tachycardia and irregular rhythms, and breathing artefact.<sup>127</sup>

Clinical use of T2W CMR for the qualitative or semi-quantitative detection of myocardial oedema and inflammation has improved since its inception. Limitations of conventional T2W techniques included the need for a normal reference region of interest, either in remote myocardium or skeletal muscle, which could lead to false-negative results when these reference areas are also affected by a systemic condition. Quantification of T2 myocardial relaxation times promises to circumvent these limitations and is achieved by collecting multiple images with different T2W imaging, thus providing multiple points along the T2 decay curve for fitting of an exponential signal.<sup>128</sup>

#### ***2.3.2.7 Early gadolinium enhancement***

Directly after gadolinium administration, in the case of vasodilatation and hyperaemia, the concentration of gadolinium increase in the affected myocardium and shows up as areas of brighter signal, in comparison to the normal surrounding myocardium. Early phase enhancement imaging is performed with a short-axis T1-weighted fast spin-echo sequence within the first 2-3 minutes after administration of contrast agent.<sup>129</sup> Contrast-enhanced T1 map values are variable and highly dependent on a) variable weight-based contrast agent dosing, b) the exact time elapsed after contrast agent administration before images are acquired, c) renal clearance of the contrast agent and d) displacement of contrast material by the haematocrit.<sup>126</sup>

Inflammation-induced hyperaemia causes increased accumulation of gadopentate dimeglumine in the myocardium during the early washout period that is indicative of myocardial inflammation or hyperaemia. Although visual identification may be possible, quantitative evaluation of myocardial early gadolinium enhancement ratio (EGEr), is helpful. EGER involves a global approach, and depending on the section orientation chosen for cardiac MR imaging, some myocardial segments may not be available for image analysis and interpretation. Respiratory motion artefacts can unfortunately also severely degrade image quality to a non-diagnostic degree. Furthermore, normalisation of the signal intensity on T1-weighted images to that of skeletal muscle may be hampered by coexisting myositis.<sup>130</sup> Early gadolinium enhancement can detect salvageable myocardium, indicating that the kinetics of gadolinium plays an important role in assessing the area at risk in relation to the imaging time.<sup>131</sup>

Myocardial hyperaemia represents another CMR marker for active inflammation in the acute stage of myocarditis, however, the usefulness beyond the acute stage is questionable. As early gadolinium enhancement imaging is time-consuming, susceptible to artefacts, and offers only sparse diagnostic value, it is infrequently performed in myocarditis.<sup>130</sup>

#### ***2.3.2.8 Late gadolinium enhancement (LGE) CMR imaging***

LGE images are acquired 10-15 minutes following gadolinium chelate contrast administration.

Gadolinium circulates in the extracellular space and is excluded by intact myocardial cell membranes. It accumulates in areas of abnormal myocardium, resulting in T1 shortening manifesting as higher signal intensity on T1-weighted images. Gadolinium can migrate through damaged myocyte membranes into the cells (e.g. in the case of myocardial infarction), or accumulates in the enlarged interstitial space (in the case of scar tissue) (Figure 11). Enhancement is therefore found in the intravascular space, in the interstitial space as well as within nonviable cells. After the initial insult, once scar formation takes place, the interstitial space increases in between a relatively small intracellular space within the fibroblasts. Both AMI and infarcted scar tissue therefore display increased enhancement in comparison

to normal myocardium. LGE plays an important diagnostic and prognostic role in patients with ischaemic heart disease.<sup>132-134</sup>

Total infarct size and scar burden can be ascertained by LGE CMR and is a strong predictor of future events in patients with coronary artery disease.<sup>135, 136</sup> The absence of contrast enhancement during the first 2 minutes after contrast injection in the centre of an area of infarction that may persist on the LGE images, points to microvascular obstruction, which is associated with a worse prognosis and outcome.<sup>137-139</sup> Gadolinium is an extracellular agent and can enter damaged myocytes, or it can accumulate in areas where the extracellular space is bigger (see figure 11).

When the cell membranes rupture the gadolinium molecules enter and accumulate in the cell. This manifests as white areas on the T1 images because it shortens the T1 time. The gadolinium also accumulates in the extracellular areas (due to scar formation) and once again manifests as white areas within the myocardium on T1-weighted sequences.

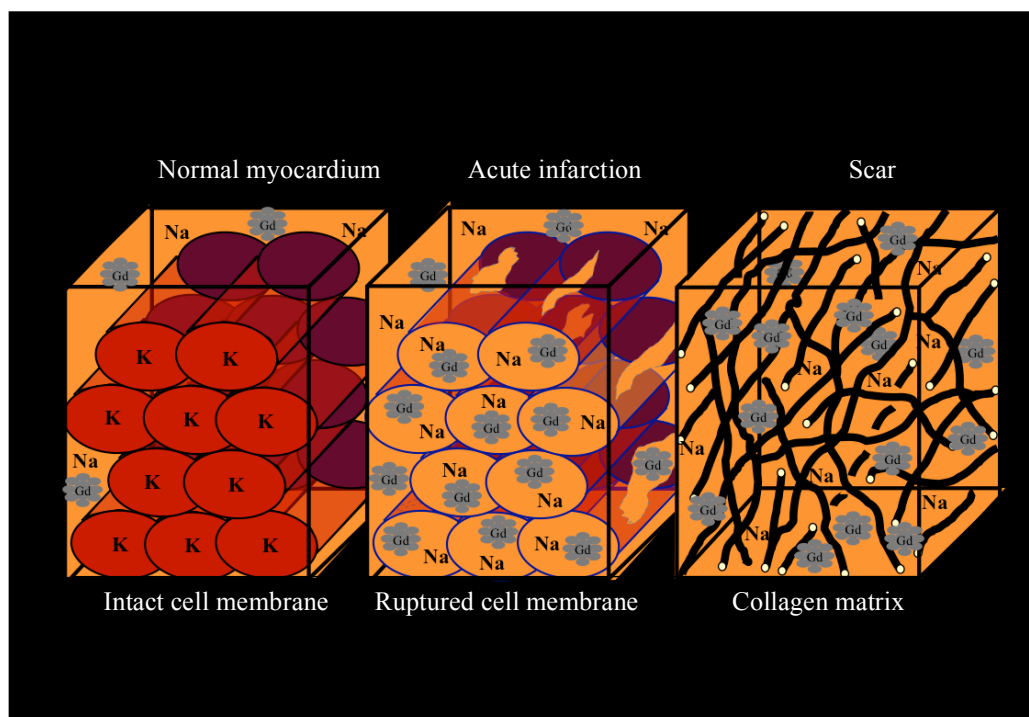


Figure 11. Potential mechanisms of hyperenhancement in acute and chronic myocardial infarction. Kim RJ, Choi KM, Judd RM, Higgins CB, de Roos A, eds. Cardiovascular MRI and MRA. Philadelphia, PA: Lippincott Williams and Wilkins; 2003: 209-237.



The presence of LGE has also been shown to be a marker for adverse outcomes in several other non ischaemic cardiomyopathies.<sup>140, 141</sup> LGE CMR can help to differentiate between ischaemic and non-ischaemic cardiomyopathy (see Figure 12).<sup>142</sup>

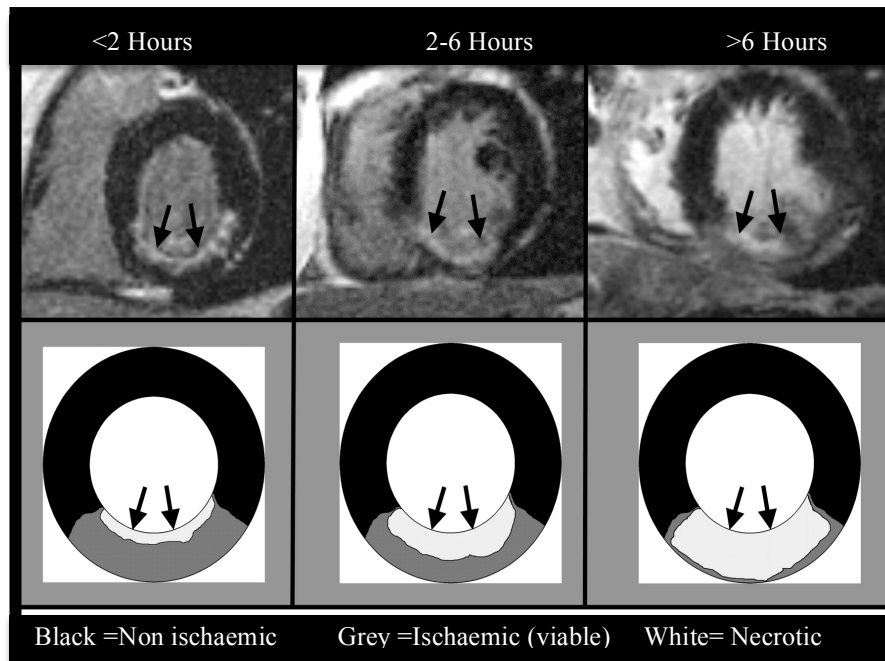


Figure 12. The typical pattern of evolving myocardial infarction secondary to acute coronary occlusion can be explained by the pathophysiology of ischaemia progressing to transmural necrosis. Little or no cellular necrosis is found until about 15 minutes after occlusion. After 15 minutes, a ‘wave-front’ of necrosis begins in the subendocardium and gradually extends towards the epicardium over the next few hours. During this period the extent of the infarcted region within the ischaemic zone increases continuously towards transmuraliity.<sup>1</sup>

Hyperenhancement patterns differ with each clinical setting and can point to the underlying cause of the myocardial involvement (see Figure 13).

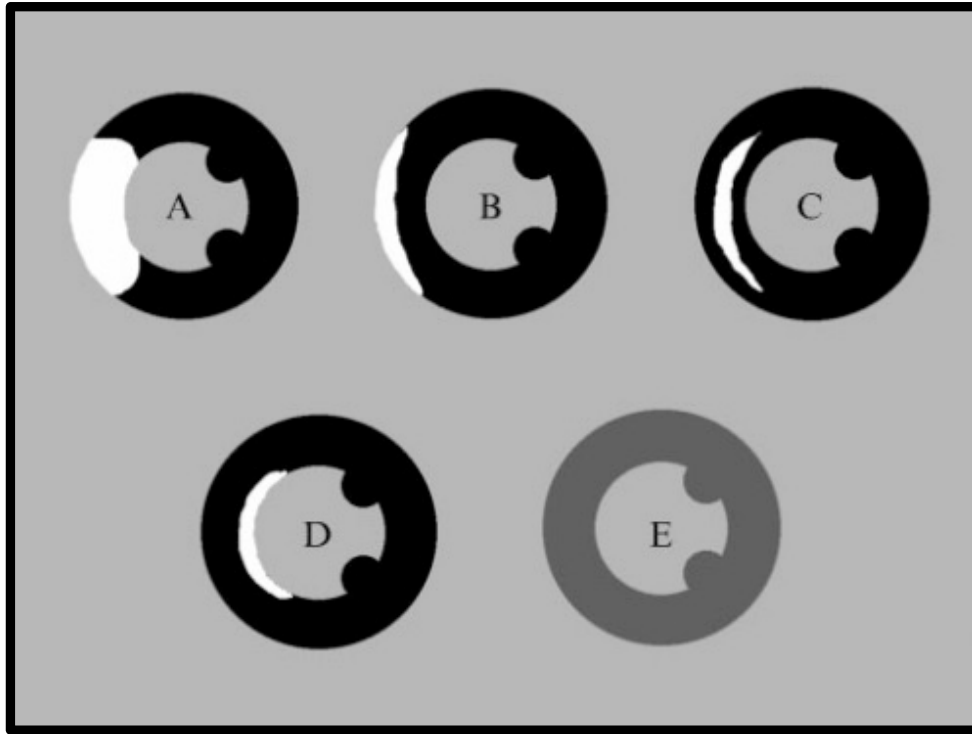


Figure 13. Patterns of late gadolinium enhancement encountered in clinical practice.<sup>143</sup>

- A. Transmural: infarct, severe myocarditis or sarcoidosis
- B. Subepicardial: myocarditis, sarcoidosis
- C. Midmyocardial: dilated cardiomyopathy, hypertrophic cardiomyopathy, pulmonary hypertension
- D. Subendocardial: infarct, amyloid, hypereosinophilic syndrome
- E. Diffuse: amyloid, hypertrophic cardiomyopathy

### 2.3.2.9 T1 mapping

T1 mapping refers to parametric maps generated from a series of images acquired with different T1 weighting so each pixel can be assigned a T1 value. T1 maps can be displayed using colour or threshold scales to enable quantitative visual interpretation. This consists of quantifying the T1 relaxation time of a tissue by using analytical expressions of image-based signal intensities. Each tissue type exhibits a characteristic range of normal T1 relaxation times at a particular field strength, and any deviation may be indicative of disease. Measured myocardial T1 values are influenced by various physiological and technical factors, including temperature, disease, age, sex, heart rate and the pulse sequence used.<sup>128</sup> All tissues have an inherent T1 (i.e. longitudinal or spin-lattice) relaxation time that is based on a composite of their cellular and interstitial components (e.g. water, protein, fat, and iron content). At a fixed magnetic field strength and in the absence of exogenous contrast agents (e.g., gadolinium chelate), the native T1 value of normal tissue falls within a predictable range (e.g., at 1.5T, normal myocardium

has a relaxation time of  $960 \pm 30$ ms).<sup>126</sup> The T1 relaxation times between different tissues vary substantially.<sup>144</sup>

Myocardial T1 mapping methods are used for native (pre-contrast) and post contrast T1 measurements. Two scientists (Look and Locker) developed the Look-Locker sequence method in 1968 where image data segments are repeatedly acquired after an inversion pulse to create multiple images along the recovery curve for fitting T1 but the Modified Look Locker Inversion (MOLLI) recovery method developed by Messroghli and colleagues in 2004<sup>145</sup> opened a new frontier of clinical applications for myocardial T1 mapping.<sup>117</sup> Newer variants based on inversion recovery, saturation-recovery, or hybrid approaches continue to emerge, enabling faster acquisition times and minimising sources of error, such as heart rate dependency, motion, off-resonance, and partial volume effects. Although MOLLI-based sequences are the most widely used and most extensively validated, newer techniques including the saturation-recovery single-shot acquisition sequence is a very promising novel approach demonstrating good T1 measurement accuracy in experimental models.

The clinical utility of native T1 mapping relies on a normal range with small variability and high sensitivity to disease. Elevated T1 times in the myocardium have been reported in a number of commonly encountered cardiac conditions including myocardial infarction, myocarditis, hypertrophic and dilated cardiomyopathy, cardiac amyloidosis, cardiac involvement in systemic diseases, and diffuse fibrosis in patients with aortic stenosis.<sup>128</sup>

Native T1 mapping techniques represent an important recent advance in the non-invasive assessment of myocardial inflammation since native myocardial T1 is prolonged by excess free water content. Post-contrast T1 mapping techniques are able to determine the expansion of interstitial space/fibrosis (extracellular volume ECV) and separate it from replacement fibrosis (such as scarred myocardium). ECV allows estimation of the extracellular matrix in quantitative terms by performing T1 mapping

before and after contrast administration, assessing the volume of distribution of gadolinium. Thus, non-ischaemic patterns of myocardial damage can be detected by T1 mapping in acute myocarditis.

Moreover, T1 mapping recently expanded current knowledge by identifying additional myocardial abnormalities in comparison to conventional LGE, since T1 values can be prolonged in apparently normal regions without any LGE.<sup>146</sup>

In a study comparing the different techniques used to assess myocardial damage the authors concluded that: a) Quantitative T1 mapping is a more robust technique compared to T2W, because T1 measurements show significantly lower variability than T2W (their acquisition is faster with a better spatial resolution), b) Non-contrast T1-mapping detects acutely injured myocardium accurately in MI patients when compared to T2W and LGE as markers of acute injury, c) The diagnostic performance of T1 mapping is at least as good as that of T2W-CMR for detecting acute myocardial injury, d) Non-contrast T1-mapping allows assessment of the extent of acute myocardial damage with similar results compared to T2W and e) T1 values are strongly related to the likelihood of functional improvement at 6 months.<sup>131</sup> The T1 value can be obtained manually by drawing a region of interest in the central portion of the LV ventricular wall, usually the septum (see Figure 14), or it can be obtained by using dedicated software that draws the endo- and epicardial borders automatically (and these can then be corrected manually).

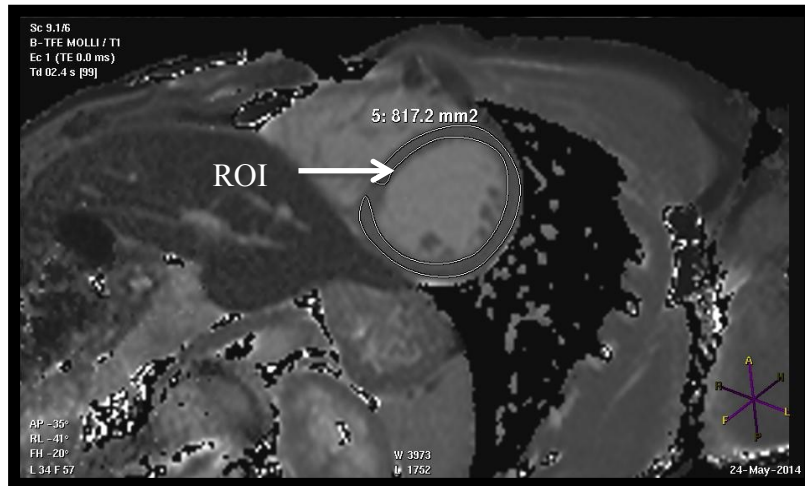


Figure 14. T1-mapping image with a region of interest (ROI) drawn manually depicting the native T1 time.

## 2.4 Cardiac remodelling

### 2.4.1 Introduction

Cardiac remodelling or plasticity is the process of adaptation of the heart during and after it has been exposed to an insult, a disease process or an increase in haemodynamic demand. Cardiac remodelling plays an important role in the clinical course of heart failure and its prognosis.<sup>147</sup> Remodelling is a complex process involving myocyte necrosis, apoptosis, vascular rarefaction, fibrosis, inflammation and electrophysiological remodelling.<sup>148, 149</sup> During the remodelling process the heart undergoes alteration in structure as well as function. This process of remodelling can result in hypertrophy (concentric or asymmetrical) or atrophy.<sup>150</sup> Remodelling can be described as physiological or pathologic, but can also be considered as adaptive or maladaptive.<sup>151</sup>

Physiological remodelling occurs during strenuous exercise (known as “athlete’s heart”) or during pregnancy when the haemodynamic demand increases. This manifests as LV hypertrophy, usually causing an increase in LV mass and chamber size.<sup>152</sup>

When pathological myocardial hypertrophy occurs, three patterns are recognised (see Figure 15):

- a. Pressure overload causes concentric hypertrophy, and this happens in patients with aortic stenosis or hypertension as an inherent myocyte coping mechanism resulting in myocyte

thickening.<sup>153</sup> This hypertrophy is possible because of an increase in protein synthesis in the individual cardiomyocytes. They respond to reduce the amount of stress on the LV wall in an effort to maintain stroke volume.<sup>154</sup>

The LaPlace Law of LV wall stress states that LV Wall stress =  $P \times R/2 \times$  LV wall thickness (where P=pressure and R=radius).

- b. Volume overload, (e.g. in valve regurgitation) or exercise leads to eccentric hypertrophy. This kind of remodelling is characterised by hypertrophy as well as cardiac chamber enlargement. This adaption process takes place to maintain forward flow.
- c. Mixed concentric and eccentric hypertrophy is encountered in patients after myocardial infarction, myocarditis or cardiomyopathies.

In all the above, remodelling may transition from an apparently compensatory process to a maladaptive state.<sup>149, 155</sup> In addition to hypertrophy, a decrease in cardiac mass (atrophy) can occur in conditions of weightlessness, bed rest and other states of ventricular unloading or assistance.<sup>156</sup>

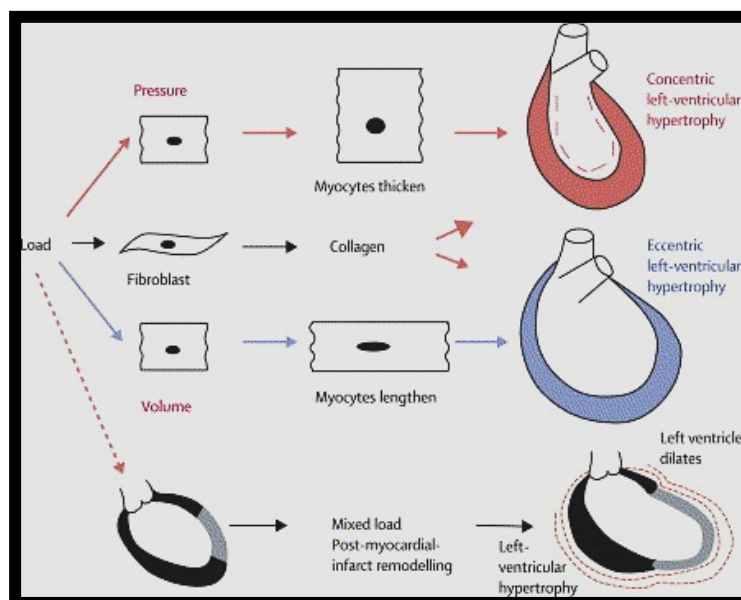


Fig 15. Three patterns of cardiac remodelling due to myocardial hypertrophy.<sup>155</sup>

All the causes and manifestations of cardiac remodelling or plasticity share common molecular, biochemical and mechanical pathways.<sup>148</sup> The cardiomyocyte forms the cornerstone in the remodelling process, but fibroblasts, collagen as well as the cardiac vasculature contributes to the process. During remodelling the heart changes in shape and size. This usually results in a change in mass as well as an alteration in the functional parameters. The initial compensatory response manifesting as remodelling may progress towards cardiac failure. This depends largely on the severity of the initial insult. Patients who develop cardiac failure may have decreased systolic function but approximately 50% of patients with heart failure have preserved ejection fraction (HFpEF).<sup>149</sup> Patients with marked remodelling have worse outcomes.<sup>147</sup> During the remodelling process a number of changes are thought to occur on the cellular and biochemical level although most of them are not completely understood as yet.

Myocytes may undergo hypertrophy, necrosis or apoptosis. Fibroblast proliferation develops<sup>150, 157</sup> with an increase in the extracellular matrix, which eventually leads to fibrosis. Myocardial fibrosis is associated with contractile dysfunction and an increase in arrhythmias as well as sudden death.<sup>148</sup> During the process of remodelling angiotensin II, norepinephrine, endothelin, aldosterone and cytokine levels increase, all of which play a part in the process of remodelling.<sup>148, 150</sup>

The result of pathologic remodelling is eventual deterioration in cardiac performance and increased neurohormonal activation. Compensatory hypertrophy *per se* may lead to an increase in wall stress which may precipitate further imbalance resulting in a vicious cycle of energy imbalance and ischaemia.<sup>158</sup> If remodelling progresses beyond a certain phase, maladaptation occurs resulting in the deterioration of cardiac failure.

#### **2.4.2 HIV and cardiac remodelling**

As discussed above the aetiology and mechanisms of development of HIV-associated cardiomyopathy are complex and multifactorial. These include damage to the myocytes, impairment of macrophage

activity as well as mitochondrial damage and vascular insufficiency, all resulting in cardiac remodelling. CMR is the ideal tool to assess remodelling as it can demonstrate the effects of several distinct pathophysiological pathways. These include oedema (which can be visualised on T2-weighted sequences) and inflammation (causing abnormal native T1 and T2 times), resulting in functional impairment (systolic and diastolic) and ventricular dilatation, which can be quantified more accurately with CMR than with any other modality.

Furthermore, subtle subclinical early abnormalities which could be a harbinger or manifestation of remodelling include abnormal diastolic strain patterns which can be assessed adequately with CMR. Early myocyte necrosis or apoptosis, as well as mild oedema and diffuse inflammation caused by HIV infection, can also be assessed with CMR.

This study was designed to evaluate, visualise and quantify the different aspects involved in the process and to assess the functional impairment as a result of cardiac remodelling due to HIV.



## Chapter 3: Materials and Methods

### 3.1 Study population

Three HIV uninfected volunteers were entered into a pilot study before commencing with the actual study. This was done in order to ascertain whether the parameters and study criteria could be met. Because the post-processing and analysis were done after the study was completed, and to avoid rejection due to poor image quality, CMR artefacts or patient movement, 77 patients in total (more than the statistical requirement-see below) were included (40 HIV infected participants and 37 HIV uninfected controls).

HIV infected patients who were potentially suitable for inclusion into the study (n=40) were selected at the HIV/AIDS clinic at The Steve Biko Academic hospital (see inclusion and exclusion criteria below). The HIV infected patients were newly diagnosed patients, and the scans were performed immediately before they were initiated on ART. All the patients were without any cardiac symptoms and signs. These patients were at least 18 years old and WHO class 2 and 3 criteria for HIV. The control group (n=37) included healthy volunteers from The Steve Biko Hospital and the Montana Private Hospital (health care workers). The groups were matched for age, sex and ethnicity. The HIV negative status of the control group of patients was confirmed with laboratory tests (blood samples were collected for the presence of HIV).

Each patient was given a number at The Steve Biko Academic hospital and patient clinical information was not provided to the radiographers performing the scans. Only the principal investigator held the key to the patient numbering code as well as the controls.

Group 1. HIV infected:

Inclusion criteria:

- a) HIV infected patients who were treatment naive
- b) Age > 18 years old
- c) The patients did not have any cardiac symptoms or signs
- d) Class 2 and 3 HIV infection according to the WHO criteria

Exclusion criteria:

- a) Intravenous drug users
- b) Patients with impaired renal function (glomerular filtration rate <60ml/min/1.73m<sup>2</sup>)
- c) Patients suffering from claustrophobia
- d) The standard contraindications for MRI scanning including metallic implants (non-MR conditional pacemakers, ICDs, older metallic valves and aneurysm coils)
- e) Uncontrolled atrial or ventricular tachyarrhythmias
- f) Signs of active pulmonary tuberculosis on chest X-ray
- g) Patients younger than 18 years and older than 60 years
- h) All cases of heart failure were excluded as well as overt cardiomegaly on chest x-ray
- i) The patients underwent a clinical evaluation prior to the CMR and any patient suffering from possible cardiovascular impairment were excluded
- j) Any patient with a history of cardiac disease (cardiomyopathy, valvular or congenital) were excluded

A resting standard ECG, echocardiography and chest X-ray were performed. NT-proBNP levels (as a measure of ventricular LV wall stress), plasma HIV viremia load (copies/ml) and mean CD4<sup>+</sup> cell count (cells/uL) were obtained. Body surface area (BSA) was calculated on all patients and the estimated glomerular filtration rate that was determined according to the Cockcroft-Gault formula on all patients (including the healthy volunteers) before the CMR.

Group 2. Healthy controls:

The healthy control group included healthy staff members matched for age, sex and ethnicity recruited from The Steve Biko Hospital and Montana Private Hospital. They were asked to undergo CMR with gadolinium contrast injection. They all underwent HIV laboratory tests (blood sampling to verify their HIV status) and confirmation obtained that they were not HIV infected. Renal function was determined before the CMR scan, and volunteers with impaired kidney function were withdrawn from the study and did not undergo the MRI scan.

## **3.2 Design and procedure**

### **3.2.1 General**

The study design was a cross-sectional study.

A standard emergency crash cart was immediately at hand in the unit. CMR studies were performed with a 1.5-Tesla whole-body clinical magnetic resonance 16 channel scanner (Achieva, Philips Medical Systems, Best, The Netherlands), and a cardiac 5-element phased-array receiver coil (SENSE coil).

Heart rate and oxygen saturation were monitored noninvasively during the examination. The two groups of patients underwent a CMR scan using the same parameters.

The patients were positioned in the MRI scanner in a supine position and with a cranial presentation.

The right cubital vein was cannulated with a 22 gauge blue Jelco cannula where after it was flushed with a 10cc syringe, filled with normal 0.9% saline solution supplied by Kendon Medical Supplies TVL (Pty) Ltd. A Y-connector tube, also filled with saline solution, was then connected to the cannula and an injector.

After completion of the scout images and precontrast images, 50% of a bolus of gadolinium (Gadodiamide 0.2 mmol/kg) was injected, followed by a 10 ml saline flush (3 - 7 ml/sec). The postcontrast perfusion sequences were performed. After that, the rest of the gadolinium was given as a

bolus and flushed with 10 ml of saline. Gadodiamide is registered as Omniscan and distributed by General Electric. The intravenous cannula was only removed once the study was completely finished.

The CMR procedure included the following sequences:

### 3.2.2 Scout images

Axial, coronal and sagittal scans, were obtained to localise and plan the rest of the study. Balanced turbo field echo sequences (BTFE), of 10 mm slice thickness were used for the scout images (see Figures 16-18).

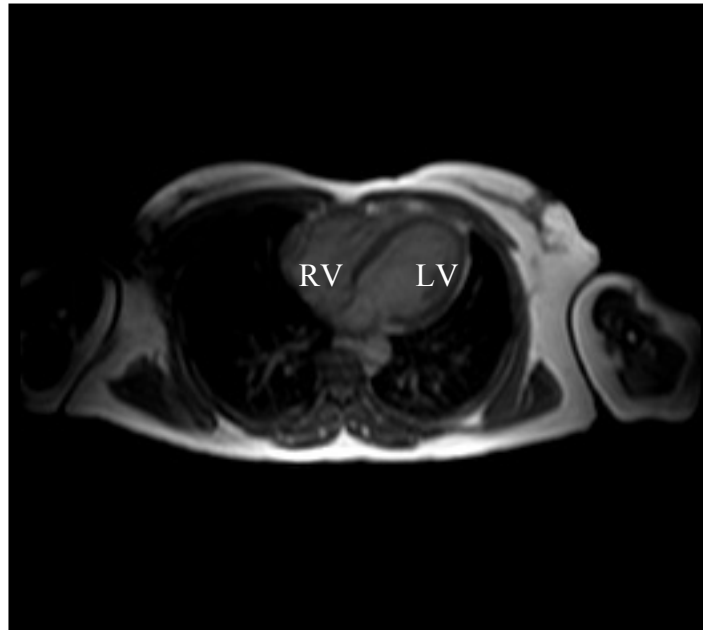


Figure 16. Axial scout image with the RV and LV on the same plane.

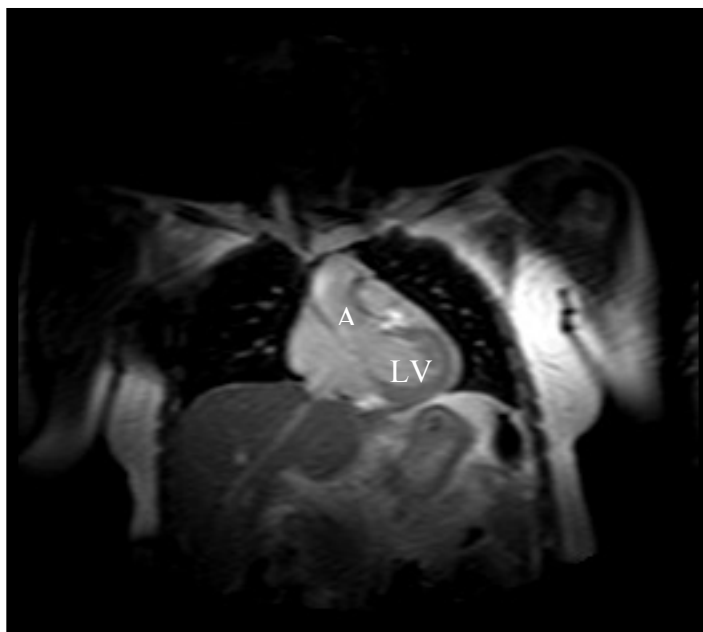


Figure 17. Coronal scout image with the LV and aorta on the same plane.

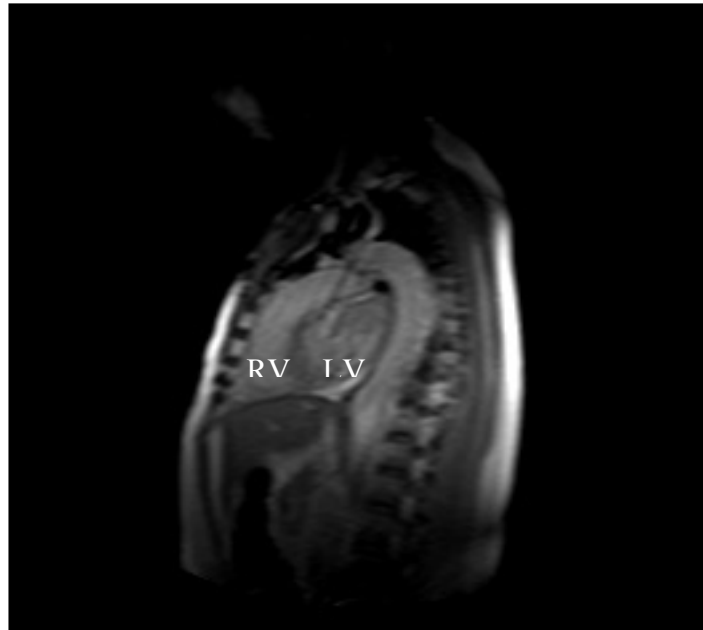


Figure 18. Sagittal scout image with the RV) in front of the LV.

### 3.2.3 Functional analysis sequences

The method to evaluate the functional status of the LV was a 2D BTFE sequence acquisition performed in 2 long axes (2- and 4-chamber view) orientations and in a contiguous short axis orientation to cover the LV from the base to the apex, with 8mm thick slices and 2mm gaps. This was done in end-expiration breath-hold, and this stack was used for the functional analysis, volume and mass assessments (see Figure 19).

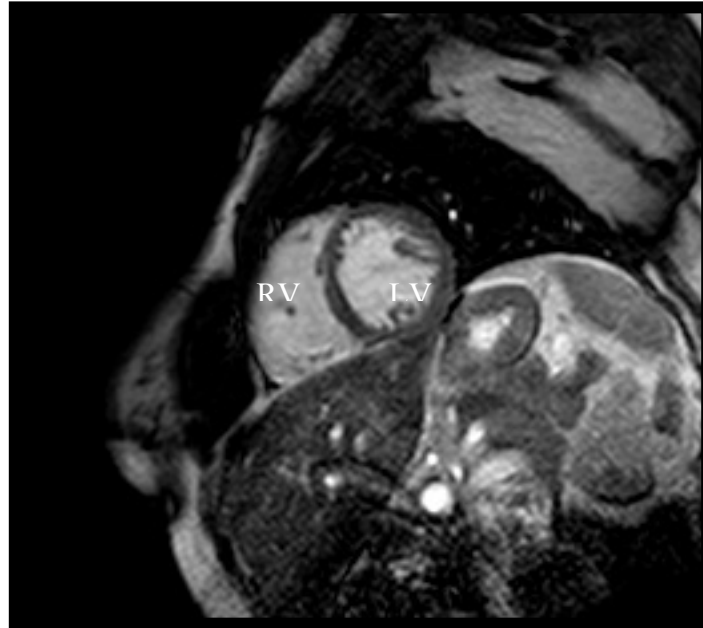


Figure 19. Short axis white blood cine images were used to perform the functional analysis, mass and volume assessments.

To assess diastolic strain patterns, tissue tracking was performed using the software module included with the dedicated software package named CVI<sup>42</sup> developed by Circle Cardiovascular Imaging, Calgary Canada. Tissue tracking used the same short-axis cine images and contours used during the systolic functional analysis.

### **3.2.4 T2 Oedema imaging sequence**

T2 weighted black blood turbo spin echo (T2 BB TSE) sequence was used to perform this. The imaging planes included a two-chamber long axis view, a four-chamber long axis view and three representative short axis slices from the apex to the base of the heart. The readout was obtained in mid-diastole (Figure 20).

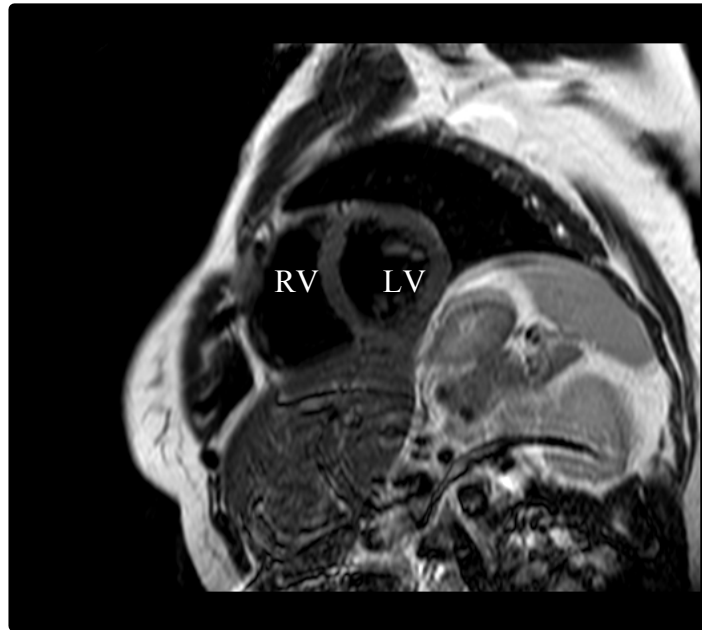


Figure 20. T2 weighted turbo spin echo short axis image. The blood pool appears black, surrounded by the myocardium.

### 3.2.5 Perfusion sequence

To assess rest perfusion a saturation-recovery imaging sequence with balanced turbo field echo pulse technique (sBTfE) was used (see Figure 21). Three short axis image slices with a slice thickness of 8 mm. each were acquired. Gadolinium was injected, (dose of 0.2 mmol/kg, 3 -7 ml/s) followed by 10 ml saline solution flush (3 - 7 ml/sec); where after imaging for 40 - 50 heart beats took place, (allowing for the gadolinium to pass through the LV myocardium) (see exact methodology in 3.2.1 above). During the acquisition there was continuous ECG monitoring. When contrast was visible in the ventricle a breath-hold command was given. Imaging lasted for 40 - 50 heartbeats until contrast had passed through the LV myocardium (after the first pass perfusion the patient was encouraged to breathe gently, if they could not hold their breath).



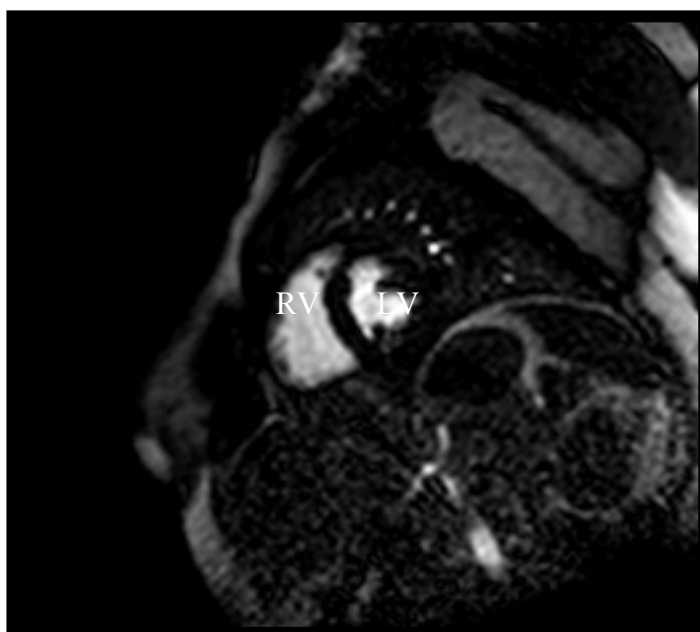


Figure 21. Short axis image during early perfusion with the contrast still in the LV and RV cavities and appearing white before perfusing the myocardial muscle.

### 3.2.6 Sequences performed for detection of hyperaemia, fibrosis, inflammation or infiltration

Two methods to detect fibrosis or infiltration were employed. The first was based on a gadolinium enhancement technique more focused on detecting focal fibrosis or infiltration, and the second upon a T1 mapping technique, more focused on identifying diffuse fibrosis, inflammation or infiltration.

During diastole, a three-dimensional (3D) T1 based segmented inversion recovery (IR) gradient echo (GRE) sequence was acquired in the short axis (SA), as well as the four chamber planes. The presence of contrast was optimised by employing a phase sensitive inversion recovery (PSIR) technique (see Figures 22 and 23). This technique is independent of TI and therefore more robust as it incorporates reference slices, which are used to correct the phase polarity of the slices at inversion time (TI), restoring TI contrast. The readout was done every other heartbeat but was modified to every heartbeat in the setting of bradycardia, and every third heart beat in the setting of tachycardia or arrhythmia. These postcontrast images were obtained directly after contrast administration (to assess hyperaemia) as well as approximately 10 minutes following contrast administration to assess late enhancement indicative of fibrosis. Before the late enhancement sequences an additional Look-Locker sequence was performed to

estimate the optimal inversion time to achieve myocardial signal nulling.

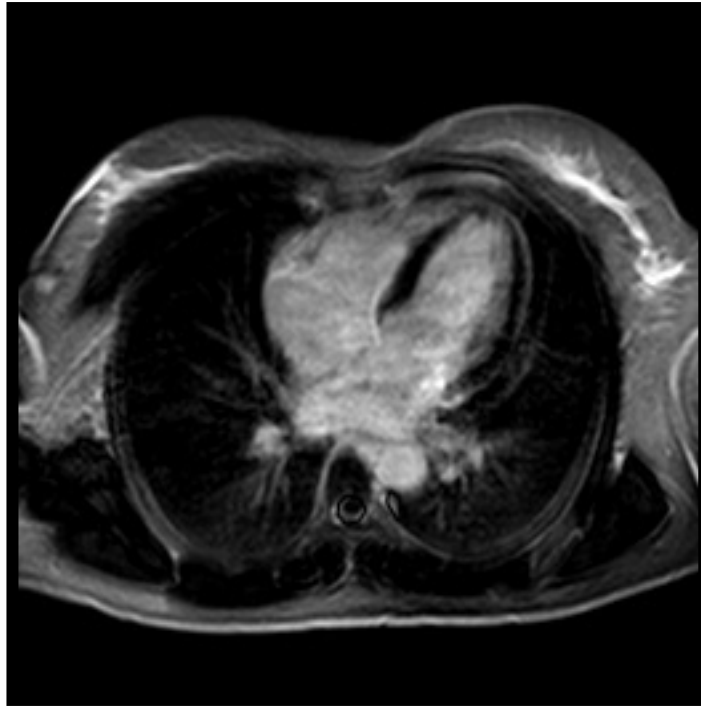


Figure 22. Four chamber PSIR LGE image with the myocardium appearing black due to effective “nulling”. Contrast enhancement would stand out as white patches.

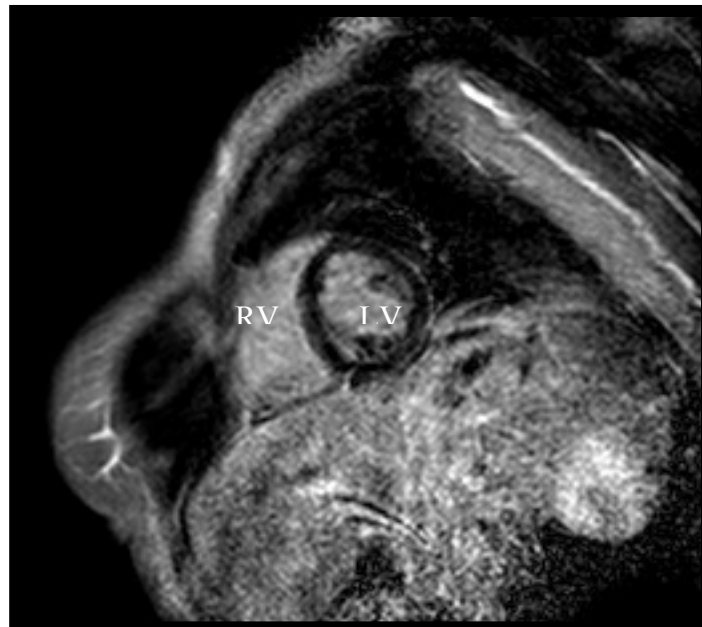


Figure 23. PSIR LGE short axis image also with the myocardium appearing black.

To detect diffuse fibrosis, an additional MOLLI sequence technique was performed both pre and post

contrast administration to obtain the T1 mapping time, in order to establish if there was diffuse fibrosis/inflammation/infiltration present (see MOLLI technique page 36). Total CMR procedure time was approximately 60 minutes. All the techniques described above (see summary in Table 2) adhered to the standardised CMR sequences, as drawn up by the Society for Cardiovascular Magnetic Resonance: Board of Trustees Task Force on Standardized Protocols.<sup>117</sup>

Table 2. Summary of the sequences performed

Description	Scout	Functional analysis	T2 oedema imaging	Perfusion	LGE	T1 mapping	Tagging
Sequence name	BTFE (balanced gradient echo)	BTFE	T2W BB TSE (black blood turbo spin echo)	sBTFE	3D IR TFE PSIR (inversion recovery turbo field echo)	MOLLI	FFE (gradient recalled echo)
Coil	Sense cardiac coil	Sense cardiac coil	Body coil	Sense cardiac coil	Sense cardiac coil	Sense cardiac coil	Sense cardiac coil
Planes	Axial Coronal Sagittal	2Ch-LA 4Ch-LA SA ( analysis)	2Ch-LA 4Ch-LA Three SA slices	SA	SA 4CH	SA 4Ch-LA	2Ch-LA 4Ch-LA SA (analysis)
Scan coverage	20 per plane	Cont. Base- apex	10 slices	Three slices	20 slices (5mm)	7 slices	Single plane +3 SA planes
Fat saturation	No	No	No	No	No	No	No
TR time	2.1ms	2.6ms	1846ms	2.3ms	5.1ms	2.1	30
TE time	0.82	1.32ms	80ms	1.14ms	2.5ms	1.1	4.98
FOV	450x450	320x320x118	320x320x8	350x350x44	320x320x100	340x255	
Matrix	192x96	160x144	228x170	116x115	176x172	192x138	176 x 141
Slice thickness	10mm	8mm	6mm	8mm	5mm	8mm	8mm
Interslice gap	2-4mm	2mm	0.8mm	0	0	0	0
Flip angle	50 degrees	60 degrees	90 degrees	50 degrees	15 degrees	35 degrees	13
Breathhold	No	End expiration	Yes	Yes	Yes	Yes	Yes
Other instruction			Readout-mid diastole		IR time set to null myocardium	Parallel imaging	

### 3.3 Post-processing analysis

#### 3.3.1 General

A blinded, experienced biomedical engineer and cardiologist performed the post-processing analysis, utilising a dedicated software package, CVI<sup>42</sup> (Circle Cardiovascular Imaging Inc.). The patient names and HIV status were not visible and a random participant identifying number was allocated to each participant.

#### 3.3.2 Functional analysis

The short axis images were evaluated with computer-aided analysis packages for planimetry of LV endocardial and epicardial borders at end-diastole and end-systole (See Figures 24a and 25a). The long axis four-chamber views were used to visualise and confirm possible areas of hypokinesia assessed via the short-axis views, as well as to cross-reference the plane of the mitral valve with the short-axis views, to improve the accuracy of the functional analysis (see Figures 24b and 25b).

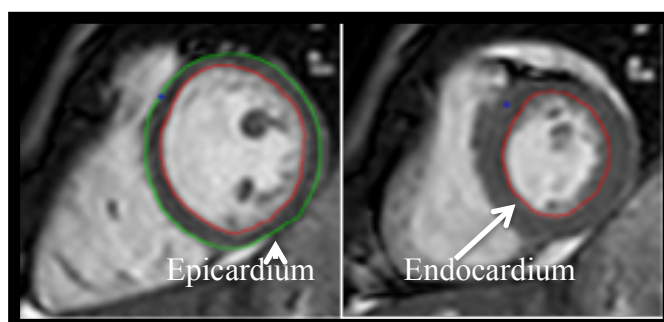


Figure 24a. Short axis images with planimetry of the endo- and epicardial borders. The endocardial line in red and the epicardium traced in green.

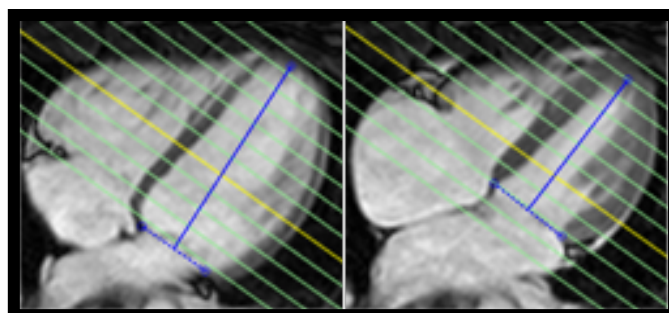


Figure 24b. Four chamber orientation to indicate the levels of the short axis images as seen in Figure 24a during diastole and systole. The yellow lines indicate the level of the prior images.

Papillary muscles were excluded in the LV mass analysis (selectable option). Computer-aided analysis included LV ejection fraction (LVEF) as a percentage, LV end systolic volume (ESV) in millilitres, LV end diastolic volume (EDV) in millilitres, stroke volume (SV) in millilitres and LV mass in grams. The LV parameters were then indexed to body surface area. The LV mass index (LVMI) = LV mass (g) divided by the body surface area. The LV end diastolic volume index (LVEDVI) = LV end diastolic volume divided by the BSA. The LV end-systolic volume index (LVESI) = LV end systolic volume divided by the BSA.

LV remodelling manifesting as hypokinesia, increased end-systolic and/or end-diastolic volumes, as well as an increase or decrease in LV mass was assessed and findings compared between the groups. Remodelling was also additionally indirectly assessed according to the ratio of LVM/LVEDV<sup>159, 160</sup> and this measurement has been associated with an increased risk and worse outcome in patients with cardiac disease. The dedicated software performed the planimetry of the endocardial and epicardial borders automatically (see Figures 25a and 25b) and the papillary muscles were excluded automatically (selectable option). The lines could be adjusted manually if necessary.

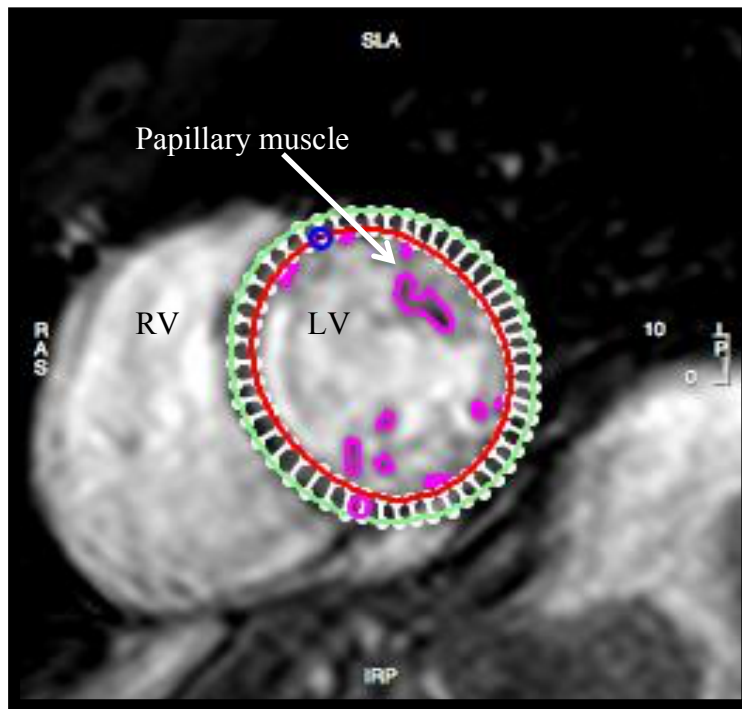


Figure 25a. The short-axis views were utilised to perform the functional analysis with dedicated software. Papillary muscles were excluded in the calculations. The endocardium once again traced with a red line and the epicardium with a green line. The papillary muscles were traced with a pink line.

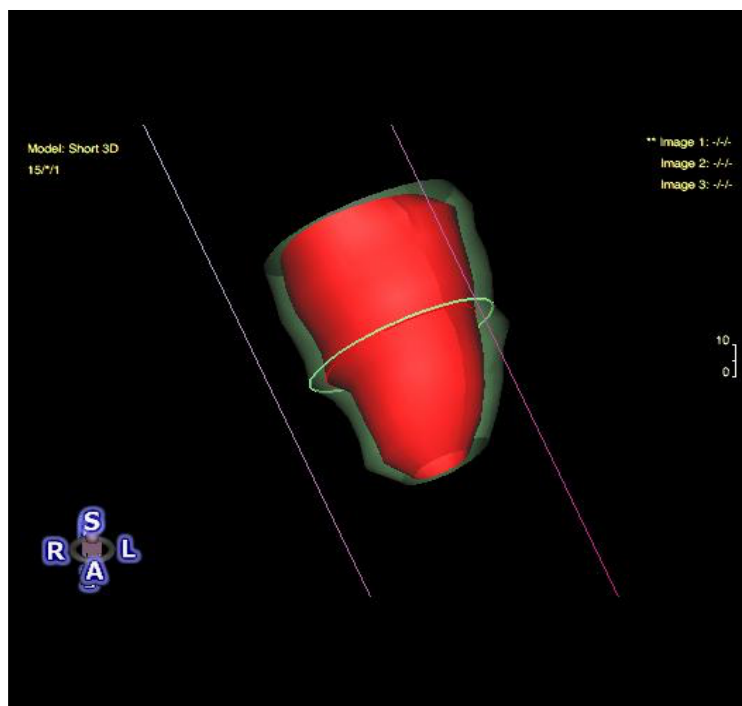


Figure 25b. Three-dimensional image indicating the level of the short axis image obtained in Figure 25a.

### 3.3.3 Oedema

The presence/absence of oedema was documented using the 17-segment AHA model, (see Figure 31). T2-weighted short axis images were evaluated for oedema using computer-aided analysis (see Figure 26). LV epicardial and endocardial borders and a region of interest (ROI) in isolated skeletal muscle were drawn for each slice (see Figure 26). Care was taken to avoid papillary muscles and blood pool near the endocardial border because the blood pool values and papillary muscles could influence the oedema score. An overlay showing a visual representation of the T2 signal intensity ratio (SIR) can be seen in Figure 26. The ratio between the signal in the myocardial and skeletal muscle ROIs, was then used to draw a reference ROI in healthy tissue. An algorithm (mean + 2SD) of the reference ROI was then used to quantify the degree of oedema.

The degree of oedema was graded and scored from 0 to 4 for each segment according to the following:

0 = no oedema present

1 = 1-25% density

2 = 26-50% density

3 = 51-75% density

4 = 76-100% density

A total score was calculated by adding up all the individual scores for each of the segments. The signal intensity ratio (SIR) between the myocardial and skeletal muscle contours was used to give an overall assessment of the presence of oedema (see Figure 26).



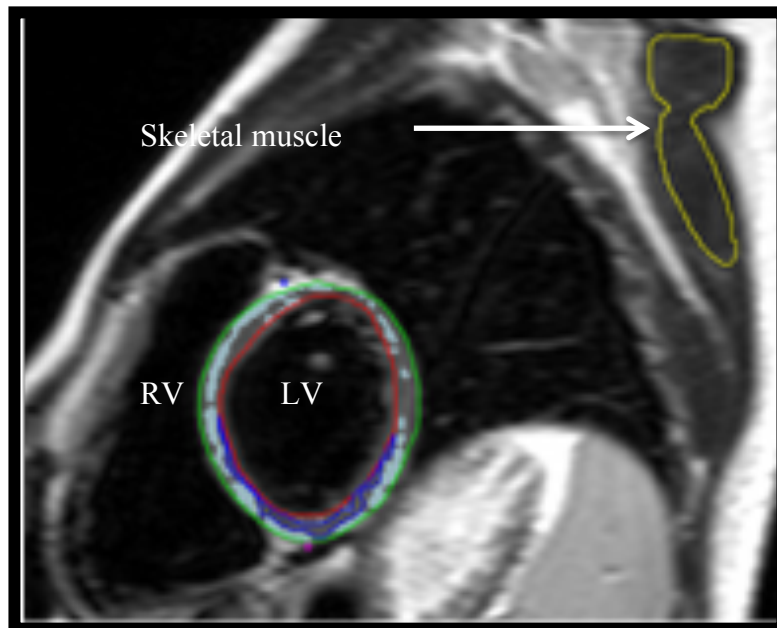


Figure 26. T2-weighted short axis images were evaluated for oedema using computer-aided analysis. The areas of oedema were colour coded according to its signal intensity.

### 3.3.4 Perfusion

Abnormal perfusion indicating underlying vascular insufficiency or impaired blood flow, which can be at a vascular or microvascular level, manifests as dark areas between normally perfused myocardium. The findings were documented using the 17-segment AHA segment model (see Figure 31).

### 3.3.5 Hyperaemia (early enhancement)

The presence/absence of hyperaemia was documented using the 17-segment AHA model, (see Figure 31). A total score was calculated by adding up all the individual scores for each of the segments. The presence/absence of hyperaemia was documented assessing the immediate post-contrast images and scores from 0 to 1 on the 17-segment AHA model.

### 3.3.6 Analysis of late gadolinium enhancement was done as follows

Visual interpretation using an AHA 17-segment model was used, and each segment received a score from 0 to 4. The papillary muscles were excluded. The inversion time was set to null the normal myocardium, and the value calculated from the Look-Locker sequence. Normal myocardium appears

dark. Fibrosis, scar tissue or infiltration by abnormal tissue shows up as areas of brightness (increased signal) between normal darker myocardium.

Phase-sensitive inversion recovery (PSIR) late gadolinium enhancement images were used to perform the analysis on. LV epicardial and endocardial borders were drawn on each slice taking care not to include papillary muscles and blood pool in the endocardial border. A reference ROI was drawn over normal appearing myocardium in each slice where after an algorithm (mean + 3SD) of the reference ROI was applied to quantify the extent of the late gadolinium enhancement.

Three parameters were assessed and the totals of all the segments added up namely:

The presence of late gadolinium enhancement (score 0-4):

0 = no late enhancement

1 = 1-25% density

2 = 26-50% density

3 = 51-75% density

4 = 76-100% density

Whether the late gadolinium enhancement was transmural or not was also categorised as a dichotomous variable (score 0-1).

Finally, the volume of the enhanced areas was calculated and summated up for all the segments individually. The volume was given in millilitres as a percentage of the total area of myocardium (see Figure 27).

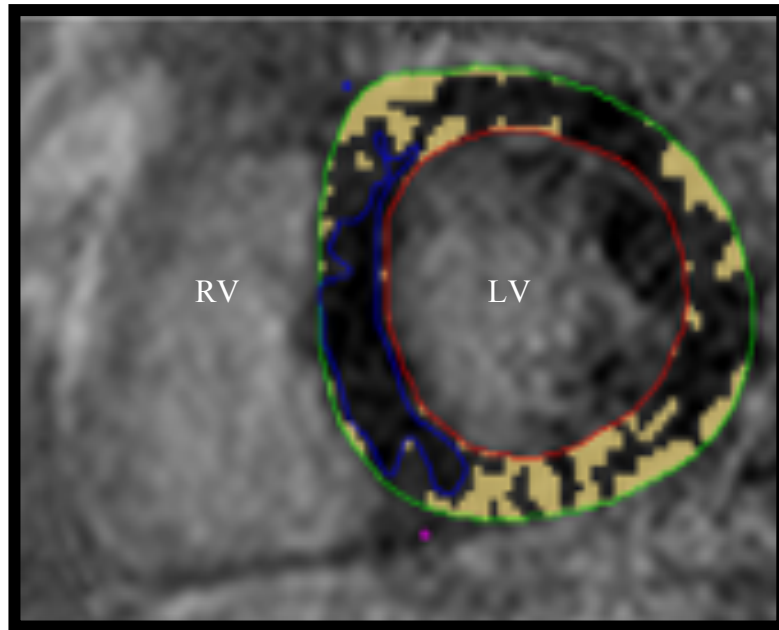


Figure 27: Intensity of LGE in the LV myocardium (colour coded in yellow).

### 3.3.7 Quantifying fibrosis using LGE and T1 mapping

The native and post-contrast T1 mapping sequences (MOLLI) were used for this measurement.

Quantitative analysis for T1 values was performed with the same dedicated software. The program automatically derived myocardial contours (see Figure 28). Contours could then be manually adjusted to ensure only myocardium was included in the analysis. Endocardial, epicardial and blood pool contours were drawn on the mid-short axis slice for each patient. T1 times, in milliseconds, were given for the whole contour in the native T1 series and the contrast administered series.

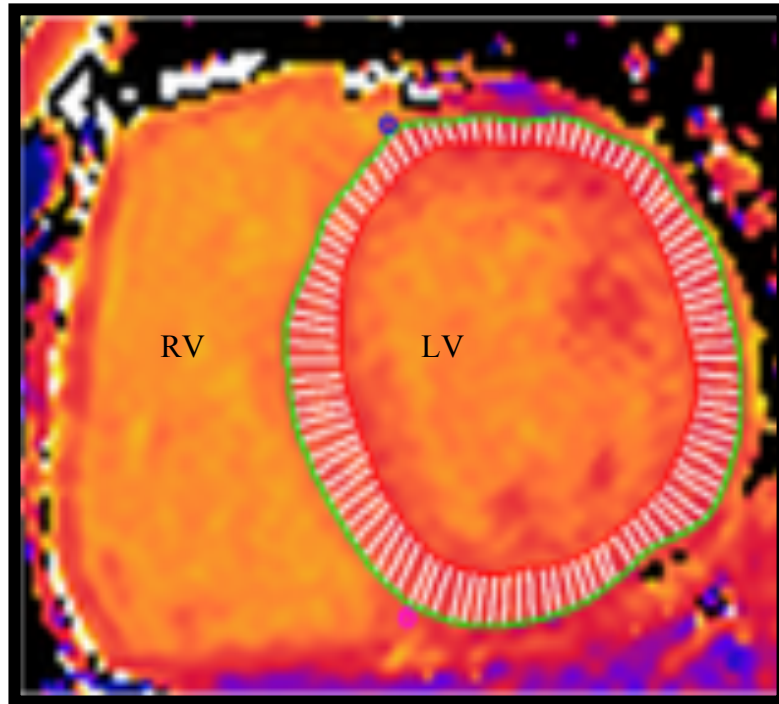


Figure 28. T1 mapping was performed on the short axis images. The T1 time was colour coded in shades of red and orange in this image, according to its value.

### 3.3.8 Assessment of LV strain and diastolic function using tissue tracking

Tissue tracking was performed using the software module included with the dedicated software package, CVI<sup>42</sup>. Tissue tracking uses the same short-axis cine images and contours used during the functional analysis (see Figure 29). Two long axis series, the 2- and 4-chamber views, were also used and required manual contouring of the endo- and epicardial borders. The strain and strain rates were then calculated using an advanced image tracking algorithm. Longitudinal, circumferential, and radial strains were documented.

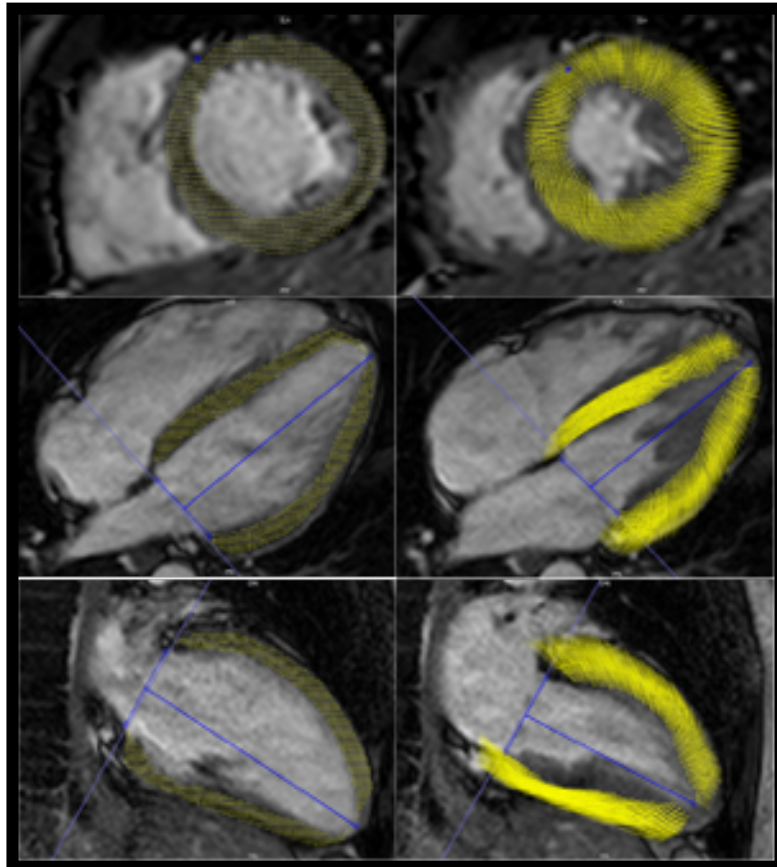


Figure 29. Tissue tracking was performed using the software module included with the dedicated software package, CVI<sup>42</sup>. The fine yellow gridlines can be seen in the overlay over the LV myocardium and the distortion during contractility used to calculate the strain.

Strain is expressed as the fractional change in length of a particular segment ( $\Delta L/L$ ) during contraction and, because the heart shortens in its longitudinal axis during contraction, this results in a negative value when assessed on the long axis. In the short axis, the radial diameter of the segments lengthens during contraction resulting in a positive value and the circumferential length shortens, resulting in a negative value (see Figure 30). Tissue tracking was used to analyse the systolic as well as the diastolic strain patterns. With the CVI<sup>42</sup> software, the myocardium is automatically tracked throughout the cardiac cycle. The endocardial and epicardial borders are manually traced. The distance moved between individual points in the matrix during systole and diastole were automatically calculated to obtain the different strain patterns. The strain rate was obtained by calculating the ratio between the distance and the time interval between the frames.

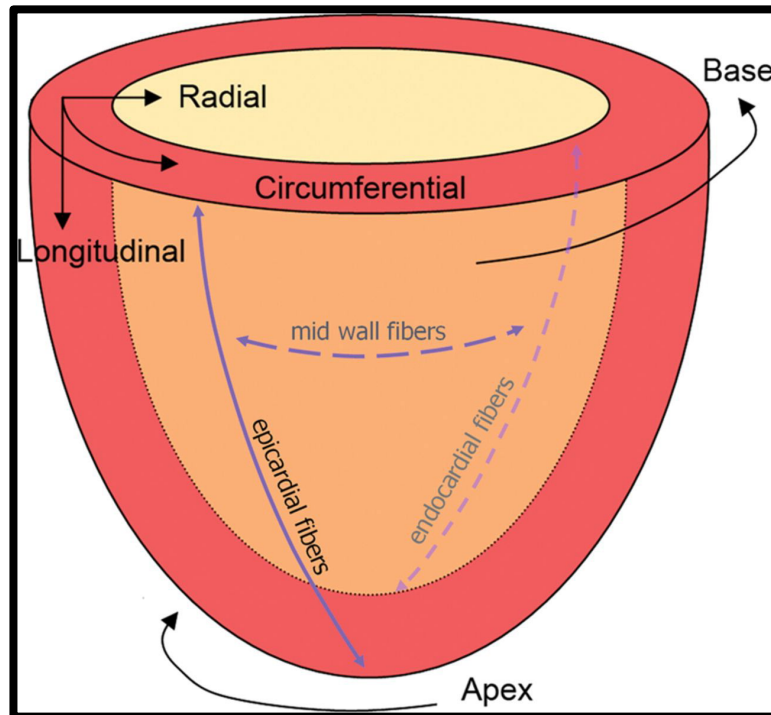


Figure 30. The three types of strain patterns. The fibres shorten in the longitudinal and circumferential plane and lengthens in the radial plane.<sup>161</sup>

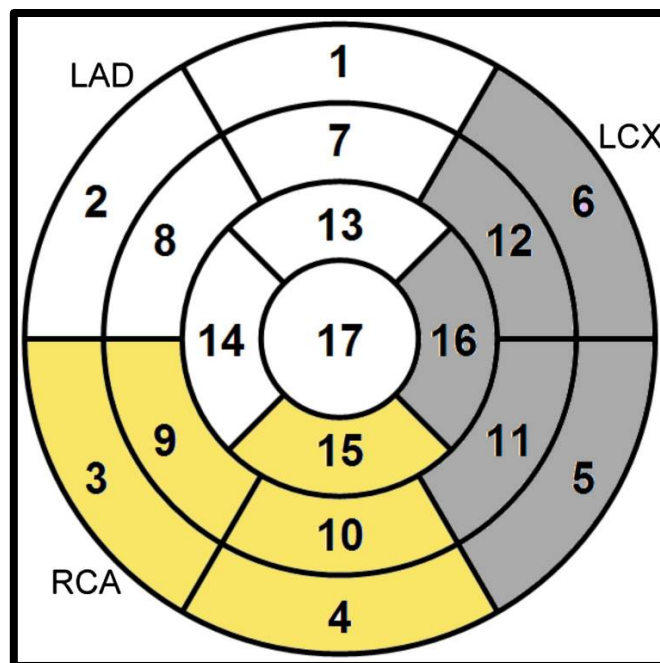


Figure 31. Coronary artery territories and LV segments according to the AHA model. There are seventeen segments and they correspond to the three main coronary artery territories with the right coronary artery supplying mainly the inferior region, the left anterior descending coronary artery supplying the apex, anterior and septal region and the circumflex artery supplying the lateral wall mainly.

### 3.3.9 Data analysis summary

The following data was collected for each patient and the control patients:

- a) Left ventricular (LV) ejection fraction (EF)% (normal for men=48-69, normal for women=51-70)
- b) End-diastolic volume (EDV) in millilitres (ml) (normal for men=109-218 ml, normal for women=88-161 ml)
- c) End-systolic volume (ESV) in millilitres (ml) (normal for men=39-97 ml, normal for women=31-68 ml)
- d) Stroke volume (SV) in millilitres (ml) (normal for men=59-132 ml, normal for women=49-100 ml)
- e) LV mass in grams (normal for men=64-141 g, normal for women=46-93 g)
- f) Oedema present/absent using the 17-segment American Heart (AHA) model
- g) Non matched perfusion defects using the 17-segment American Heart (AHA) model
- h) Late gadolinium enhancement present (LGE) using the AHA 17-segment model
- i) Native and post contrast T1 (ms) (normal native T1 time=975+/- 62 ms, normal post contrast T1 time=564+/-23 ms)
- j) Diastolic dysfunction analysis (nine parameters):
  - Peak circumferential diastolic strain rate (%/s)
  - Peak circumferential systolic strain rate (%/s)
  - Peak circumferential systolic strain (%)
  - Peak longitudinal diastolic strain rate (%/s)
  - Peak longitudinal systolic strain rate (%/s)
  - Peak longitudinal systolic strain (%)
  - Peak radial diastolic strain rate (%/s)
  - Peak radial systolic strain rate (%/s)
  - Peak radial systolic strain (%)

## 3.4 Statistics

### 3.4.1 Statistical considerations

The objective of analytical interest in this study was to compare the treatment naïve HIV infected and the HIV negative groups with respect to the functional and structural CMR findings

Sample size:

Sample size estimation for the study was based on testing for a clinically relevant difference between the HIV infected and control groups in mean EDV values, using the Student two-sample t test. With a sample size of 39 in each group the t test, performed at a two-sided significance level of 5%, would have 90% power to detect a mean difference of 15 (the difference between a mean of 80 in the HIV infected group and 65 in the control group) assuming that the common standard deviation is 20. Sample size estimation was done on nQuery Advanced (Statistical Solutions Ltd, Cork, Ireland), Release 8.0.

Data analysis:

Descriptive summary statistics are reported for all variables. Categorical variables are summarised by frequency counts and percentage calculations. Continuous variables are summarised by mean, standard deviation, median, interquartile range, minimum and maximum values.

Inferential statistics included significance tests for percentages, mean and median values, as well as correlation and linear regression analyses. The Fisher exact test was applied to test for differences in percentages. Student's two-sample t test was applied to test for differences in mean values with equal variances. Satterthwaite's t test was applied in the case of unequal variances. Application of the t test is based on the assumption of normality of the underlying distributions. The sample sizes achieved in the study (40 in the HIV infected group and 37 in the control group) are too small to allow for reliable normality testing. Nevertheless the Kolmogorov–Smirnov test was used to test for normality in all variables concerned. Together with each t test, the nonparametric Wilcoxon rank sum test, not



depending on normality and allowing for moderate skewness, was applied to median values to test for differences in location. All statistical tests were two-tailed, with p values  $\leq 0.05$  considered statistically significant. All the statistical procedures were performed on SAS (SAS Institute Inc, Carey, NC, USA), Release 9.4.

Validity and reliability:

Three patients were scanned before commencing the study in order to validate the procedures that would be followed in the study.

### **3.4.2 Control of potential Bias**

We recruited the HIV-infected as well as the control patients at The Steve Biko Academic hospital and they were slotted in (on an ad hoc basis) amongst the other patients.

The data analysts were blinded to the clinical data and they were not present during the scan. The scan protocols were the same for each patient and a radiologist not involved with the study administered the contrast.

The technicians performing the scans did not have access to the patients HIV status before or during the CMR scans.

The data was analysed at a different site and the analysts did not have access to the site where the scans or the selection took place. The analysts received the images on a numbered disc without having access to the HIV-status of the patients.

The HIV status was only disclosed after the whole study was completed.

### **3.5 Safety**

CMR is regarded as a very safe modality and does not involve ionising radiation. The reported frequency of adverse events after injection of gadolinium contrast ranges from 0.07-2.4%. The majority

of these reactions are mild, including coldness at the injection site, nausea, vomiting, dizziness, and itching. Reactions resembling an “allergic” response are rare and vary in frequency from 0.0034-0.013%.<sup>162</sup> A rash or hives are the most frequent of this group, and bronchospasm is very rare. Severe, life-threatening anaphylactoid reactions are also exceedingly rare (1-10/100,000). To date, only one published death has been clearly related to the administration of gadolinium-based contrast. Individuals who have pre-existing kidney disease and are given gadolinium-based contrast agent may have a small risk of developing a very rare disease called nephrogenic systemic fibrosis (NSF). To date this disease has only been found in patients with kidney disease, and the vast majority, if not all, had severe pre-existing kidney disease. NSF is often associated with thickening and tightening of the skin (usually involving the arms and/or legs, but occasionally associated with the trunk) and scarring. NSF may rarely get worse or cause death. Importantly, NSF has not been reported with newer generations of gadolinium contrast agents. All the patients enrolled in the study had undergone renal functional analysis and those with impaired kidney function (GFR <60 ml/min) were excluded.

### **3.6 Ethical considerations**

Informed consent was sought from each patient and the control patients for the CMR scan, which also included consent for intravenous gadolinium contrast injection (see Appendix 1). The patients and controls were asked to complete a screening form to address and confirm the absence of any detrimental metal implants or devices (see Appendix 2). Each patient was given a unique number and patient clinical information was not provided to the radiographers performing the scans. It must be emphasized that the HIV-infected patients were selected at the time of their initial presentation and the scans were performed immediately.

The protocol was submitted to and approved by the Ethics Committee of the Faculty of Health Sciences, University of Pretoria (RET\_2014\_UP02/201) and the extended period approved (see Appendix 3).

## Chapter 4: Results

### 4.1 Demographics and weight

Table 3. Demographics, weight and BSA

Characteristic	HIV infected (n=40)	Controls (n=37)	p value*
<b>Gender ratio</b>			
Males	9 (22.5%)	11 (29.7%)	0.604
Females	31 (77.5%)	26 (70.3%)	0.604
<b>Age, years</b>			
Mean ( $\pm$ SD)	36.2 ( $\pm$ 9.42)	35.4 ( $\pm$ 10.87)	0.723
Median (IQR)	36 (29–39)	34 (27–40)	0.683
Min/Max	21/59	18/59	
<b>Weight, kg</b>			
Mean ( $\pm$ SD)	67.8 ( $\pm$ 16.22)	68.0 ( $\pm$ 16.24)	0.953
Median (IQR)	64 (57–76)	66 (56–78)	0.736
Min/Max	45/122	41/127	
<b>BSA, m<sup>2</sup></b>			
Mean ( $\pm$ SD)	1.74 ( $\pm$ 0.20)	1.73 ( $\pm$ 0.22)	0.930
Median (IQR)	1.71 (1.61–1.85)	1.73 (1.58–1.89)	0.923
Min/Max	1.37/2.44	1.35/2.38	

\* Fisher Exact test for percentages, t tests for means, and the Wilcoxon rank sum test for medians

Interpretation:

- The group consisted of 40 HIV-infected patients and 37 controls.
- No statistically significant differences were found between the HIV infected and Control groups.

The two groups were statistically comparable in respect of the baseline demographic characteristics considered above.

## 4.2 Serological markers

Table 4. Baseline serological markers

Characteristic	HIV infected (n=40)	Controls (n=37)	p value
NT-proBNP, pg/mL			
n	36		
Median (IQR)	12 (8–22)	-	n/a
Min/Max	3/205		
CD4 <sup>+</sup> count, cm <sup>3</sup>			
n	39		
Median (IQR)	272 (62–526)	-	n/a
Min/Max	5/913		
Viremia load, copies/mL			
n	31		
Median (IQR)	51014 (8977 - 302654)	-	n/a
Min/Max	259/593076		

Interpretation:

- The median NT-proBNP of the infected patients was 12 pg/mL and the IQR 8-22 pg/mL (normal value is below 125pg/mL).
- The median CD4<sup>+</sup> count of the infected patients was 272 cells / $\mu$ L and the IQR between 62 and 526 cells/ $\mu$ L (normal CD4<sup>+</sup> count varies between 500-1600 cells/ $\mu$ L depending on the specific laboratory) and the median viremia load was 51014 copies/mL with an IQR of 8977 - 302654 copies/mL.
- The CD4<sup>+</sup> and viremia load were not performed on the control group of patients because they were proven to be uninfected.
- NT-proBNP values were also not obtained in the control group because they had been shown to be uninfected.

### 4.3 Structural and functional analyses

Table 5a. Summary of the results of the systolic functional analysis

<b>Characteristic</b>	<b>HIVinfected (n=40)</b>	<b>Controls (n=37)</b>	<b>Difference / p value*</b>
<b>EF, %</b>			
Mean ( $\pm$ SD)	58.8 ( $\pm$ 20.88)	60.9 ( $\pm$ 28.62)	2.1 / 0.719
Median (IQR)	55.5 (50.7-59.4)	54.7 (50.2-59.8)	-0.8 /0.783
Min/Max	30.8 / 155.6	40.4 / 175.6	
<b>LVED indexed to BSA, mL/m<sup>2</sup></b>			
Mean ( $\pm$ SD)	72.1 ( $\pm$ 15.62)	70.7 ( $\pm$ 13.63)	-1.4 / 0.677
Median (IQR)	78.0 (64.68–1.0)	72.7 (63.57–8.5)	-5.3 /0.657
<b>LVESV indexed to BSA, mL/m<sup>2</sup></b>			
Mean ( $\pm$ SD)	34.4 ( $\pm$ 9.50)	34.3 ( $\pm$ 8.94)	-0.1 /0.970
Median (IQR)	33.2 (28.2-39.4)	33.6 (28.8-38.8)	0.4 /0.988

Min/Max	17.8 / 59.4	15.3 / 59.0	
<b>LVSV, mL</b>			
Mean ( $\pm$ SD)	68.8 ( $\pm$ 15.15)	66.9 ( $\pm$ 13.19)	-1.9 / 0.557
Median (IQR)	68.3 (57.07–8.2)	69.3 (54.07–4.9)	1.0 / 0.610
Min/Max	36.7 / 102.8	42.3 / 93.8	
<b>LVSV indexed to BSA, mL/m<sup>2</sup></b>			
Mean ( $\pm$ SD)	39.8 ( $\pm$ 8.84)	38.7 ( $\pm$ 6.84)	-1.1 / 0.563
Median (IQR)	40.4 (33.44–4.1)	40.4 (33.5–43.5)	0 / 0.691
Min/Max	24.5 / 63.9	25.3 / 54.2	

Table 5b. Results of the LV mass assessment

<b>Characteristic</b>	<b>HIV infected (n=40)</b>	<b>Controls (n=37)</b>	<b>Difference / p value*</b>
<b>LV mass indexed to BSA, g/m<sup>2</sup></b>			
Mean ( $\pm$ SD)	52.2 ( $\pm$ 13.47)	50.0 ( $\pm$ 6.95 )	-2.2 / 0.355
Median (IQR)	49.4 (43.8–57.9)	47.8 (45.1–55.7)	-1.6 / 0.721
Min/Max	31.2 / 100.1	37.1 / 64.3	
<b>LV mass/LVEDV, g/L</b>			
Mean ( $\pm$ SD)	0.74 ( $\pm$ 0.20)	0.72 ( $\pm$ 0.19)	-0.02 / 0.666
Median (IQR)	0.68 (0.64–0.79)	0.68 (0.63–0.72)	0 / 0.514
Min/Max	0.48 / 1.35	0.55 / 1.46	

\*tests for means, and Wilcoxon rank sum tests for medians

Interpretation:

- The differences in mean and median values of all the systolic functional and LV mass characteristics were statistically insignificant.

Table 6. Results for the circumferential strain patterns

<b>Characteristic</b>	<b>HIV infected (n=40)</b>	<b>Controls (n=37)</b>	<b>Difference / p vale*</b>
<b>Peak systolic circumferential strain, %</b>			
Mean ( $\pm$ SD)	-18.1 ( $\pm$ 6.75)	-17.2 ( $\pm$ 8.39)	0.9 / 0.606
Median (IQR)	-19.1 (-21.1;-17.4)	-19.0 (-20.1;-17.2)	0.1 / 0.596
Min/Max	-23.8 / 19.3	-24.7 / 18.7	
<b>Peak diastolic circumferential strain rate, 1/s</b>			
Mean ( $\pm$ SD)	1.3 ( $\pm$ 0.31)	1.4 ( $\pm$ 0.47)	0.1 / 0.334
Median (IQR)	1.2 (1.1–1.5)	1.3 (1.1–1.7)	0.1 / 0.724
Min/Max	0.9 / 2.0	0.8 / 2.8	
<b>Peak systolic circumferential strain rate, 1/s</b>			
Mean ( $\pm$ SD)	-1.2 ( $\pm$ 0.56)	-1.0 ( $\pm$ 0.22)	0.2 / 0.044**
Median (IQR)	-1.2 (-1.3; -1.0)	-0.9 (-1.1; -0.8)	0.3 / <0.001**
Min/Max	-2.2 / 1.7	-1.7 / -0.6	

\*tests for means, and Wilcoxon rank sum tests for medians

Table 7. Results for the radial strain patterns

<b>Peak systolic radial strain, %</b>			
Mean ( $\pm$ SD)	34.9 ( $\pm$ 8.80)	34.0 ( $\pm$ 7.37)	-0.9 / 0.604
Median (IQR)	35.0 (29.3–39.6)	33.0 (29.7–36.2)	-2.0 / 0.506
Min/Max	16.9 / 55.5	20.8 / 52.1	
<b>Peak diastolic radial strain rate, 1/s</b>			
Mean ( $\pm$ SD)	-2.4 ( $\pm$ 0.93)	-2.6 ( $\pm$ 1.1)	-0.2 / 0.440
Median (IQR)	-2.3 (-2.8;-1.9)	-2.3 (-3.1;-1.9)	0 / 0.905
Min/Max	-5.2 / 1.2	-6.6 / -1.2	
<b>Peak systolic radial strain rate, 1/s</b>			
Mean ( $\pm$ SD)	2.2 ( $\pm$ 0.67)	1.8 ( $\pm$ 0.55)	-0.4 / 0.004**
Median (IQR)	2.0 (1.8–2.7)	1.7 (1.5–2.1)	-0.3 / 0.005**
Min/Max	1.2 / 3.8	0.9 / 3.4	

\*tests for means, and Wilcoxon rank sum tests for medians

Table 8. Results for the longitudinal strain patterns

<b>Characteristic</b>	<b>HIV infected (n=40)</b>	<b>Controls (n=37)</b>	<b>Difference / p value*</b>
<b>Peak systolic longitudinal strain, %</b>			
n	40	37	
Mean ( $\pm$ SD)	-18.9 ( $\pm$ 2.72)	-18.2 ( $\pm$ 7.29)	0.7 / 0.614
Median (IQR)	-19.2 (-20.8;-17.1)	-18.3 (-20.3;-17.1)	0.9 / 0.768
Min/Max	-24.2 / -9.4	-29.0 / 20.8	



<b>Peak diastolic longitudinal strain rate, 1/s</b>			
n	40	37	
Mean ( $\pm$ SD)	1.2 ( $\pm$ 0.26)	1.1 ( $\pm$ 0.30)	-0.1 / 0.356
Median (IQR)	1.2 (1.0–1.3)	1.0 (0.9–1.3)	-0.2 / 0.121
Min/Max	0.5 / 1.7	0.7 / 1.9	
<b>Peak systolic longitudinal strain rate, 1/s</b>			
n	40	36	
Mean ( $\pm$ SD)	-1.0 ( $\pm$ 0.23)	-0.8 ( $\pm$ 0.43)	0.2 / 0.014**
Median (IQR)	-1.0 (-1.1; -0.9)	-0.9 (-1.0; -0.8)	0.1 / 0.002**
Min/Max	-1.9 / -0.7	-1.5 / 0.9	

\*tests for means, and Wilcoxon rank sum tests for medians

Interpretation:

- The diastolic circumferential, radial and longitudinal strain patterns did not differ statistically significantly between the two groups but the systolic circumferential, radial and longitudinal systolic strain rates did differ significantly ( $p < 0.001$ , 0.005 and 0.002 respectively).
- This finding implies an early decreased rate of myocardial shortening and thickening during systole. Strain rate decreases early in the presence of myocardial dysfunction and impaired relaxation of the ventricle.

#### 4.4 Tissue characterisation analyses

Table 9. Tissue characterisation results

Characteristic	HIV infected (n=40)	Controls (n=37)	Difference / p value*
<b>T2 SIR</b>			
n	23	24	
Mean ( $\pm$ SD)	1.95 ( $\pm$ 0.41)	2.14 ( $\pm$ 0.31)	0.0824
<b>Native T1, ms</b>			
n	39	37	
Mean ( $\pm$ SD)	1084 ( $\pm$ 64.8)	1058 ( $\pm$ 62.9)	-26 / 0.074
Median (IQR)	1085 (10321–121)	1052 (10231–079)	-33 / 0.037**
Min/Max	992 / 1277	962 / 1315	
<b>Presence of LGE</b>			
Yes	31 (83.8%)	17 (48.6%)	-35.2 / 0.002**
No	6 (16.2%)	18 (51.4%)	35.2 / 0.002**
Total	37 (100%)	35 (100%)	
<b>Post contrast T1, ms</b>			
n	39	36	
Mean ( $\pm$ SD)	532.4 ( $\pm$ 65.97)	516.9 ( $\pm$ 61.56)	-15.5 / 0.299
Median (IQR)	539 (485–564)	512 (483–547)	-27 / 0.211
Min/Max	377 / 663	412 / 680	
<b>Volume fraction of LGE at 3SD</b>			
N	34	29	
Mean ( $\pm$ SD)	25.6 ( $\pm$ 6.54)	25.8 ( $\pm$ 9.13)	0.2 / 0.914
Median (IQR)	25.6 (22.3 – 28.9)	26.5 (22.7 – 31.7)	0.9 / 0.499
Min/Max	7.7 / 45.5	0 / 41.2	
<b>Total number of LGE</b>			
n	35	28	
Mean ( $\pm$ SD)	25.7 ( $\pm$ 4.31)	25.3 ( $\pm$ 4.27)	-0.4 / 0.690
Median (IQR)	25 (23–29)	25 (22–28)	0 / 0.627
Min/Max	18 / 38	18 / 34	

\*Student t tests for means, and the Wilcoxon rank sum tests for medians

\*\* Statistically significant

Interpretation:

- The median value of native T1 time in the HIV-infected group was statistically significantly greater than in the Control group ( $p=0.037$ ). Normality of the underlying distributions could not be supported by the Shapiro-Wilk test. The preferred measure of location in this case is the median.
- The presence of LGE in the HIV infected group (83.8%) and the Control group (48.6%) differ significantly (Fisher Exact test,  $p=0.002$ ).
- Enhancement was more commonly present in the inferolateral wall as reported in prior studies.<sup>16</sup>
- The differences in mean and median values of post contrast T1, volume fraction of LGE at 3SD, and total number of LGE were statistically insignificant.
- The differences in mean value of T2 weighted SIR in the HIV infected and Control groups were not statistically significant.

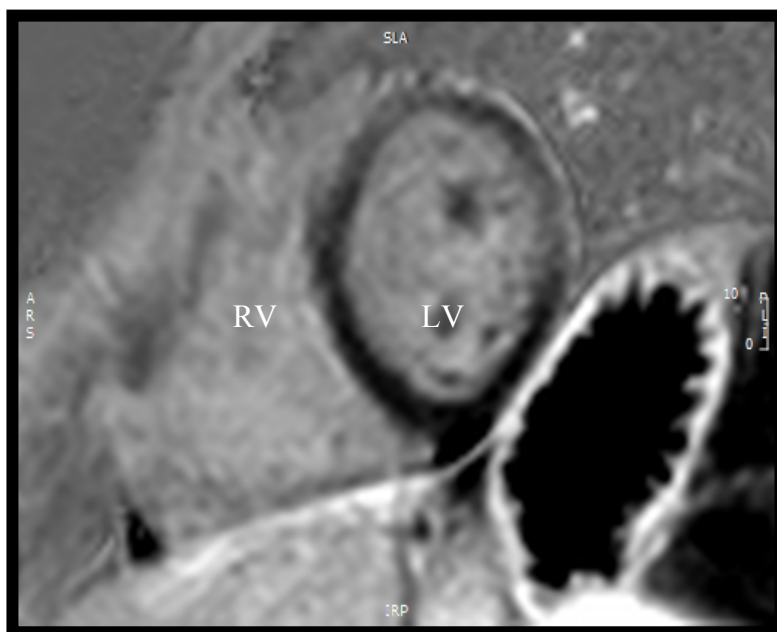


Figure 32a. LGE PSIR-TFE image of an HIV uninfected individual.

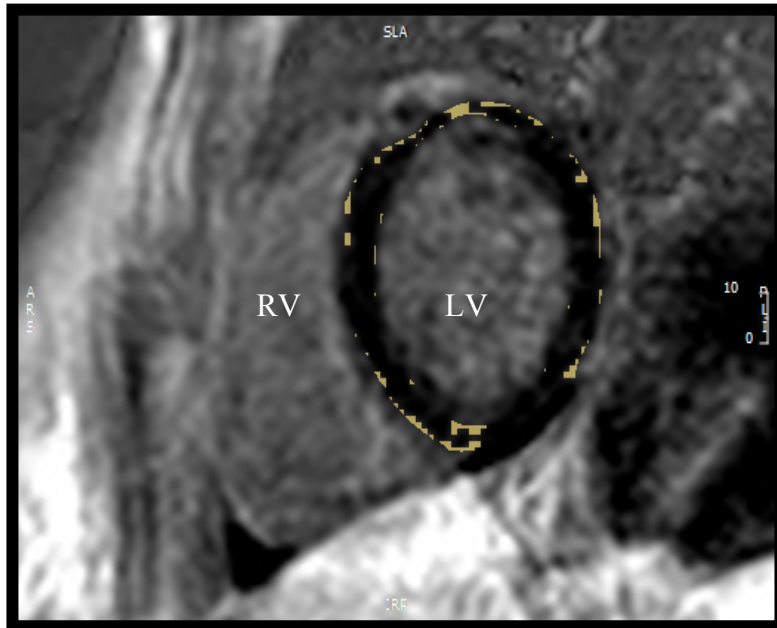


Figure 32b. LGE in the same uninfected individual with yellow colour overlay in the areas of enhancement colour coded according to the intensity of the enhancement. In uninfected individuals the myocardium appears black, and the colour coded areas of enhancement minimal.

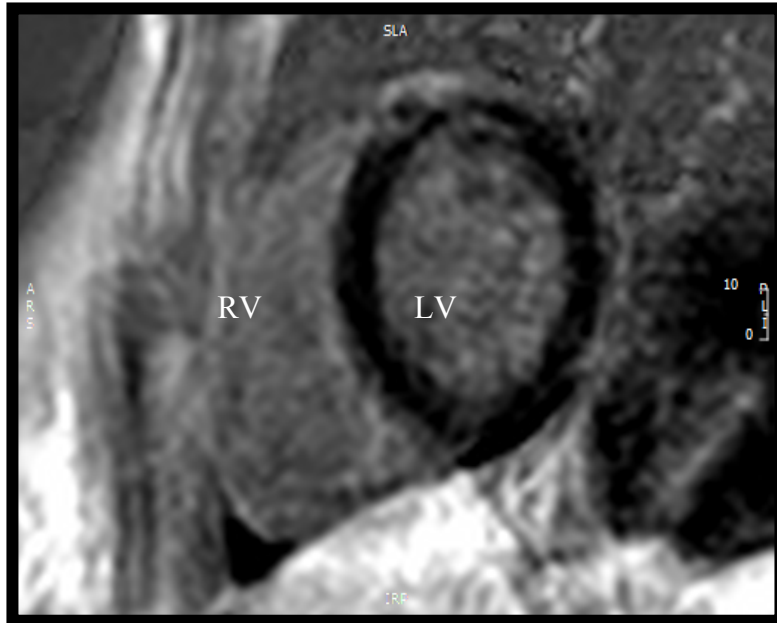


Figure 33a. LGE PSIR-TFE image of an HIV infected patient showing brighter areas of enhancement in the anterolateral wall and septum. Enhancement occurs more often in the inferolateral wall but can occur anywhere in the myocardium.

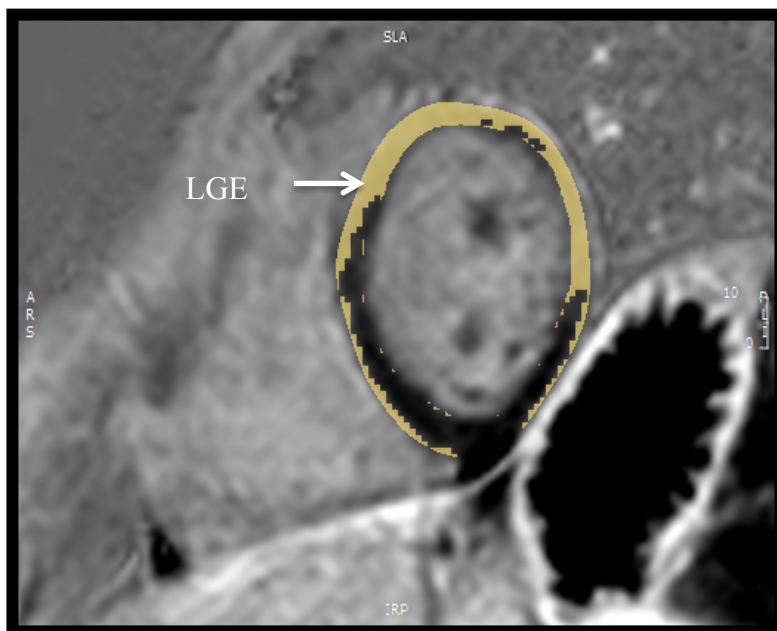


Figure 33b. The same LGE image with colour overlay in the areas of enhancement. The yellow areas indicate enhancement.

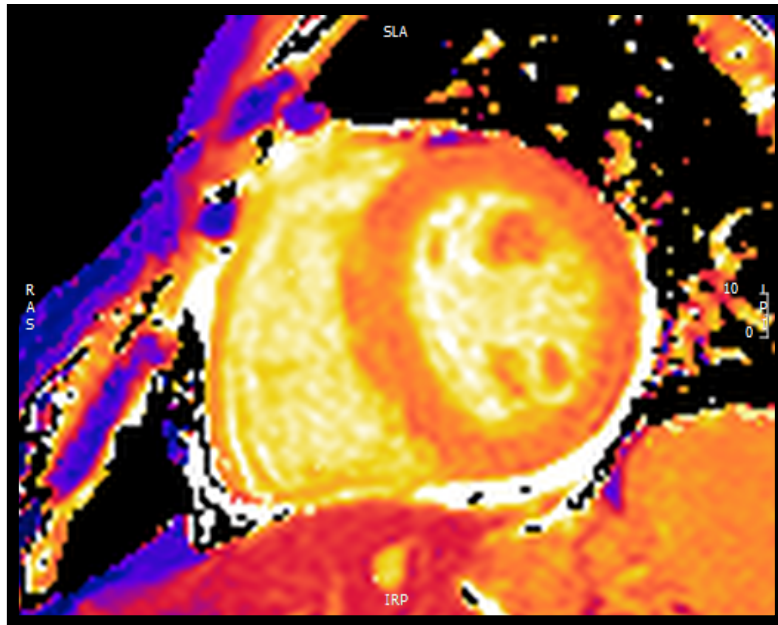


Figure 34a. T1 map of an uninfected individual in the control group.

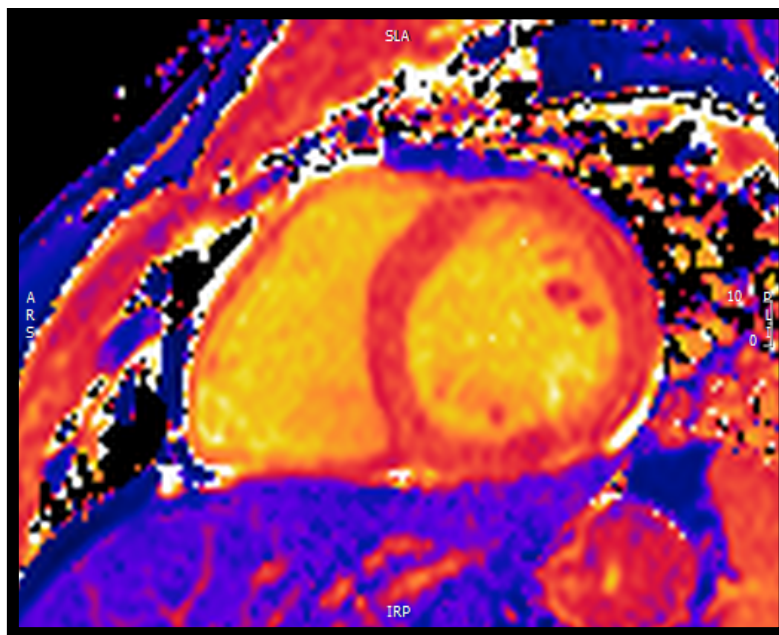


Figure 34b. Abnormal T1 map of one of the HIV-infected patients. The T1 time in ms is colour coded in orange/red with darker intensity in areas of abnormality in the HIV infected patient in comparison to the uninfected patient in Figure 34a. This is a common occurrence observed in HIV-infected individuals.<sup>17</sup>

## Chapter 5: Discussion

To the best of my knowledge, this is the first comprehensive CMR study performed on HIV-infected patients in SSA evaluating the effects of only HIV disease in the absence of ART on the myocardium. Moreover, since the MRI studies antedate the initiation of retroviral therapy, the abnormal findings are likely the consequence of the disease per se independent of any changes that could be attributed to ART therapy. Opportunistic infections could also be the culprit and cannot be excluded with certainty although the asymptomatic status of these patients argues against OI's as a cause of the cardiac abnormalities.

In contrast to prior studies in Europe and the USA, our patients were younger and had not yet received antiretroviral therapy.<sup>16-18</sup>

Systolic function was not impaired in our patients, which differs from some other prior studies.<sup>16-18</sup>

On the other hand, there was a significant impairment in strain rate in our patients in addition to the presence of abnormal native T1 times as well as the presence of LGE, suggesting that these are the earliest effects of HIV infection on the heart in asymptomatic patients without overt cardiac involvement using routine evaluation techniques.<sup>16-18</sup>

Strain becomes abnormal before the ejection fraction does and it can be used as an early marker of myocardial dysfunction. The updated EACVI/ASE/Industry Task Force recommendation was published after the protocol of this study was finalised and it states that global strain patterns (calculated by using the entire myocardial line length) should be used rather than the segmental individual measurements, to simplify and standardise future studies.<sup>163</sup>

Global strain can also be calculated by averaging the three segmental samples.

CMR is now becoming more accessible in SSA, and the fact that a study, which includes T1 mapping and strain assessment, can provide accurate detection of cardiovascular involvement due to HIV infection provides clinicians with an opportunity to detect the manifestations at an earlier phase of the disease. While T1 mapping is limited to assessment with magnetic resonance, strain can be assessed by echocardiography, which is cheaper and more widely available implying that T1 mapping can play a

potential important role in future. What will be of interest and should stimulate additional investigation is the natural history of these early cardiovascular changes, their response to retroviral therapy and whether the initiation of specific CV therapy, e.g. beta blockers, ACEi/ARB and aldosterone antagonists will alter the natural history and prevent the future development of overt symptomatic CV disease. Prompt and effective treatment of the cardiovascular complications can help to reduce mortality and morbidity in HIV-infected patients, mainly because the cardiovascular manifestations often go undetected.

A novel finding in this study is the abnormal strain patterns and native T1 times, which strongly suggest that these myocardial abnormalities in patients who had not yet been started on retroviral therapy were caused by the HIV virus itself or conceivably by OI's and not ART.

The study by Thiara and co-workers included 95 HIV-infected patients, who were all on treatment.<sup>18</sup>

The study by Leutgens and co-workers included 50 patients on ARTs.<sup>63</sup> The study by Holloway and that by Ntusi and their co-workers included 90 patients, of which 68% were on treatment<sup>16, 17</sup>

Our study showed no significant difference in systolic function (EF) when comparing HIV-infected patients to the control group. The majority of the prior studies reported decreased systolic function in HIV-infected patients, compared to controls. Potential explanations for these differences could be because our study was performed earlier during the disease in addition to the possibility of adverse effects on systolic function as a consequence of retroviral therapy.

These prior studies included patients that had been on therapy for several years as reported on in a recent meta-analysis.<sup>164</sup> The HIV-infected patients in the study by Thiara and coworkers<sup>18</sup> and Ntusi and coworkers<sup>17</sup>, reported no difference in the EF between infected patients and controls. In contrast Leutgens and his coworkers<sup>19</sup> did demonstrate lower EF values in HIV-infected patients. The subclinical systolic strain parameters, however, (peak systolic circumferential strain) were in fact modestly impaired in the studies by Thiara and Ntusi.<sup>17, 18</sup> The systolic radial strain and systolic radial strain rates were also impaired in the study by Thiara.<sup>18</sup>



Another differentiating feature between our and prior studies is a significant age difference. The mean age in the group studied by Leutgens, was 49 years,<sup>19</sup> 49 years in the series of Thiara, 49 years<sup>18</sup> and 43 years and 45 years in the series of Holloway<sup>16</sup> and Ntusi<sup>17</sup> respectively. In contrast, our patients were much younger with a median age of our patients was 36 years.

Left ventricular volumes in all the studies, including our own did not differ between HIV-infected patients and controls, except for the ESV that was modestly larger in the study by Ntusi (7%).<sup>17</sup>

LV mass did not differ significantly between the groups in any of the studies, including our own.

Our findings regarding the strain impairment confirmed the results of prior studies:

The systolic strain rate was impaired in our study and Ntusi and his co-workers reported abnormal diastolic strain in HIV infected patients (29% lower in the HIV-infected patients)<sup>17</sup> and this was also impaired in the study by Leutgens and his coworkers.<sup>19</sup>

We observed areas of LGE in 75% of the HIV-infected patients (30 out of the 40 patients), similar to the studies by Ntusi and Leutgens, who observed patchy areas of LGE in 83% and 82% of the patients respectively.<sup>17, 19</sup> The study by Thiara reported lower percentages in their HIV-infected patients (8.6%).<sup>18</sup>

The native T1 mapping times, a marker of diffuse fibrosis, were significantly increased in all the studies, including our own.

Thiara and co-workers showed an association between ART-treated HIV and myocardial fibrosis.<sup>18</sup> The subsequent studies by Ntusi and Leutgens and their co-workers alluded to a possible underlying inflammatory cause for the fibrosis and associated, (mainly diastolic) functional impairment, in patients on treatment.<sup>17, 63</sup> Our patients were not on treatment, but the findings were similar, strongly suggesting that HIV infection per se could be the major aetiological factor.

This implies that the changes and abnormal parameters in our study were due to the HIV virus itself or to OI's affecting the myocardium.

A limitation of the study is the lack of follow up CMR scans to ascertain whether the abnormalities improved or progressed over time and in response to therapy once patients were treated with ART. The

effects of cardioprotective therapies, like renin-angiotensin-aldosterone system (RAAS) inhibitors and beta-blockers were not assessed in this study, and this could be a fertile area for further investigation including prospective randomised trials using CMR as a surrogate endpoint and clinical outcomes in more extensive studies. Another limitation is the fact that the sample size was small due to financial restraints as well as the fact that the control patients that were included could have had underlying asymptomatic heart disease.

## **Chapter 6: Impact of the Study and future considerations**

There is a pandemic of HIV infection in Sub-Saharan Africa with a dire impact on the socio-economy of the region. The protean manifestations of the HIV syndrome are multifactorial and include the impact of comorbidities and underlying nutritional status of the patient population, in addition to other factors such as the regional infrastructure, which determines the accessibility to retroviral therapy, drug adherence and prompt treatment of the complications of the disease. In this respect, this study makes an original contribution by enhancing our understanding of the early onset of cardiac manifestations of HIV infection in SSA. An example of the international differences is the well-documented prevalence of premature vascular disease in long-term survivors of retroviral therapy in high-income countries, whereas the impact of retroviral therapy in association with emerging risk factors for CVD in SSA is unknown.

This study does provide a novel insight into the early effects of HIV in a young population with a low likelihood of CVD, and as such the functional, morphologic and tissue characteristics described are likely the result of the HIV infection alone. All the previous studies, which evaluated the effects of HIV infection on function, structure and myocardial tissue included patients almost exclusively on treatment and adverse effects of antiretroviral drugs on the myocardium and vasculature are well known in addition to their proclivity to cause dyslipidaemia, the metabolic syndrome and accelerated atherosclerosis.<sup>91, 165,166, 167</sup>

The increased risk of hyperglycaemia, the metabolic syndrome in HIV-infected patients on treatment is well documented.

We therefore addressed one of the important gaps in the literature by demonstrating:

- a. Early manifestations of cardiac involvement in untreated asymptomatic individuals without cardiac symptoms (and normal systolic functional analysis) are present in several strain parameters.

- b. These patients were not on therapy implying that the abnormal findings can be attributed to the effects of viral infection per se or perhaps opportunistic infections.

The study provides the following insights:

- a. There is a striking lack of any measurable impact upon systolic ejection fraction and structure in asymptomatic untreated patients. This highlights the potential importance of identifying abnormal strain patterns as the earliest harbinger of cardiac involvement and perhaps a target for early cardiac-specific therapies. Earlier detection and treatment may, in turn, have the potential to modify the natural progression of the disease.
- b. We demonstrated that the native T1 time could also be used as early markers of diffuse myocardial involvement. Also, these parameters can be utilised to diagnose and follow the progression of cardiac involvement.

Implications for the future include the following:

- a. CMR parameters may provide a target or parameter for future clinical trials of antiviral and cardiac-specific therapy.
- b. CMR may provide additional insight into the natural history of these abnormalities and links to subsequent disease, e.g. CVD, heart failure and arrhythmias
- c. Ultimately clinical trials will be needed to assess whether treatments based upon these parameters can affect outcomes.
- d. The CMR sequences we used to evaluate function, structure and tissue characteristics included sophisticated software tools to assess diastolic function, but also T1 mapping that is now a commercially available tool and is easy to perform and does not require the use of contrast. It can be traced manually, without access to sophisticated software and potentially at a lower cost than a full comprehensive CMR study.

- e. Awareness of the potential for cardiac involvement at an early subclinical phase of the disease must be cultivated among physicians.
- f. The broader availability of CMR may have a role to play in the earlier identification of subclinical disease in HIV as well as in the assessment of the effect of cardioprotective therapies like RAAS inhibitors once cardiovascular manifestations occur.
- g. Earlier detection of the cardiovascular manifestations may improve mortality and morbidity in HIV-infected patients as well as its effect on the economy and workforce.
- h. It would be prudent for future policy to include routine native T1 CMR scanning of asymptomatic patients before commencing with ART.
- i. Symptomatic patients should undergo a routine native T1 CMR scan, if the symptoms cannot be attributed to underlying intrapulmonary or other systemic pathologies.

HIV infection is a cost to society and the economy and prevention as well as prompt treatment with ARTs is the only way to counteract this. Whether the early detection of cardiac involvement may reduce future cardiovascular and coronary disease events and as such may help to reduce the clinical impact of the epidemic of CVD in SSA, a region that already struggles under the burden of many other diseases, including the complications of HIV, will remain to be determined. Nonetheless, the potential therapeutic implication of early detection is exciting.

## Chapter 7: Published articles, articles under review and planned articles

Articles published on the same topic before registration for the degree:

1. Editorial: L Scholtz Cardiovascular imaging in South Africa. SA Journal of Radiology September 2011
2. Vascular manifestations of HIV/AIDS Cardiovasc Intervent Radiol (2004) 27:422–426 DOI: 10.1007/s00270-004-0016-6

Articles published since registration for the PhD:

1. L Scholtz, A Sarkin, Z Lockhat Current clinical applications of cardiovascular magnetic resonance imaging *Cardiovasc J Afr* 2014; 25: 185–190 DOI: 10.5830/CVJA-2014-021
2. Editorial: Scholtz L. Cardiovascular imaging in South Africa: Is the heartache easing? *S Afr J Radiol* 2016;20(2), a1045 <http://dx.doi.org/10.4102/sajr.v20i2.1045>
3. Preliminary results of the systolic functional evaluation were reported in the local SA Journal of Radiology: Scholtz L, Du Plessis A, Andronikou S, *et al.* Systolic function evaluated with cardiovascular magnetic resonance imaging in HIV-infected patients. *S Afr J Rad.* 2016;20(2), a1044. <http://dx.doi.org/10.4102//sajr.v20i2.1044>
4. Article titled, “Cardiovascular manifestations of HIV/AIDS: An African perspective on the evolving epidemiology and clinical course with emphasis upon diagnostic imaging challenges.” has been sent to Cardiovascular journal of Africa and awaits acceptance.
5. The full results including the full functional evaluation, hyperaemia, oedema and LGE as well as the T1 mapping findings will be submitted for publication to a peer-reviewed journal. The journals that will be considered include *Circulation*, *JACC Imaging*, *European Heart Journal Cardiovascular Imaging*, etc.

## Appendix 1

**PIC 1 (a)**

### **PATIENT / PARTICIPANT'S INFORMATION LEAFLET & INFORMED CONSENT FORM FOR CLINICAL MEDICATION TRIAL /**

**TRIAL TITLE:**

**Cardiovascular Magnetic Resonance in patients with HIV: assessing the structural and functional abnormalities associated with remodeling of the myocardium**

**SPONSOR: None**

**Principal Investigator:**

**Professor Leonie Scholtz**

**Institution:**

**Montana Private Hospital and University of Pretoria**

**DAYTIME AND AFTER HOURS TELEPHONE NUMBER(S):**

**Daytime numbers: 0125481002 or 0828235729**

**Afterhours: 0825552912**

**DATE AND TIME OF FIRST INFORMED CONSENT DISCUSSION:**

<b>dd</b>	<b>mm</b>	<b>yyyy</b>

<b>:</b>
<b>Time</b>

**Dear Patient**

## **INTRODUCTION**

You are invited to volunteer for a research study. This information leaflet is to help you to decide if you would like to participate. Before you agree to take part in this study, you should fully understand what is involved. If you have any questions, which are not fully explained in this leaflet, do not hesitate to ask the investigator. You should not agree to take part unless you are completely happy about all the procedures involved. In the best interests of your health, it is strongly recommended that you discuss with or inform your personal doctor of your possible participation in this study, wherever possible.

## **WHAT IS THE PURPOSE OF THE RESEARCH TRIAL?**

You have been diagnosed as suffering from HIV infection and the investigator would like you to consider taking part in the research of a new imaging tool, called Cardiovascular Magnetic Resonance Imaging.

The objective of this study is to image and document the heart abnormalities associated with HIV infection.

We are going to characterize the structural changes (tissue abnormalities) affecting the heart muscle in patients with HIV and verify whether these changes are due to swelling, scar tissue or inflammation based on Cardiovascular Magnetic Resonance (CMR) imaging findings.

We are going to compare the functional and structural CMR findings between HIV infected and HIV-uninfected patients (controls).

## **WHAT IS THE DURATION OF THIS TRIAL?**

If you decide to take part you will be one of approximately 35 patients. The CMR will take approximately one hour.

## **DESCRIPTION OF PROCEDURES**

This study involves answering some questions with regard to your illness, examination of yourself, ECG, weight and height, measurements, blood tests and an ultrasound test.

It is important that you let the investigator know of any medicines (both prescriptions or over-the-counter medicines), alcohol or other substances that you are currently taking.

You will be asked to remove all metal objects and you will wear a gown given to you by the radiographer. During the scan itself, you will lie on a table that slides into a horizontal cylinder slightly wider than your body. You will be asked to lie still, but you will be able to hear and speak to the MRI personnel/research staff.

## **HAS THE TRIAL RECEIVED ETHICAL APPROVAL?**

This clinical trial Protocol was submitted to the Faculty of Health Sciences Research Ethics Committee, University of Pretoria, telephone numbers 012 3541677 / 012 3541330 and written approval has been granted by that committee. The study has been structured in accordance with the Declaration of Helsinki (last update: October 2008), which deals with the recommendations guiding doctors in biomedical research involving human/subjects. A copy of the Declaration may be obtained from the investigator should you wish to review it.

## **WHAT ARE YOUR RIGHTS AS A PARTICIPANT IN THIS TRIAL?**

Your participation in this trial is entirely voluntary and you can refuse to participate or stop at any time without stating any reason. Your withdrawal will not affect your access to other medical care. The



investigator retains the right to withdraw you from the study if it is considered being in your best interest. If it is detected that you did not give an accurate history or did not follow the guidelines of the trial and the regulations of the trial facility, you may be withdrawn from the trial at any time.

### **IS ALTERNATIVE IMAGING AVAILABLE?**

Alternative imaging of the heart muscle is not currently available.

### **MAY ANY OF THESE TRIAL PROCEDURES RESULT IN DISCOMFORT OR INCONVENIENCE?**

Some people experience anxiety, panic, or a sensation of claustrophobia when lying in the MRI machine. If you think this may happen to you, please tell the researchers before you have the scan. The scanner also makes loud noises during imaging. Ear protection will be provided to reduce the noise level. If you feel uncomfortable for any reason before or during the procedure, please tell the researchers. If for any reason during the procedure you want to stop, you may do so at any time. You will be given an intravenous injection of contrast material called Gadolinium during the scan. It may result in a bruise at the puncture site, or less commonly fainting or swelling of the vein, infection and bleeding from the site. Your protection is that the procedures are performed under sterile conditions by experienced personnel. A total of 10ml of contrast (i.e. 1 tablespoon) will be injected.

### **WHAT ARE THE BENEFITS TO YOU**

This particular scan normally carries a high cost and in your case it will be free of charge. The findings resulting from the study might add additional information regarding your medical condition and utilized by your doctor during your treatment.

### **WHAT ARE THE RISKS INVOLVED IN THIS TRIAL?**

MR imaging is generally considered being safe; but accidents, injuries, and even deaths have occurred during MRI procedures. Serious complications can occur in people who have metal pacemakers, metallic dust in the eyes, or certain types of metal prostheses, implants, or surgical clips. MRI is also dangerous for anyone wearing any metal objects, including jewellery, watches, hair holders, eyeglasses or metal on clothing, as well as eye shadow, which sometimes contains metallic substances. In addition, if you enter the MRI room with any magnetic cards, such as ATM and credit cards, you will risk having the data on the cards erased by the MRI machine. For these reasons, a researcher or technician will review safety information with you before the scan. In order to determine whether it is safe for you to undergo the scanning procedure, it will be important that you tell the technician about any metallic objects or devices in, on, or on, your body. In this research study, an injection of Gadolinium, an MRI contrast media, is used to enhance the quality of your MRI images. Gadolinium will be administered by intravenous injection. Gadolinium generally gives very few reactions. However, injections carry a small risk of harm including allergic reaction, injury at the injection site, or infection. The reported frequency of adverse events after an injection of Gadolinium contrast ranges from 0.07-2.4%. The majority of these reactions are mild, including coldness at the injection site, nausea, vomiting, dizziness, and itching. Reactions resembling an "allergic" response are rare and vary in frequency from 0.004-0.07. A rash or hives are the most frequent of this group and very rarely there may be bronchospasm. Severe, life threatening anaphylactoid reactions are exceedingly rare (1-10/100,000) In an accumulated series of 687,000 doses there were only 5 severe reactions. In another survey based on 20 million administered doses there were 55 cases of anaphylactic shock. To date, only one published death has been clearly related to the administration of gadolinium- based contrast. The staff and physicians are trained to handle problems that may arise with the contrast injection. **If you previously had an "allergic-type" reaction to contrast media used in MRI, please notify the technologist so that they can plan your examination**

**accordingly.**

People who have kidney disease who are given gadolinium-based contrast agent may have a very small risk of developing a very rare disease called Nephrogenic Systemic Fibrosis (NSF). We have screened you and your kidney function fell within the normal range. To date this disease has only been found in patients with kidney disease, and the vast majority, if not all, have severe kidney disease. NSF is often associated with thickening and tightening of the skin (usually involving the arms and/or legs but occasionally associated with the trunk) and scarring. NSF may rarely continue to get worse and can even cause death. **If you have any questions, feel free to ask the technologist.**

## **ARE THERE ANY WARNINGS OR RESTRICTIONS CONCERNING MY PARTICIPATION IN THIS TRIAL?**

Magnetic Resonance Imaging (MRI) uses a powerful magnet to take pictures of your body. Because the MRI machine exposes the body to a very strong magnetic force, you will have to follow certain safety precautions to make sure you do not have any metal objects in, or on, your body. Before you undergo your MRI scan, a researcher or technician will ask whether your body contains any metallic medical devices or equipment, including heart pacemakers, metal prostheses, implants or surgical clips. You also will be asked whether you have had any prior injury from shrapnel or grinding metal, and you will be asked whether your eyes have been exposed to metallic dust or metallic shavings. You, or the researcher or technician, will also complete a checklist that addresses issues of MRI safety. If you have no metallic objects or particles in your body, you will be asked before entering the MRI room to remove from your person all metal objects, including jewellery, watches, hair holders, or eyeglasses; and you will be asked to empty your pockets of all materials, including keys, wallets, and magnetic cards such as ATM and credit cards. In addition, if your clothing has more than a minimal amount of metal content, you may be asked to change into a hospital gown or other suitable garment. Finally, you will be asked to remove any eye shadow you may be wearing, because eye shadow sometimes contains metallic substances.

**FOR WOMEN:** The safety of MR imaging during pregnancy has not been proved. If you are, or might be, pregnant, you cannot take part in this study.

## **INSURANCE AND FINANCIAL ARRANGEMENTS**

The scans will be performed at the Netcare Montana Private Hospital. You will be transported from and back to Steve Biko Hospital free of charge.

The investigator will provide payment for all trial procedures and reasonable medical expenses, which you may incur as a direct result of this trial as determined by the investigator. Neither you nor your medical scheme will be expected to pay for any study medication or trial procedures.

The investigator has obtained insurance for you and the investigator in the event of such trial related injury. Further detailed information on the payment of medical treatment and compensation due to injury can be obtained from the investigator should you desire to review it. You will not be paid to participate in this trial. The investigator will determine if you are eligible to receive reimbursement for out-of-pocket and/or travel expenses. Please note that if you have a life insurance policy, you should enquire whether your insurance company requires notification of your intention to participate in a clinical trial. Our information to date is that it should not affect any life insurance policy taken out. Nevertheless you are strongly advised to clarify this with the company concerned.

**SOURCE OF ADDITIONAL INFORMATION**

For the duration of the trial, you will be under the care of Professors Scholtz and Stoltz. If at any time between your visits you feel that any of your symptoms are causing you any problems, or you have any questions during the trial, please do not hesitate to contact him/her. The 24 hour telephone number is 0825552912, through which you can reach him/her or another authorized person.

**CONFIDENTIALITY**

All information obtained during this trial is strictly confidential. Data that may be reported in scientific journals will not include any information which identifies you as a patient in this trial.

**INFORMED CONSENT**

I hereby confirm that I have been informed by the investigator, Dr..... about the nature, conduct, benefits and risks of clinical imaging trial. I have also received, read and understood the above written information (Patient Information Leaflet and Informed Consent) regarding the clinical trial.

I am aware that the results of the trial, including personal details regarding my sex, age, date of birth, initials and diagnosis will be anonymously processed into a trial report.

I may, at any stage, without prejudice, withdraw my consent and participation in the trial. I have had sufficient opportunity to ask questions and (of my own free will) declare myself prepared to participate in the trial.

Patient's name \_\_\_\_\_  
(Please print)  
Patient's signature \_\_\_\_\_ Date \_\_\_\_\_

I, Dr ..... herewith confirm that the above patient has been informed fully about the nature, conduct and risks of the above trial.

Investigator's name \_\_\_\_\_  
(Please print)  
Investigator's signature \_\_\_\_\_ Date \_\_\_\_\_

Witness's name\* \_\_\_\_\_ Witness's signature \_\_\_\_\_ Date \_\_\_\_\_  
(Please print)

**\*Consent procedure should be witnessed whenever possible.**

**VERBAL PATIENT INFORMED CONSENT** (applicable when patients cannot read or write)

I, the undersigned, Dr ....., have read and have explained fully to the patient, named ..... and/or is/her relative, the patient information leaflet, which has indicated the nature and purpose of the trial in which I have asked the patient to participate. The explanation I have given has mentioned both the possible risks and benefits of the trial and the alternative treatments available for his/her illness. The patient indicated that he/she understands that he/she will be free to withdraw from the trial at any time for any reason and without jeopardizing his/her subsequent injury attributable to the drug(s) used in the clinical trial, to which he/she agrees.

I hereby certify that the patient has agreed to participate in this trial.

Patient's Name \_\_\_\_\_  
(Please print)

Investigator's Name \_\_\_\_\_  
(Please print)

Investigator's Signature \_\_\_\_\_ Date \_\_\_\_\_

Witness's Name \_\_\_\_\_ Witness's Signature \_\_\_\_\_ Date \_\_\_\_\_  
(Please print)

**(Witness - sign that he/she has witnessed the process of informed consent**

## Appendix 2

### MRI Pre Scan Safety Questionnaire

This questionnaire is designed to screen for various conditions in a potential MRI participant, which could lead to moderate or serious injury during MRI scanning. It is VERY important that you complete it as honestly and comprehensively as possible—please ask if you have any questions.

NAME: \_\_\_\_\_ DATE: \_\_\_\_\_  
ID No. \_\_\_\_\_  
DATE OF BIRTH: \_\_\_\_\_ HEIGHT: \_\_\_\_\_ WEIGHT: \_\_\_\_\_  
STUDY/PROJECT NAME: \_\_\_\_\_

**Please circle if any of the following are relevant to you:**

Do you have or have you ever had a cardiac pacemaker?	YES/NO
Do you have an implanted cardiac defibrillator?	YES/NO
Do you have an aneurysm clip or been treated for an aneurysm in the head?	YES/NO
Do you have a cochlear or stapes Implant?	YES/NO
Do you have a neurostimulator or spinal cord stimulator?	YES/NO
Do you have any implanted electronic or magnetically activated devices?	YES/NO
Have you ever had any metal enter your eyes? (Cutting metal, grinding or welding)	YES/NO
If yes, was it removed by a doctor?	YES/NO

**Please indicate if you have any of the following: (Please circle)**

Hip replacement or artificial joint?	YES/NO
Pin, plate or screw?	YES/NO
Prosthesis -eye, limb, penile implant?	YES/NO
Implanted coil, filter, shunt or stent?	YES/NO
Eyeliner or other facial make up?	YES/NO
Piercings or any jewellery?	YES/NO
Hearing aid?	YES/NO
Eyelid spring or wire?	YES/NO
Do you have any tattoos?	YES/NO
Artificial heart valve?	YES/NO
Contraceptive IUD?	YES/NO
Inflatable breast implant?	YES/NO
Are you/could you be pregnant?	YES/NO
Medication patches applied?	YES/NO
Wire mesh Implanted?	YES/NO
Spine or head shunt?	YES/NO

Vascular port or catheter?	YES/NO
Any other implanted metal?	YES/NO
Any metal foreign bodies?	YES/NO
Other concerns?	YES/NO
Are you breast-feeding?	YES/NO
Do you suffer from claustrophobia?	YES/NO
Do you suffer from epilepsy or ever had a seizure?	YES/NO
Do you wear braces, a dental plate or false teeth?	YES/NO
Do you suffer from any heart condition that would make you susceptible to an increased risk of cardiac arrest?	YES/NO
Have you ever had a surgical operation? If yes, please provide details of body area (head, arm) and medical condition	YES/NO

.....

.....

Have you had a MRI scan before?	YES/NO
If yes, where? .....	
Did you experience any problems while having an MRI scan?	YES/NO
Do you have any allergies?	YES/NO
If yes, details:	

.....

I have read the above information and am aware of the risks and benefits of undergoing an MRI examination.

I have been provided with the opportunity to have any questions answered and I therefore give my consent to an MRI scan. I confirm that the questions have been answered to the best of my knowledge.

PARTICIPANTS NAME.....

SIGNATURE..... DATE.....

MRI STAFF MEMBER NAME: .....

SIGNATURE..... DATE.....

Please empty your pockets of all magnetic items including wallet, bank cards and coins. You will also need to remove shoes, metal belt buckles and any jewellery you have on. You will also need to remove your eye glasses (the radiographer will provide you with alternatives)

## Appendix 3

The Research Ethics Committee, Faculty Health Sciences, University of Pretoria complies with ICH-GCP guidelines and has US Federal wide Assurance.

- FWA 00002567, Approved dd 22 May 2002 and Expires 20 Oct 2016.
- IRB 0000 2235 IORG0001762 Approved dd 22/04/2014 and Expires 22/04/2017.



UNIVERSITEIT VAN PRETORIA  
UNIVERSITY OF PRETORIA  
YUNIBESITHI YA PRETORIA

Faculty of Health Sciences Research Ethics Committee

12/08/2014

### Approval Certificate New Application

**Ethics Reference No.: 239/2014**

**Title:** Cardiovascular Magnetic Resonance in patients with HIV: assessing the structural and functional abnormalities associated with remodelling of the myocardium

Dear Prof Magdalena Scholtz

The **New Application** as supported by documents specified in your cover letter for your research received on the 3/06/2014, was approved by the Faculty of Health Sciences Research Ethics Committee on the 12/08/2014.

Please note the following about your ethics approval:

- Ethics Approval is valid for 2 years.
- Please remember to use your protocol number (**239/2014**) on any documents or correspondence with the Research Ethics Committee regarding your research.
- Please note that the Research Ethics Committee may ask further questions, seek additional information, require further modification, or monitor the conduct of your research.

**Ethics approval is subject to the following:**

- The ethics approval is conditional on the receipt of 6 monthly written Progress Reports, and
- The ethics approval is conditional on the research being conducted as stipulated by the details of all documents submitted to the Committee. In the event that a further need arises to change who the investigators are, the methods or any other aspect, such changes must be submitted as an Amendment for approval by the Committee.

We wish you the best with your research.

Yours sincerely

A handwritten signature in black ink, appearing to read 'R Sommers', written over a horizontal line.

**Dr R Sommers**; MBChB; MMed (Int); MPharMed.  
**Deputy Chairperson** of the Faculty of Health Sciences Research Ethics Committee, University of Pretoria

*The Faculty of Health Sciences Research Ethics Committee complies with the SA National Act 61 of 2003 as it pertains to health research and the United States Code of Federal Regulations Title 45 and 46. This committee abides by the ethical norms and principles for research, established by the Declaration of Helsinki, the South African Medical Research Council Guidelines as well as the Guidelines for Ethical Research: Principles Structures and Processes 2004 (Department of Health).*

☎ 012 354 1677    ☎ 0866516047    ✉ [deepeka.behari@up.ac.za](mailto:deepeka.behari@up.ac.za)    🌐 <http://www.healthethics-up.co.za>  
✉ Private Bag X323, Arcadia, 0007 - 31 Bophelo Road, HW Snyman South Building, Level 2, Room 2.33, Gezina, Pretoria



The Research Ethics Committee, Faculty Health Sciences, University of Pretoria complies with ICH-GCP guidelines and has US Federal wide Assurance.

- FWA 00002567, Approved dd 22 May 2002 and Expires 20 Oct 2016.
- IRB 0000 2235 IORG0001762 Approved dd 22/04/2014 and Expires 22/04/2017.



UNIVERSITEIT VAN PRETORIA  
UNIVERSITY OF PRETORIA  
YUNIBESITHI YA PRETORIA

Faculty of Health Sciences Research Ethics Committee

28/05/2015

**Approval Certificate  
Amendment  
(to be read in conjunction with the main approval certificate)**

Ethics Reference No.: 239/2014

**Title:** Cardiovascular Magnetic Resonance in patients with HIV: assessing the structural and functional abnormalities associated with remodelling of the myocardium

Dear Prof Magdalena Scholtz

The **Amendment** as described in your documents specified in your cover letter dated 7/05/2015 received on 7/05/2015 was approved by the Faculty of Health Sciences Research Ethics Committee on its quorate meeting of 27/05/2015.

Please note the following about your ethics amendment:

- Please remember to use your protocol number (**239/2014**) on any documents or correspondence with the Research Ethics Committee regarding your research.
- Please note that the Research Ethics Committee may ask further questions, seek additional information, require further modification, or monitor the conduct of your research.

**Ethics amendment is subject to the following:**

- The ethics approval is conditional on the receipt of 6 monthly written Progress Reports, and
- The ethics approval is conditional on the research being conducted as stipulated by the details of all documents submitted to the Committee. In the event that a further need arises to change who the investigators are, the methods or any other aspect, such changes must be submitted as an Amendment for approval by the Committee.

We wish you the best with your research.

Yours sincerely

**Dr R Sommers**, MBChB, MMed (Int); MPharMed.  
Deputy Chairperson of the Faculty of Health Sciences Research Ethics Committee, University of Pretoria

*The Faculty of Health Sciences Research Ethics Committee complies with the SA National Act 61 of 2003 as it pertains to health research and the United States Code of Federal Regulations Title 45 and 46. This committee abides by the ethical norms and principles for research, established by the Declaration of Helsinki, the South African Medical Research Council Guidelines as well as the Guidelines for Ethical Research: Principles Structures and Processes 2004 (Department of Health).*

◆ Tel: 012-3541330     ◆ Fax: 012-3541367     Fax2Email: 0866515924     ◆ E-Mail: fhsethics@up.ac.za  
◆ Web: //www.healthethics-up.co.za     ◆ H W Snyman Bld (South) Level 2-34     ◆ Private Bag x 323, Arcadia, Pta, S.A., 0007



The Research Ethics Committee, Faculty Health Sciences, University of Pretoria complies with ICH-GCP guidelines and has US Federal wide Assurance.

- FWA 00002567, Approved dd 22 May 2002 and Expires 03/20/2022.
- IRB 0000 2235 IORG0001762 Approved dd 22/04/2014 and Expires 03/14/2020.

14 March 2019

**Approval Certificate  
Amendment**

**Ethics Reference No.: 239/2014**

**Title: Cardiovascular Magnetic Resonance in patients with HIV Infection: Assessing the structural and functional abnormalities associated with remodelling of the myocardium**

Dear Prof ME Scholtz

The **Amendment** as supported by documents received between 2019-02-22 and 2019-03-14 for your research, was approved by the Faculty of Health Sciences Research Ethics Committee on its quorate meeting of 2019-03-13.

Please note the following about your ethics approval:

- Please remember to use your protocol number (239/2014 ) on any documents or correspondence with the Research Ethics Committee regarding your research.
- Please note that the Research Ethics Committee may ask further questions, seek additional information, require further modification, monitor the conduct of your research, or suspend or withdraw ethics approval.

**Ethics approval is subject to the following:**

- The ethics approval is conditional on the research being conducted as stipulated by the details of all documents submitted to the Committee. In the event that a further need arises to change who the investigators are, the methods or any other aspect, such changes must be submitted as an Amendment for approval by the Committee.

We wish you the best with your research.

**Yours sincerely**



---

**Dr R Sommers**

MBChB MMed (Int) MPharmMed PhD

**Deputy Chairperson** of the Faculty of Health Sciences Research Ethics Committee, University of Pretoria

*The Faculty of Health Sciences Research Ethics Committee complies with the SA National Act 61 of 2003 as it pertains to health research and the United States Code of Federal Regulations Title 45 and 46. This committee abides by the ethical norms and principles for research, established by the Declaration of Helsinki, the South African Medical Research Council Guidelines as well as the Guidelines for Ethical Research: Principles Structures and Processes, Second Edition 2015 (Department of Health).*

## References

1. Mahrholdt H, Wagner A, Judd RM, Sechtem U and Kim RJ. Delayed enhancement cardiovascular magnetic resonance assessment of non-ischaemic cardiomyopathies. *Eur Heart J.* 2005; 26: 1461-74.
2. <UNAIDS\_Global\_Report\_2013\_en\_1.pdf>.
3. Kharsany AB, Frohlich JA, Yende-Zuma N, Mahlase G, Samsunder N, Dellar RC, Zuma-Mkhonza M, Abdool Karim SS and Abdool Karim Q. Trends in HIV Prevalence in Pregnant Women in Rural South Africa. *J Acquir Immune Defic Syndr.* 2015; 70: 289-95.
4. <http://www.unaids.org/en/resources/fact-sheet>. Fact sheet - Latest statistics on the status of the AIDS epidemic. Global HIV statistics 2016.
5. <http://www.statssa.gov.za/publications/P0302/P03022017.pdf> SSASrPM-ypehotIcNAf.
6. UNAIDS. Fact sheet - Latest statistics on the status of the AIDS epidemic. Global HIV statistics. <http://www.unaids.org/en/resources/fact-sheet> 2016
7. Lempicki RA, Kovacs JA, Baseler MW, Adelsberger JW, Dewar RL, Natarajan V, Bosche MC, Metcalf JA, Stevens RA, Lambert LA, Alvord WG, Polis MA, Davey RT, Dimitrov DS and Lane HC. Impact of HIV-1 infection and highly active antiretroviral therapy on the kinetics of CD4+ and CD8+ T cell turnover in HIV-infected patients. *Proc Natl Acad Sci U S A.* 2000; 97: 13778-83.
8. [https://www.avert.org/professionals/hiv-around-world/global-response/funding-footnote10\\_ngo9aeb\\_AGiaeoha](https://www.avert.org/professionals/hiv-around-world/global-response/funding-footnote10_ngo9aeb_AGiaeoha).
9. <http://www.kas.de/suedafrika/en/pages/1848/TioHAotSAEK-A-S>.
10. Pennell DJ, Sechtem UP, Higgins CB, Manning WJ, Pohost GM, Rademakers FE, van Rossum AC, Shaw LJ and Yucel EK. Clinical indications for cardiovascular magnetic resonance (CMR): Consensus Panel report. *European heart journal.* 2004; 25: 1940-65.
11. Bellenger NG, Burgess MI, Ray SG, Lahiri A, Coats AJ, Cleland JG and Pennell DJ. Comparison of left ventricular ejection fraction and volumes in heart failure by echocardiography, radionuclide ventriculography and cardiovascular magnetic resonance; are they interchangeable? *Eur Heart J.* 2000; 21: 1387-96.
12. Bellenger NG, Francis JM, Davies CL, Coats AJ and Pennell DJ. Establishment and performance of a magnetic resonance cardiac function clinic. *J Cardiovasc Magn Reson.* 2000; 2: 15-22.
13. Gardner BI, Bingham SE, Allen MR, Blatter DD and Anderson JL. Cardiac magnetic resonance versus transthoracic echocardiography for the assessment of cardiac volumes and regional function after myocardial infarction: an intrasubject comparison using simultaneous intrasubject recordings. *Cardiovasc Ultrasound.* 2009; 7: 38.
14. Petersen SE, Aung N, Sanghvi MM, Zemrak F, Fung K, Paiva JM, Francis JM, Khanji MY, Lukaschuk E, Lee AM, Carapella V, Kim YJ, Leeson P, Piechnik SK and Neubauer S. Reference ranges for cardiac structure and function using cardiovascular magnetic resonance (CMR) in Caucasians from the UK Biobank population cohort. *J Cardiovasc Magn Reson.* 2017; 19: 18.
15. Lumsden RH and Bloomfield GS. The Causes of HIV-Associated Cardiomyopathy: A Tale of Two Worlds. *Biomed Res Int.* 2016; 2016: 8196560.
16. Holloway CJ, Ntusi N, Suttie J, Mahmood M, Wainwright E, Clutton G, Hancock G, Beak P, Tajar A, Piechnik SK, Schneider JE, Angus B, Clarke K, Dorrell L and Neubauer S. Comprehensive cardiac magnetic resonance imaging and spectroscopy reveal a high burden of myocardial disease in HIV patients. *Circulation.* 2013; 128: 814-22.
17. Ntusi N, O'Dwyer E, Dorrell L, Wainwright E, Piechnik S, Clutton G, Hancock G, Ferreira V, Cox P, Badri M, Karamitsos T, Emmanuel S, Clarke K, Neubauer S and Holloway C. HIV-1-Related Cardiovascular Disease Is Associated With Chronic Inflammation, Frequent Pericardial Effusions, and Probable Myocardial Edema. *Circ Cardiovasc Imaging.* 2016; 9: e004430.
18. Thiara DK, Liu CY, Raman F, Mangat S, Purdy JB, Duarte HA, Schmidt N, Hur J, Sibley CT, Bluemke DA and Hadigan C. Abnormal Myocardial Function Is Related to Myocardial Steatosis and Diffuse Myocardial Fibrosis in HIV-Infected Adults. *J Infect Dis.* 2015; 212: 1544-51.
19. Luetkens JA, Homsy R, Dabir D, Kuetting DL, Marx C, Doerner J, Schlesinger-Irsch U, Andrie R, Sprinkart AM, Schmeel FC, Stehning C, Fimmers R, Gieseke J, Naehle CP, Schild HH and Thomas

- DK. Comprehensive Cardiac Magnetic Resonance for Short-Term Follow-Up in Acute Myocarditis. *J Am Heart Assoc.* 2016; 5.
20. Ntsekhe M and Mayosi BM. Cardiac manifestations of HIV infection: an African perspective. *Nat Clin Pract Cardiovasc Med.* 2009; 6: 120-7.
21. Ntusi NAB. HIV and myocarditis. *Curr Opin HIV AIDS.* 2017; 12: 561-5.
22. Adler Y, Charron P, Imazio M, Badano L, Baron-Esquivias G, Bogaert J, Brucato A, Gueret P, Klingel K, Lionis C, Maisch B, Mayosi B, Pavie A, Ristic AD, Tenas MS, Seferovic P, Swedberg K and Tomkowski W. [2015 ESC Guidelines for the diagnosis and management of pericardial diseases]. *Kardiol Pol.* 2015; 73: 1028-91.
23. Mutyaba AK, Balkaran S, Cloete R, du Plessis N, Badri M, Brink J and Mayosi BM. Constrictive pericarditis requiring pericardiectomy at Groote Schuur Hospital, Cape Town, South Africa: causes and perioperative outcomes in the HIV era (1990-2012). *J Thorac Cardiovasc Surg.* 2014; 148: 3058-65 e1.
24. Fink L, Reichel N and Sutton MG. Cardiac abnormalities in acquired immune deficiency syndrome. *Am J Cardiol.* 1984; 54: 1161-3.
25. Ntsekhe M, Wiysonge CS, Gumedze F, Maartens G, Commerford PJ, Volmink JA and Mayosi BM. HIV infection is associated with a lower incidence of constriction in presumed tuberculous pericarditis: a prospective observational study. *PLoS One.* 2008; 3: e2253.
26. Cegielski JP, Lwakatare J, Dukes CS, Lema LE, Lallinger GJ, Kitinya J, Reller LB and Sheriff F. Tuberculous pericarditis in Tanzanian patients with and without HIV infection. *Tuber Lung Dis.* 1994; 75: 429-34.
27. Sagrista-Sauleda J, Permanyer-Miralda G and Soler-Soler J. Tuberculous pericarditis: ten year experience with a prospective protocol for diagnosis and treatment. *J Am Coll Cardiol.* 1988; 11: 724-8.
28. Mayosi BM, Wiysonge CS, Ntsekhe M, Volmink JA, Gumedze F, Maartens G, Aje A, Thomas BM, Thomas KM, Awotedu AA, Thembela B, Mntla P, Maritz F, Blackett KN, Nkouonlack DC, Burch VC, Rebe K, Parish A, Sliwa K, Vezi BZ, Alam N, Brown BG, Gould T, Visser T, Shey MS, Magula NP and Commerford PJ. Clinical characteristics and initial management of patients with tuberculous pericarditis in the HIV era: the Investigation of the Management of Pericarditis in Africa (IMPI Africa) registry. *BMC Infect Dis.* 2006; 6: 2.
29. Reuter H, Burgess LJ and Doubell AF. Role of chest radiography in diagnosing patients with tuberculous pericarditis. *Cardiovasc J S Afr.* 2005; 16: 108-11.
30. Strang JI, Kakaza HH, Gibson DG, Allen BW, Mitchison DA, Evans DJ, Girling DJ, Nunn AJ and Fox W. Controlled clinical trial of complete open surgical drainage and of prednisolone in treatment of tuberculous pericardial effusion in Transkei. *Lancet.* 1988; 2: 759-64.
31. Geske JB, Anavekar NS, Nishimura RA, Oh JK and Gersh BJ. Differentiation of Constriction and Restriction: Complex Cardiovascular Hemodynamics. *J Am Coll Cardiol.* 2016; 68: 2329-47.
32. Mayosi BM, Wiysonge CS, Ntsekhe M, Gumedze F, Volmink JA, Maartens G, Aje A, Thomas BM, Thomas KM, Awotedu AA, Thembela B, Mntla P, Maritz F, Blackett KN, Nkouonlack DC, Burch VC, Rebe K, Parrish A, Sliwa K, Vezi BZ, Alam N, Brown BG, Gould T, Visser T, Magula NP and Commerford PJ. Mortality in patients treated for tuberculous pericarditis in sub-Saharan Africa. *S Afr Med J.* 2008; 98: 36-40.
33. Mayosi BM, Ntsekhe M, Bosch J, Pandie S, Jung H, Gumedze F, Pogue J, Thabane L, Smieja M, Francis V, Joldersma L, Thomas KM, Thomas B, Awotedu AA, Magula NP, Naidoo DP, Damasceno A, Chitsa Banda A, Brown B, Manga P, Kirenga B, Mondo C, Mntla P, Tsitsi JM, Peters F, Essop MR, Russell JB, Hakim J, Matenga J, Barasa AF, Sani MU, Olunuga T, Ogah O, Ansa V, Aje A, Danbauchi S, Ojji D, Yusuf S and Investigators IT. Prednisolone and Mycobacterium indicus pranii in tuberculous pericarditis. *N Engl J Med.* 2014; 371: 1121-30.
34. Barbaro G, Di Lorenzo G, Grisorio B and Barbarini G. Cardiac involvement in the acquired immunodeficiency syndrome: a multicenter clinical-pathological study. Gruppo Italiano per lo Studio Cardiologico dei pazienti affetti da AIDS Investigators. *AIDS Res Hum Retroviruses.* 1998; 14: 1071-7.

35. Longo-Mbenza B, Seghers LV, Vita EK, Tonduang K and Bayekula M. Assessment of ventricular diastolic function in AIDS patients from Congo: a Doppler echocardiographic study. *Heart*. 1998; 80: 184-9.
36. Herskowitz A, Wu TC, Willoughby SB, Vlahov D, Ansari AA, Beschorner WE and Baughman KL. Myocarditis and cardiotropic viral infection associated with severe left ventricular dysfunction in late-stage infection with human immunodeficiency virus. *J Am Coll Cardiol*. 1994; 24: 1025-32.
37. Shaboodien G, Maske C, Wainwright H, Smuts H, Ntsekhe M, Commerford PJ, Badri M and Mayosi BM. Prevalence of myocarditis and cardiotropic virus infection in Africans with HIV-associated cardiomyopathy, idiopathic dilated cardiomyopathy and heart transplant recipients: a pilot study: cardiovascular topic. *Cardiovasc J Afr*. 2013; 24: 218-23.
38. Barbaro G. Reviewing the cardiovascular complications of HIV infection after the introduction of highly active antiretroviral therapy. *Curr Drug Targets Cardiovasc Haematol Disord*. 2005; 5: 337-43.
39. Friedrich MG, Sechtem U, Schulz-Menger J, Holmvang G, Alakija P, Cooper LT, White JA, Abdel-Aty H, Gutberlet M, Prasad S, Aletras A, Laissy JP, Paterson I, Filipchuk NG, Kumar A, Pauschinger M, Liu P and International Consensus Group on Cardiovascular Magnetic Resonance in M. Cardiovascular magnetic resonance in myocarditis: A JACC White Paper. *J Am Coll Cardiol*. 2009; 53: 1475-87.
40. Lurz P, Eitel I, Adam J, Steiner J, Grothoff M, Desch S, Fuernau G, de Waha S, Sareban M, Luecke C, Klingel K, Kandolf R, Schuler G, Gutberlet M and Thiele H. Diagnostic performance of CMR imaging compared with EMB in patients with suspected myocarditis. *JACC Cardiovasc Imaging*. 2012; 5: 513-24.
41. Kuhl U, Lauer B, Souvatzoglu M, Vosberg H and Schultheiss HP. Antimyosin scintigraphy and immunohistologic analysis of endomyocardial biopsy in patients with clinically suspected myocarditis--evidence of myocardial cell damage and inflammation in the absence of histologic signs of myocarditis. *J Am Coll Cardiol*. 1998; 32: 1371-6.
42. Kan H, Xie Z and Finkel MS. HIV gp120 enhances NO production by cardiac myocytes through p38 MAP kinase-mediated NF-kappaB activation. *Am J Physiol Heart Circ Physiol*. 2000; 279: H3138-43.
43. Shannon RP, Simon MA, Mathier MA, Geng YJ, Mankad S and Lackner AA. Dilated cardiomyopathy associated with simian AIDS in nonhuman primates. *Circulation*. 2000; 101: 185-93.
44. Lipshultz SE, Fisher SD, Lai WW and Miller TL. Cardiovascular monitoring and therapy for HIV-infected patients. *Ann N Y Acad Sci*. 2001; 946: 236-73.
45. Raidel SM, Haase C, Jansen NR, Russ RB, Sutliff RL, Velsor LW, Day BJ, Hoit BD, Samarel AM and Lewis W. Targeted myocardial transgenic expression of HIV Tat causes cardiomyopathy and mitochondrial damage. *Am J Physiol Heart Circ Physiol*. 2002; 282: H1672-8.
46. Remick J, Georgiopoulou V, Marti C, Ofotokun I, Kalogeropoulos A, Lewis W and Butler J. Heart failure in patients with human immunodeficiency virus infection: epidemiology, pathophysiology, treatment, and future research. *Circulation*. 2014; 129: 1781-9.
47. Frerichs FC, Dingemans KP and Brinkman K. Cardiomyopathy with mitochondrial damage associated with nucleoside reverse-transcriptase inhibitors. *N Engl J Med*. 2002; 347: 1895-6.
48. Sliwa K, Wilkinson D, Hansen C, Ntyintyane L, Tibazarwa K, Becker A and Stewart S. Spectrum of heart disease and risk factors in a black urban population in South Africa (the Heart of Soweto Study): a cohort study. *Lancet*. 2008; 371: 915-22.
49. Magula NP and Mayosi BM. Cardiac involvement in HIV-infected people living in Africa: a review. *Cardiovasc J S Afr*. 2003; 14: 231-7.
50. Ntsekhe M and Hakim J. Impact of human immunodeficiency virus infection on cardiovascular disease in Africa. *Circulation*. 2005; 112: 3602-7.
51. Twagirumukiza M, Nkeramihigo E, Seminega B, Gasakure E, Boccara F and Barbaro G. Prevalence of dilated cardiomyopathy in HIV-infected African patients not receiving HAART: a multicenter, observational, prospective, cohort study in Rwanda. *Curr HIV Res*. 2007; 5: 129-37.

52. Sliwa K, Carrington MJ, Becker A, Thienemann F, Ntsekhe M and Stewart S. Contribution of the human immunodeficiency virus/acquired immunodeficiency syndrome epidemic to de novo presentations of heart disease in the Heart of Soweto Study cohort. *Eur Heart J.* 2012; 33: 866-74.
53. Nzuobontane D, Blackett KN and Kuaban C. Cardiac involvement in HIV infected people in Yaounde, Cameroon. *Postgrad Med J.* 2002; 78: 678-81.
54. Ntusi NN, M. Human immunodeficiency virus-associated heart failure in sub-Saharan Africa: evolution in the epidemiology, pathophysiology, and clinical manifestations in the antiretroviral era. *ESC Heart Failure.* 2016; 3: 158-67.
55. Akinbami A, Balogun B, Balogun M, Dosunmu O, Oshinaike O, Adediran A and Adegboyega K. Chest X-ray findings in HIV- infected Highly Active Antiretroviral Treatment (HAART)-naive patients. *Pan Afr Med J.* 2012; 12: 78.
56. Du Plessis V, Andronikou S, Struck G, McKerrow N and Stoker A. Baseline chest radiographic features of HIV-infected children eligible for antiretroviral therapy. *S Afr Med J.* 2011; 101: 829-34.
57. Borlaug BA and Kass DA. Ventricular-vascular interaction in heart failure. *Heart Fail Clin.* 2008; 4: 23-36.
58. Reinsch N, Kahlert P, Esser S, Sundermeyer A, Neuhaus K, Brockmeyer N, Potthoff A, Erbel R, Buck T and Neumann T. Echocardiographic findings and abnormalities in HIV-infected patients: results from a large, prospective, multicenter HIV-heart study. *Am J Cardiovasc Dis.* 2011; 1: 176-84.
59. Mondy KE, Gottdiener J, Overton ET, Henry K, Bush T, Conley L, Hammer J, Carpenter CC, Kojic E, Patel P, Brooks JT and Investigators SUNS. High Prevalence of Echocardiographic Abnormalities among HIV-infected Persons in the Era of Highly Active Antiretroviral Therapy. *Clin Infect Dis.* 2011; 52: 378-86.
60. Olusegun-Joseph DA, Ajuluchukwu JN, Okany CC, Mbakwem AC, Oke DA and Okubadejo NU. Echocardiographic patterns in treatment-naive HIV-positive patients in Lagos, south-west Nigeria. *Cardiovasc J Afr.* 2012; 23: e1-6.
61. Wever-Pinzon O, Bangalore S, Romero J, Silva Enciso J and Chaudhry FA. Inotropic contractile reserve can risk-stratify patients with HIV cardiomyopathy: a dobutamine stress echocardiography study. *JACC Cardiovasc Imaging.* 2011; 4: 1231-8.
62. Hofman P, Drici MD, Gibelin P, Michiels JF and Thyss A. Prevalence of toxoplasma myocarditis in patients with the acquired immunodeficiency syndrome. *Br Heart J.* 1993; 70: 376-81.
63. Luetkens JA, Doerner J, Schwarze-Zander C, Wasmuth JC, Boesecke C, Sprinkart AM, Schmeel FC, Homsy R, Gieseke J, Schild HH, Rockstroh JK and Naehle CP. Cardiac Magnetic Resonance Reveals Signs of Subclinical Myocardial Inflammation in Asymptomatic HIV-Infected Patients. *Circ Cardiovasc Imaging.* 2016; 9: e004091.
64. Currie PF, Jacob AJ, Foreman AR, Elton RA, Brettell RP and Boon NA. Heart muscle disease related to HIV infection: prognostic implications. *BMJ.* 1994; 309: 1605-7.
65. Felker GM, Thompson RE, Hare JM, Hruban RH, Clemetson DE, Howard DL, Baughman KL and Kasper EK. Underlying causes and long-term survival in patients with initially unexplained cardiomyopathy. *N Engl J Med.* 2000; 342: 1077-84.
66. Sanchez-Torres RJ and Garcia-Palmieri MR. Cardiovascular disease in HIV infection. *P R Health Sci J.* 2006; 25: 249-54.
67. Fingerhood M. Full recovery from severe dilated cardiomyopathy in an HIV-infected patient. *AIDS Read.* 2001; 11: 333-5.
68. Sliwa K, Davison BA, Mayosi BM, Damasceno A, Sani M, Ogah OS, Mondo C, Ojji D, Dzudie A, Kouam Kouam C, Suliman A, Schrueder N, Yonga G, Ba SA, Maru F, Alemayehu B, Edwards C and Cotter G. Readmission and death after an acute heart failure event: predictors and outcomes in sub-Saharan Africa: results from the THESUS-HF registry. *Eur Heart J.* 2013; 34: 3151-9.
69. Lai H, Redheuil A, Tong W, Bluemke DA, Lima JA, Ren S and Lai S. HIV infection and abnormal regional ventricular function. *Int J Cardiovasc Imaging.* 2009; 25: 809-17.
70. Mendes L, Silva D, Miranda C, Sa J, Duque L, Duarte N, Brito P, Bernardino L and Pocas J. Impact of HIV infection on cardiac deformation. *Rev Port Cardiol.* 2014; 33: 501-9.

71. Reinsch N, Neuhaus K, Esser S, Potthoff A, Hower M, Brockmeyer NH, Erbel R, Neumann T, German Competence Network for Heart F and German Competence Network for HA. Prevalence of cardiac diastolic dysfunction in HIV-infected patients: results of the HIV-HEART study. *HIV Clin Trials*. 2010; 11: 156-62.
72. Nayak G, Ferguson M, Tribble DR, Porter CK, Rapena R, Marchicelli M and Decker CF. Cardiac diastolic dysfunction is prevalent in HIV-infected patients. *AIDS Patient Care STDS*. 2009; 23: 231-8.
73. Nelson MD, Szczepaniak LS, LaBounty TM, Szczepaniak E, Li D, Tighiouart M, Li Q, Dharmakumar R, Sannes G, Fan Z, Yumul R, Hardy WD and Hernandez Conte A. Cardiac steatosis and left ventricular dysfunction in HIV-infected patients treated with highly active antiretroviral therapy. *JACC Cardiovasc Imaging*. 2014; 7: 1175-7.
74. Diaz-Zamudio M, Dey D, LaBounty T, Nelson M, Fan Z, Szczepaniak LS, Hsieh BP, Rajani R, Berman D, Li D, Dharmakumar R, Hardy WD and Conte AH. Increased pericardial fat accumulation is associated with increased intramyocardial lipid content and duration of highly active antiretroviral therapy exposure in patients infected with human immunodeficiency virus: a 3T cardiovascular magnetic resonance feasibility study. *J Cardiovasc Magn Reson*. 2015; 17: 91.
75. Lopes de Campos WR, Chirwa N, London G, Rotherham LS, Morris L, Mayosi BM and Khati M. HIV-1 subtype C unproductively infects human cardiomyocytes in vitro and induces apoptosis mitigated by an anti-Gp120 aptamer. *PLoS One*. 2014; 9: e110930.
76. Shaboodien G, Engel ME, Syed FF, Poulton J, Badri M and Mayosi BM. The mitochondrial DNA T16189C polymorphism and HIV-associated cardiomyopathy: a genotype-phenotype association study. *BMC Med Genet*. 2009; 10: 37.
77. Duong M, Dubois C, Buisson M, Eicher JC, Grappin M, Chavanet P and Portier H. Non-Hodgkin's lymphoma of the heart in patients infected with human immunodeficiency virus. *Clin Cardiol*. 1997; 20: 497-502.
78. Gopal M, Bhaskaran A, Khalife WI and Barbagelata A. Heart Disease in Patients with HIV/AIDS-An Emerging Clinical Problem. *Curr Cardiol Rev*. 2009; 5: 149-54.
79. Nakazono T, Jeudy J and White CS. HIV-related cardiac complications: CT and MRI findings. *AJR Am J Roentgenol*. 2012; 198: 364-9.
80. d'Amati G, di Gioia CR and Gallo P. Pathological findings of HIV-associated cardiovascular disease. *Ann N Y Acad Sci*. 2001; 946: 23-45.
81. Whitby S, Madu EC and Bronze MS. Case report: *Candida zeylanoides* infective endocarditis complicating infection with the human immunodeficiency virus. *Am J Med Sci*. 1996; 312: 138-9.
82. Barbaro G. Cardiovascular manifestations of HIV infection. *Circulation*. 2002; 106: 1420-5.
83. Currie PF, Sutherland GR, Jacob AJ, Bell JE, Brettle RP and Boon NA. A review of endocarditis in acquired immunodeficiency syndrome and human immunodeficiency virus infection. *Eur Heart J*. 1995; 16 Suppl B: 15-8.
84. Garcia I, Fainstein V, Rios A, Luna M, Mansell P, Reuben J and Hersh E. Nonbacterial thrombotic endocarditis in a male homosexual with Kaposi's sarcoma. *Arch Intern Med*. 1983; 143: 1243-4.
85. Thuny F, Gaubert JY, Jacquier A, Tessonnier L, Cammilleri S, Raoult D and Habib G. Imaging investigations in infective endocarditis: current approach and perspectives. *Arch Cardiovasc Dis*. 2013; 106: 52-62.
86. Paton P, Tabib A, Loire R and Tete R. Coronary artery lesions and human immunodeficiency virus infection. *Res Virol*. 1993; 144: 225-31.
87. Khunnawat C, Mukerji S, Havlichek D, Jr., Touma R and Abela GS. Cardiovascular manifestations in human immunodeficiency virus-infected patients. *Am J Cardiol*. 2008; 102: 635-42.
88. Becker AC, Sliwa K, Stewart S, Libhaber E, Essop AR, Zambakides CA and Essop MR. Acute coronary syndromes in treatment-naive black South africans with human immunodeficiency virus infection. *J Interv Cardiol*. 2010; 23: 70-7.

89. Becker AC, Jacobson B, Singh S, Sliwa K, Stewart S, Libhaber E and Essop MR. The thrombotic profile of treatment-naïve HIV-positive Black South Africans with acute coronary syndromes. *Clin Appl Thromb Hemost*. 2011; 17: 264-72.
90. Rerkpattanapipat P, Wongpraparut N, Jacobs LE and Kotler MN. Cardiac manifestations of acquired immunodeficiency syndrome. *Arch Intern Med*. 2000; 160: 602-8.
91. Klein D, Hurley LB, Quesenberry CP, Jr. and Sidney S. Do protease inhibitors increase the risk for coronary heart disease in patients with HIV-1 infection? *J Acquir Immune Defic Syndr*. 2002; 30: 471-7.
92. Group DADS, Friis-Moller N, Reiss P, Sabin CA, Weber R, Monforte A, El-Sadr W, Thiebaut R, De Wit S, Kirk O, Fontas E, Law MG, Phillips A and Lundgren JD. Class of antiretroviral drugs and the risk of myocardial infarction. *N Engl J Med*. 2007; 356: 1723-35.
93. Hsue PY, Giri K, Erickson S, MacGregor JS, Younes N, Shergill A and Waters DD. Clinical features of acute coronary syndromes in patients with human immunodeficiency virus infection. *Circulation*. 2004; 109: 316-9.
94. Onen CL. Epidemiology of ischaemic heart disease in sub-Saharan Africa. *Cardiovasc J Afr*. 2013; 24: 34-42.
95. Gilbert JM, Fitch KV and Grinspoon SK. HIV-Related Cardiovascular Disease, Statins, and the REPRIEVE Trial. *Top Antivir Med*. 2015; 23: 146-9.
96. Triant VA, Lee H, Hadigan C and Grinspoon SK. Increased acute myocardial infarction rates and cardiovascular risk factors among patients with human immunodeficiency virus disease. *J Clin Endocrinol Metab*. 2007; 92: 2506-12.
97. Lang S, Mary-Krause M, Cotte L, Gilquin J, Partisani M, Simon A, Boccara F, Costagliola D and Clinical Epidemiology Group of the French Hospital Database on HIV. Impact of individual antiretroviral drugs on the risk of myocardial infarction in human immunodeficiency virus-infected patients: a case-control study nested within the French Hospital Database on HIV ANRS cohort CO4. *Arch Intern Med*. 2010; 170: 1228-38.
98. Boccara F, Lang S, Meuleman C, Ederhy S, Mary-Krause M, Costagliola D, Capeau J and Cohen A. HIV and coronary heart disease: time for a better understanding. *J Am Coll Cardiol*. 2013; 61: 511-23.
99. Miller TL, Orav EJ, Lipshultz SE, Arheart KL, Duggan C, Weinberg GA, Bechard L, Furuta L, Nicchitta J, Gorbach SL and Shevitz A. Risk factors for cardiovascular disease in children infected with human immunodeficiency virus-1. *J Pediatr*. 2008; 153: 491-7.
100. Gersh BJ, Sliwa K, Mayosi BM and Yusuf S. Novel therapeutic concepts: the epidemic of cardiovascular disease in the developing world: global implications. *Eur Heart J*. 2010; 31: 642-8.
101. Hsue PY, Lo JC, Franklin A, Bolger AF, Martin JN, Deeks SG and Waters DD. Progression of atherosclerosis as assessed by carotid intima-media thickness in patients with HIV infection. *Circulation*. 2004; 109: 1603-8.
102. Post WS, Budoff M, Kingsley L, Palella FJ, Jr., Witt MD, Li X, George RT, Brown TT and Jacobson LP. Associations between HIV infection and subclinical coronary atherosclerosis. *Ann Intern Med*. 2014; 160: 458-67.
103. D'Ascenzo F, Cerrato E, Calcagno A, Grossomarra W, Ballocca F, Omede P, Montefusco A, Veglia S, Barbero U, Gili S, Cannillo M, Pianelli M, Mistretta E, Raviola A, Salera D, Garabello D, Mancone M, Estrada V, Escaned J, De Marie D, Abbate A, Bonora S, Zoccai GB, Moretti C and Gaita F. High prevalence at computed coronary tomography of non-calcified plaques in asymptomatic HIV patients treated with HAART: a meta-analysis. *Atherosclerosis*. 2015; 240: 197-204.
104. Gharib AM, Abd-Elmoniem KZ, Pettigrew RI and Hadigan C. Noninvasive coronary imaging for atherosclerosis in human immunodeficiency virus infection. *Curr Probl Diagn Radiol*. 2011; 40: 262-7.
105. Mariano-Goulart D, Jacquet JM, Molinari N, Bourdon A, Benkiran M, Sainmont M, Cornillet L, Macia JC, Reynes J and Ben Bouallegue F. Should HIV-infected patients be screened for silent myocardial ischaemia using gated myocardial perfusion SPECT? *Eur J Nucl Med Mol Imaging*. 2013; 40: 271-9.

106. Subramanian S, Tawakol A, Burdo TH, Abbara S, Wei J, Vijayakumar J, Corsini E, Abdelbaky A, Zanni MV, Hoffmann U, Williams KC, Lo J and Grinspoon SK. Arterial inflammation in patients with HIV. *JAMA*. 2012; 308: 379-86.
107. Yarasheski KE, Laciny E, Overton ET, Reeds DN, Harrod M, Baldwin S and Davila-Roman VG. 18FDG PET-CT imaging detects arterial inflammation and early atherosclerosis in HIV-infected adults with cardiovascular disease risk factors. *J Inflamm (Lond)*. 2012; 9: 26.
108. Almodovar S, Hsue PY, Morelli J, Huang L, Flores SC and Lung HIVS. Pathogenesis of HIV-associated pulmonary hypertension: potential role of HIV-1 Nef. *Proc Am Thorac Soc*. 2011; 8: 308-12.
109. Opravil M and Sereni D. Natural history of HIV-associated pulmonary arterial hypertension: trends in the HAART era. *AIDS*. 2008; 22 Suppl 3: S35-40.
110. Weiss JR, Pietra GG and Scharf SM. Primary pulmonary hypertension and the human immunodeficiency virus. Report of two cases and a review of the literature. *Arch Intern Med*. 1995; 155: 2350-4.
111. Petitpretz P, Brenot F, Azarian R, Parent F, Rain B, Herve P and Simonneau G. Pulmonary hypertension in patients with human immunodeficiency virus infection. Comparison with primary pulmonary hypertension. *Circulation*. 1994; 89: 2722-7.
112. Dellegrottaglie S, Garcia-Alvarez A, Guarini P, Perrone-Filardi P, Fuster V and Sanz J. Prevalence and severity of ventricular dysfunction in patients with HIV-related pulmonary arterial hypertension. *Heart Lung*. 2014; 43: 256-61.
113. Thienemann F, Dzudie A, Mocumbi AO, Blauwet L, Sani MU, Karaye KM, Ogah OS, Mbanze I, Mbakwem A, Udo P, Tibazarwa K, Damasceno A, Keates AK, Stewart S and Sliwa K. The causes, treatment, and outcome of pulmonary hypertension in Africa: Insights from the Pan African Pulmonary Hypertension Cohort (PAPUCO) Registry. *Int J Cardiol*. 2016; 221: 205-11.
114. Shehata ML, Lossnitzer D, Skrok J, Boyce D, Lechtzin N, Mathai SC, Girgis RE, Osman N, Lima JA, Bluemke DA, Hassoun PM and Vogel-Claussen J. Myocardial delayed enhancement in pulmonary hypertension: pulmonary hemodynamics, right ventricular function, and remodeling. *AJR Am J Roentgenol*. 2011; 196: 87-94.
115. Mehta NJ, Khan IA, Mehta RN and Sepkowitz DA. HIV-Related pulmonary hypertension: analytic review of 131 cases. *Chest*. 2000; 118: 1133-41.
116. Knesewitsch T, Meierhofer C, Rieger H, Rossler J, Frank M, Martinoff S, Hess J, Stern H and Fratz S. Demonstration of value of optimizing ECG triggering for cardiovascular magnetic resonance in patients with congenital heart disease. *J Cardiovasc Magn Reson*. 2013; 15: 3.
117. Kramer CM, Barkhausen J, Flamm SD, Kim RJ, Nagel E and Society for Cardiovascular Magnetic Resonance Board of Trustees Task Force on Standardized P. Standardized cardiovascular magnetic resonance (CMR) protocols 2013 update. *J Cardiovasc Magn Reson*. 2013; 15: 91.
118. Grothues F, Moon JC, Bellenger NG, Smith GS, Klein HU and Pennell DJ. Interstudy reproducibility of right ventricular volumes, function, and mass with cardiovascular magnetic resonance. *Am Heart J*. 2004; 147: 218-23.
119. Grothues F, Smith GC, Moon JC, Bellenger NG, Collins P, Klein HU and Pennell DJ. Comparison of interstudy reproducibility of cardiovascular magnetic resonance with two-dimensional echocardiography in normal subjects and in patients with heart failure or left ventricular hypertrophy. *Am J Cardiol*. 2002; 90: 29-34.
120. Persson E, Carlsson M, Palmer J, Pahlm O and Arheden H. Evaluation of left ventricular volumes and ejection fraction by automated gated myocardial SPECT versus cardiovascular magnetic resonance. *Clin Physiol Funct Imaging*. 2005; 25: 135-41.
121. Ioannidis JP, Trikalinos TA and Danias PG. Electrocardiogram-gated single-photon emission computed tomography versus cardiac magnetic resonance imaging for the assessment of left ventricular volumes and ejection fraction: a meta-analysis. *J Am Coll Cardiol*. 2002; 39: 2059-68.
122. Abdel-Aty H, Cocker M, Meek C, Tyberg JV and Friedrich MG. Edema as a very early marker for acute myocardial ischemia: a cardiovascular magnetic resonance study. *J Am Coll Cardiol*. 2009; 53: 1194-201.



123. Abdel-Aty H, Zagrosek A, Schulz-Menger J, Taylor AJ, Messroghli D, Kumar A, Gross M, Dietz R and Friedrich MG. Delayed enhancement and T2-weighted cardiovascular magnetic resonance imaging differentiate acute from chronic myocardial infarction. *Circulation*. 2004; 109: 2411-6.
124. Fuernau G, Eitel I, Franke V, Hildebrandt L, Meissner J, de Waha S, Lurz P, Gutberlet M, Desch S, Schuler G and Thiele H. Myocardium at risk in ST-segment elevation myocardial infarction comparison of T2-weighted edema imaging with the MR-assessed endocardial surface area and validation against angiographic scoring. *JACC Cardiovasc Imaging*. 2011; 4: 967-76.
125. Graham MM, Faris PD, Ghali WA, Galbraith PD, Norris CM, Badry JT, Mitchell LB, Curtis MJ, Knudtson ML and Investigators A. Validation of three myocardial jeopardy scores in a population-based cardiac catheterization cohort. *Am Heart J*. 2001; 142: 254-61.
126. Hamlin SA, Henry TS, Little BP, Lerakis S and Stillman AE. Mapping the future of cardiac MR imaging: case-based review of T1 and T2 mapping techniques. *Radiographics*. 2014; 34: 1594-611.
127. Ferreira VM, Piechnik SK, Dall'Armellina E, Karamitsos TD, Francis JM, Ntusi N, Holloway C, Choudhury RP, Kardos A, Robson MD, Friedrich MG and Neubauer S. T(1) mapping for the diagnosis of acute myocarditis using CMR: comparison to T2-weighted and late gadolinium enhanced imaging. *JACC Cardiovasc Imaging*. 2013; 6: 1048-58.
128. Ferreira VM, Piechnik SK, Robson MD, Neubauer S and Karamitsos TD. Myocardial tissue characterization by magnetic resonance imaging: novel applications of T1 and T2 mapping. *J Thorac Imaging*. 2014; 29: 147-54.
129. Hoey ET, Gulati GS, Ganeshan A, Watkin RW, Simpson H and Sharma S. Cardiovascular MRI for assessment of infectious and inflammatory conditions of the heart. *AJR Am J Roentgenol*. 2011; 197: 103-12.
130. Luetkens JA, Doerner J, Thomas DK, Dabir D, Gieseke J, Sprinkart AM, Fimmers R, Stehning C, Homs R, Schwab JO, Schild H and Naehle CP. Acute myocarditis: multiparametric cardiac MR imaging. *Radiology*. 2014; 273: 383-92.
131. Dall'Armellina E, Piechnik SK, Ferreira VM, Si QL, Robson MD, Francis JM, Cuculi F, Kharbada RK, Banning AP, Choudhury RP, Karamitsos TD and Neubauer S. Cardiovascular magnetic resonance by non contrast T1-mapping allows assessment of severity of injury in acute myocardial infarction. *J Cardiovasc Magn Reson*. 2012; 14: 15.
132. Cheong BY, Muthupillai R, Wilson JM, Sung A, Huber S, Amin S, Elayda MA, Lee VV and Flamm SD. Prognostic significance of delayed-enhancement magnetic resonance imaging: survival of 857 patients with and without left ventricular dysfunction. *Circulation*. 2009; 120: 2069-76.
133. Ishida M, Kato S and Sakuma H. Cardiac MRI in ischemic heart disease. *Circ J*. 2009; 73: 1577-88.
134. Kwon DH, Halley CM, Carrigan TP, Zysek V, Popovic ZB, Setser R, Schoenhagen P, Starling RC, Flamm SD and Desai MY. Extent of left ventricular scar predicts outcomes in ischemic cardiomyopathy patients with significantly reduced systolic function: a delayed hyperenhancement cardiac magnetic resonance study. *JACC Cardiovasc Imaging*. 2009; 2: 34-44.
135. Kelle S, Roes SD, Klein C, Kokocinski T, de Roos A, Fleck E, Bax JJ and Nagel E. Prognostic value of myocardial infarct size and contractile reserve using magnetic resonance imaging. *J Am Coll Cardiol*. 2009; 54: 1770-7.
136. Shah DJ, Kim HW, James O, Parker M, Wu E, Bonow RO, Judd RM and Kim RJ. Prevalence of regional myocardial thinning and relationship with myocardial scarring in patients with coronary artery disease. *JAMA*. 2013; 309: 909-18.
137. Beek AM, Kuhl HP, Bondarenko O, Twisk JW, Hofman MB, van Dockum WG, Visser CA and van Rossum AC. Delayed contrast-enhanced magnetic resonance imaging for the prediction of regional functional improvement after acute myocardial infarction. *J Am Coll Cardiol*. 2003; 42: 895-901.
138. Friedrich MG. Tissue characterization of acute myocardial infarction and myocarditis by cardiac magnetic resonance. *JACC Cardiovasc Imaging*. 2008; 1: 652-62.
139. Rezkalla SH and Kloner RA. No-reflow phenomenon. *Circulation*. 2002; 105: 656-62.

140. Assomull RG, Prasad SK, Lyne J, Smith G, Burman ED, Khan M, Sheppard MN, Poole-Wilson PA and Pennell DJ. Cardiovascular magnetic resonance, fibrosis, and prognosis in dilated cardiomyopathy. *J Am Coll Cardiol.* 2006; 48: 1977-85.
141. Wu KC, Weiss RG, Thiemann DR, Kitagawa K, Schmidt A, Dalal D, Lai S, Bluemke DA, Gerstenblith G, Marban E, Tomaselli GF and Lima JA. Late gadolinium enhancement by cardiovascular magnetic resonance heralds an adverse prognosis in nonischemic cardiomyopathy. *J Am Coll Cardiol.* 2008; 51: 2414-21.
142. McCrohon JA, Moon JC, Prasad SK, McKenna WJ, Lorenz CH, Coats AJ and Pennell DJ. Differentiation of heart failure related to dilated cardiomyopathy and coronary artery disease using gadolinium-enhanced cardiovascular magnetic resonance. *Circulation.* 2003; 108: 54-9.
143. Sueyoshi E, Sakamoto I, Hayashida T and Uetani M. Quantification of enhancement of left ventricular myocardium in patients with dilated cardiomyopathy using delayed enhanced MR imaging. *Comput Med Imaging Graph.* 2009; 33: 547-52.
144. Burt JR, Zimmerman SL, Kamel IR, Halushka M and Bluemke DA. Myocardial T1 mapping: techniques and potential applications. *Radiographics.* 2014; 34: 377-95.
145. Messroghli DR, Radjenovic A, Kozerke S, Higgins DM, Sivananthan MU and Ridgway JP. Modified Look-Locker inversion recovery (MOLLI) for high-resolution T1 mapping of the heart. *Magn Reson Med.* 2004; 52: 141-6.
146. Greulich S, Arai AE, Sechtem U and Mahrholdt H. Recent advances in cardiac magnetic resonance. *F1000Res.* 2016; 5.
147. Azevedo PS, Polegato BF, Minicucci MF, Paiva SA and Zornoff LA. Cardiac Remodeling: Concepts, Clinical Impact, Pathophysiological Mechanisms and Pharmacologic Treatment. *Arq Bras Cardiol.* 2016; 106: 62-9.
148. Schirone L, Forte M, Palmerio S, Yee D, Nocella C, Angelini F, Pagano F, Schiavon S, Bordin A, Carrizzo A, Vecchione C, Valenti V, Chimenti I, De Falco E, Sciarretta S and Frati G. A Review of the Molecular Mechanisms Underlying the Development and Progression of Cardiac Remodeling. *Oxid Med Cell Longev.* 2017; 2017: 3920195.
149. Burchfield JS, Xie M and Hill JA. Pathological ventricular remodeling: mechanisms: part 1 of 2. *Circulation.* 2013; 128: 388-400.
150. Hill JA and Olson EN. Cardiac plasticity. *N Engl J Med.* 2008; 358: 1370-80.
151. Dorn GW, 2nd, Robbins J and Sugden PH. Phenotyping hypertrophy: eschew obfuscation. *Circulation research.* 2003; 92: 1171-5.
152. Baggish AL and Wood MJ. Athlete's heart and cardiovascular care of the athlete: scientific and clinical update. *Circulation.* 2011; 123: 2723-35.
153. Frey N, Katus HA, Olson EN and Hill JA. Hypertrophy of the heart: a new therapeutic target? *Circulation.* 2004; 109: 1580-9.
154. Grossman W, Jones D and McLaurin LP. Wall stress and patterns of hypertrophy in the human left ventricle. *The Journal of clinical investigation.* 1975; 56: 56-64.
155. Opie LH, Commerford PJ, Gersh BJ and Pfeffer MA. Controversies in ventricular remodeling. *Lancet.* 2006; 367: 356-67.
156. Perhonen MA, Franco F, Lane LD, Buckley JC, Blomqvist CG, Zerwekh JE, Peshock RM, Weatherall PT and Levine BD. Cardiac atrophy after bed rest and spaceflight. *J Appl Physiol.* 2001; 91: 645-53.
157. Villarreal FJ, Kim NN, Ungab GD, Printz MP and Dillmann WH. Identification of functional angiotensin II receptors on rat cardiac fibroblasts. *Circulation.* 1993; 88: 2849-61.
158. Anversa P, Olivetti G and Capasso JM. Cellular basis of ventricular remodeling after myocardial infarction. *The American journal of cardiology.* 1991; 68: 7D-16D.
159. Bluemke DA, Kronmal RA, Lima JA, Liu K, Olson J, Burke GL and Folsom AR. The relationship of left ventricular mass and geometry to incident cardiovascular events: the MESA (Multi-Ethnic Study of Atherosclerosis) study. *J Am Coll Cardiol.* 2008; 52: 2148-55.
160. Gaasch WH and Zile MR. Left ventricular structural remodeling in health and disease: with special emphasis on volume, mass, and geometry. *J Am Coll Cardiol.* 2011; 58: 1733-40.

161. Jeung MY, Germain P, Croisille P, El ghannudi S, Roy C and Gangi A. Myocardial tagging with MR imaging: overview of normal and pathologic findings. *Radiographics*. 2012; 32: 1381-98.
162. Prince MR, Zhang H, Zou Z, Staron RB and Brill PW. Incidence of immediate gadolinium contrast media reactions. *AJR American journal of roentgenology*. 2011; 196: W138-43.
163. Voigt JU, Pedrizzetti G, Lysyansky P, Marwick TH, Houle H, Baumann R, Pedri S, Ito Y, Abe Y, Metz S, Song JH, Hamilton J, Sengupta PP, Kolias TJ, d'Hooge J, Aurigemma GP, Thomas JD and Badano LP. Definitions for a common standard for 2D speckle tracking echocardiography: consensus document of the EACVI/ASE/Industry Task Force to standardize deformation imaging. *J Am Soc Echocardiogr*. 2015; 28: 183-93.
164. Cerrato E, D'Ascenzo F, Biondi-Zoccai G, Calcagno A, Frea S, Grosso Marra W, Castagno D, Omede P, Quadri G, Sciuto F, Presutti D, Frati G, Bonora S, Moretti C and Gaita F. Cardiac dysfunction in pauci symptomatic human immunodeficiency virus patients: a meta-analysis in the highly active antiretroviral therapy era. *Eur Heart J*. 2013; 34: 1432-6.
165. Grinspoon S and Carr A. Cardiovascular risk and body-fat abnormalities in HIV-infected adults. *N Engl J Med*. 2005; 352: 48-62.
166. Samaras K, Wand H, Law M, Emery S, Cooper D and Carr A. Prevalence of metabolic syndrome in HIV-infected patients receiving highly active antiretroviral therapy using International Diabetes Foundation and Adult Treatment Panel III criteria: associations with insulin resistance, disturbed body fat compartmentalization, elevated C-reactive protein, and [corrected] hypoadiponectinemia. *Diabetes Care*. 2007; 30: 113-9.
167. Vergara-Rodriguez P, Vibhakkar S and Watts J. Metabolic syndrome and associated cardiovascular risk factors in the treatment of persons with human immunodeficiency virus and severe mental illness. *Pharmacol Ther*. 2009; 124: 269-78.